University of Concepción
Graduate School
Faculty of Natural and Oceanographic Sciences
PhD in Oceanography

Biogeographic and diversity patterns of pelagic copepods in the South Pacific Ocean

Patrones biogeográficos y diversidad de copépodos pelágicos en el Océano Pacífico Sur

Thesis presented to the Faculty of Natural and Oceanographic Sciences
to qualify for the degree of PhD in Oceanography

by

Manuela Isabel Pérez Aragón

Rubén Escribano Veloso, PhD; Thesis Advisor

Cristián E. Hernández, PhD; Co-advisor

Concepción - Chile

December 2024

University of Concepción

Graduate School Direction

The Doctoral Thesis in Oceanography entitled "Biogeographic and diversity patterns of pelagic copepods in the South Pacific Ocean", by Mrs. Manuela Isabel Pérez Aragón and carried out at the Faculty of Natural and Oceanographic Sciences, University of Concepción, has been approved by the following Evaluation Commission:

Professor Rubén Escribano, PhD
Thesis advisor
Universidad de Concepción _____

Cristián E. Hernández, PhD
Co-advisor
Universidad de Concepción _____

Reinaldo Rivera Jara, PhD
Thesis Committee Member
Universidad de Concepción _____

Humberto E. González, PhD
External Examiner
Universidad Austral de Chile _____

Pamela Hidalgo, PhD
Director
PhD Program in Oceanography
Universidad de Concepción _____

ACKNOWLEDGEMENTS

I would like to express my gratitude to my advisors Dr. Ruben Escribano and Dr. Cristián Hernández for their guidance throughout the development of this PhD thesis. Also, I am especially grateful to Dr. Reinaldo Rivera for his patience and the tools he taught me to use for achieving this.

I would like to thank the Agencia Nacional de Investigación y Desarrollo and the Instituto Milenio de Oceanografía for the funding granted at pursuing this PhD work.

I would like to express my appreciation to the teachers of the Program for being considered sometimes beyond curricular matters, especially Dr. Ruben Escribano and Dr. Pamela Hidalgo who encouraged me and helped me to focus for my degree examination.

Finally, I would like to acknowledge the constant support, both in Concepción and at distance of my cohort colleagues and friends *Los Pichicuyanos*; as well as of Sonia Yáñez, Luis Pinto, Pedro Torres and Gisela Letelier.

This thesis work is dedicated to my late mother Corina Aragón, my father Manuel Pérez, my elder sister María José, my twin sister Corina; and to the family we formed with my partner Ignacio and our son Vicente.

Curriculum Vitae

Manuela Isabel Pérez Aragón

Born on March 5th, 1985, Chillán, Chile

Educational Background

2017 to date	PhD in Oceanography. University of Concepción. Concepción, Chile.
2014 – 2016	PhD in Marine Biology and Coastal Environments. Universidade Federal Fluminense, Niterói. Rio de Janeiro, Brazil.
2011 – 2012	Erasmus Mundus Master of Science in Marine Biodiversity and Conservation. University Pierre et Marie Curie (Paris 6, Sorbonne Université), Paris, France.
2010 – 2011	Erasmus Mundus Master of Science in Marine Biodiversity and Conservation. Bremen University. Bremen, Germany.
2003 – 2009	Marine Biology. University of Concepción. Concepción, Chile.
1st semester 2008	Marine Biology. University of Gothenburg. Gothenburg, Suecia.
1991 – 2002	Primary and secondary education. Colegio Padre Hurtado. Chillán, Chile.

Research Areas

Main	Biological Oceanography
Secondary	Plankton Ecology and Biogeography

Publications

2024 **Pérez-Aragón M.**, Escribano R., Rivera R, Hidalgo P. 2024 *Biodiversity patterns of epipelagic copepods in the South Pacific Ocean: Strengths and limitations of current data bases*. DOI: https://doi.org/10.1371/journal.pone.0306440.

2024 Rivera R., Escribano R., González C., **Pérez-Aragón M.**, 2023. Latitudinal diversity of planktonic copepods in the Eastern Pacific: overcoming sampling biases and predicting patterns. DOI: 10.3389/fevo.2024.1305916

2023 Rivera R., Escribano R., González C., **Pérez-Aragón M.**, 2023. *Modelling present and future distribution of plankton populations in a coastal upwelling zone: the copepod Calanus chilensis as a study case*. Scientific Reports 13: 3158. DOI: 10.1038/s41598-023-29541-9.

2011 **Pérez-Aragón M.**, Fernández C., Escribano R., 2011. *Nitrogen excretion by mesozooplankton in a coastal upwelling area: Seasonal trends and implications for biological production*. Journal of Experimental Marine Biology and Ecology 406 (1-2), 116-124. DOI: 10.1016/j.jembe.2011.05.029.

Work Experience

June 2023 – to date	Specialist in Oceanography and Specialized Text Editing. Dinámica Costera Consulting, Valparaíso, Chile.
April – August 2010	Technical Support for Fondecyt Project 1100358. Center for Oceanographic Research in the eastern South Pacific, University of Concepción, Chile.
February 2010	Technical Support for FIP Project 2009-39. Dichato Marine Biology Station, University of Concepción, Chile.

Grant s and Scholarships

2021 – 2023	Financial support granted by Instituto Milenio de Oceanografía, IMO-Chile.
2017 – 2021	Beca de Doctorado Nacional de la Comisión Nacional de Investigación Científica y Tecnológica (CONICYT), scholarship for pursuing doctoral studies in Chile.
2014 – 2016	Bolsa da Coordenação de Aperfeiçoamento de Pessoal de Nível Superior (CAPES), scholarship for pursuing doctoral studies in Brazil.
2010 – 2012	Erasmus Mundus Scholarship for the program Master of Science in Marine Biodiversity and Conservation (2 years), for pursuing master studies in Germany, Ireland and France.
2010	Financial support granted by the Oceanography Department of the Faculty of Natural and Oceanographic Sciences of the University of Concepción, to attend the X Austral Summer Institute (ASI X), University of Concepción, Chile. Course: *Food Web Structure and*

	Management of Biodiversity in Fjord Ecosystems. Professor: Stephen R. Wing, Department of Marine Sciences, University of Otago, New Zealand.
June 2009	Participation at the internship program Programa de Pasantía D+D para Profesional Joven of Programa COPAS Sur Austral, University of Concepción. Granted by Explora Project ED13/019: Tras la Huella del Carbono en fondos marinos de Bahías y Fiordos.
1st semester 2008	Linnaeus-Palme International Exchange Program Scholarship to study during a semester at the University of Gothenburg and its Marine Research Station (Kristineberg) in Fiskebäckskil, Sweden.

Participation in Courses and Conferences

December 2023	Attendance to workshops I, II y III of the online course *Gestión de riesgos vinculados al cambio climático en las zonas costeras de América Latina y el Caribe*. Modalidad virtual (30 horas). Instituto de Hidráulica Ambiental de la Universidad de Cantabria (IHCantabria), Centro de Formación de la Cooperación Española en La Antigua Guatemala y la Oficina de la Cooperación Española en Costa Rica (OCE) de la Agencia Española de Cooperación Internacional para el Desarrollo (AECID).
October 2023	Attendance to the course: *Delimitación de Humedales Urbanos*. Modalidad e-learning (6 horas), Academia de Formación Ambiental Adriana Hoffmann. Ministerio de Medio Ambiente, Chile.
July 2023	Attendance to the course: *Ley de Protección de Humedales Urbanos*. Modalidad e-learning (8 horas), Academia de Formación Ambiental Adriana Hoffmann. Ministerio de Medio Ambiente, Chile.

April 2023	Attendance to the course: *Diagnóstico y Reparación de Humedales Costeros*. Modalidad e-learning (16 horas), Academia de Formación Ambiental Adriana Hoffmann. Ministerio de Medio Ambiente, Chile.
January 2023	Expositor at the course: *Biodiversidad marina de Chile: un enfoque multidisciplinario para su estudio, gestión y conservación*. Escuela de Verano, Universidad de Concepción. Concepción, Chile.
May 2022	*XLI Congreso de Ciencias del Mar de la Sociedad Chilena de Ciencias del Mar*. Concepción, Chile. Oral exposition: *Patrones biogeográficos de copépodos epipelágicos del Océano Pacífico Sur.* **Manuela Pérez Aragón**, Reinaldo Rivera y Rubén Escribano. IMO, Universidad de Concepción, Chile.
	Coauthor in: *Latitudinal gradient of copepod diversity of the Eastern Pacific Ocean: searching for causal processes*. Reinaldo Rivera, **Manuela Pérez Aragón**, Rubén Escribano. IMO, Universidad de Concepción, Chile.
June 2021	Attendance to the workshop: *Escritura y Edición para la Productividad Científica*. Universidad de Concepción, Chile.
October 2018	Attendance to the course (30 h) *OBIS Training Course: OBIS Nodes Train the Trainers*, hosted by University of Concepción with the support of the Ocean Teacher Global Academy of the UNESCO/IOC/IODE. Concepción, Chile.
November 2012	Member of the organizing committee at the *4th Biennial Conference of the International Pacific Marine Educators Network (IPMEN)*. Conference theme: *"One Big Ocean, Many Dreams"*. Santiago and Caleta Tortel (Patagonia), Chile.
October 2010	*XXX Congreso de Ciencias del Mar de la Sociedad Chilena de Ciencias del Mar.* Concepción, Chile. Oral exposition: *Excreción de nitrógeno por parte del mesozooplankton en un sistema de surgencia costera: variación estacional e importancia de compuestos orgánicos.*

Manuela Pérez Aragón, Camila Fernández y Rubén Escribano. COPAS Center, Universidad de Concepción, Chile.

September 2009 — *VI Congreso Iberoamericano de Educación Ambiental*. San Clemente del Tuyú, Argentina. Poster: *Transferencia hacia la comunidad educativa del nuevo conocimiento aplicado a problemáticas ambientales marinas.* Luis A. Pinto, Verónica Toledo, Alicia Carvajal, Ruth Alarcón, Paula Quiroz y **Manuela Pérez Aragón**. COPAS Center, Universidad de Concepción, Chile.

May 2009 — XXIX Congreso de Ciencias del Mar de la Sociedad Chilena de Ciencias del Mar. Hualpén, Chile. Oral exposition: Efecto de la limitación de nutrientes y riesgo de depredación sobre la conducta natatoria de dos especies de dinoflagelados. **Manuela Pérez Aragón**, Erik Selander, Josefin Titelman, Rubén Escribano. Universidad de Gotemburgo, Suecia; Universidad de Concepción, Chile.

Outreach Experience

September 2023 — Preparation of educational material for the for the Linkage Project (Proyecto de Vinculación) VRIM2397: *Océano para la enseñanza interdisciplinaria de las ciencias y matemáticas*. Universidad de Concepción, Chile.

October 2020 — Series of Talks *Semana de la Ciencia y Tecnología* 2020. Liceo La Asunción, Talcahuano. Exposición oral: *El mundo de los microorganismos marinos: curiosidades del Plancton*. **Manuela Pérez Aragón**, UdeC.

April 2013 — Logistical support at Seminario Internacional: *Chile es Mar, Educando para la Conservación Marina*. Santiago, Chile.

June 2009	Participation in the Internship Program D+D para Profesional Joven del Programa COPAS Sur Austral, Universidad de Concepción, en el marco del Proyecto Explora ED13/019: Tras la Huella del Carbono en fondos marinos de Bahías y Fiordos.
May 2009	Second Ocean Education Fair. Hualpén, Chile. Stand: Pellet Watch: Monitoreo de la contaminación mundial usando Pellets de plástico varados en las playas. Manuela Pérez Aragón, Luis Pinto Álvarez, Hideshige Takada. Centro COPAS, Universidad de Concepción, Chile; Aquasendas; Tokyo University of Agriculture and Technology, Japón.

Table of Contents

RESUMEN i

ABSTRACT iv

1. INTRODUCTION 1

1.1. MARINE BIODIVERSITY AND ITS LARGE-SCALE PATTERNS 1

1.2. COPEPODA 2

1.3. SOUTH PACIFIC OCEAN 3

1.4. OCEANOGRAPHY AND CLIMATE VARIABILITY OF THE SOUTH PACIFIC BASIN 5

1.5. VERTICALLY LAYERED (3-D) OCEAN STUDIES AND DIVERSITY PATTERNS 9

1.6. TEMPERATURE IN THE OCEAN 13

1.7. STATE OF THE ART ON BIOGEOGRAPHY AND DIVERSITY PATTERNS OF PLANKTON 14

1.8. CONCEPTUAL FRAMEWORK, SCIENTIFIC QUESTIONS AND PROPOSED HYPOTHESIS 17

2. OBJECTIVES AND HYPOTHESIS 19

2.1 GENERAL OBJECTIVE 19

2.2 HYPOTHESIS 19

2.3. SPECIFIC OBJECTIVES 20

3. MATERIALS AND METHODS 21

3.1 STUDY AREA 21

3.1.1. South Pacific Ocean (Chapter 1) 21

3.1.2. The Humboldt Current System (Chapter 2) 21

3.2. ENVIRONMENTAL DATA 24

3.3. ECOLOGICAL DATA - OBIS 26

3.4 SPATIAL ANALYSES 28

4. RESULTS 30

4.1 Chapter 1: "Biodiversity patterns of epipelagic copepods in the South Pacific Ocean: Strengths and limitations of current data bases". Scientific article published in PLOS ONE, https://doi.org/10.1371/journal.pone.0306440. 30

Abstract 30

Resumen 31

4.2 Chapter 2: "The influence of environmental stability and upwelling variation on copepod diversity in the Humboldt Current System off Chile". Scientific manuscript submitted to "Frontiers in Ecology and Evolution" journal. 67

Abstract 67

Resumen 68

5. GENERAL DISCUSSION 136

6. CONCLUSIONS 138

7. REFERENCES 139

INDEX OF TABLES

TABLES FROM THE ARTICLE "BIODIVERSITY PATTERNS OF EPIPELAGIC COPEPODS IN THE SOUTH PACIFIC OCEAN: STRENGTHS AND LIMITATIONS OF CURRENT DATA BASES"

Table 1: Summary of spatial characteristics and cells sampled per each main surface current system of the SPO. CHC=Cape Horn Current; EAC=East Australian Current; HCS=Humboldt Current System; SEC=South Equatorial Current; SPSG=South Pacific Subtropical Gyre; WWD=West Wind Drift; n.a.=not applicable 47

Table 2: GAM+RAC models for species richness. Statistics acronyms are BIC = Bayesian information criterion, ΔBIC = delta BIC (i.e., the difference in BIC score between the best model and the model being compared). Predictors' acronyms are: Tmean = mean temperature, S = salinity, Chla = chlorophyll-a concentration, MLD = mixed layer depth, autocovariate = residuals autocovariate. The best model is highlighted in bold..... 47

Table 3: GAM+RAC models for species composition. Statistics acronyms are BIC = Bayesian information criterion, ΔBIC = delta BIC (i.e., the difference in BIC score between the best model and the model being compared). Predictors' acronyms are: Tmean = mean temperature, Tstab = temperature stability, S = salinity, Chla = chlorophyll-a concentration, DO2 = dissolved oxygen concentration, MLD = mixed layer depth, autocovariate = residuals autocovariate. The best model is highlighted in bold..... 48

TABLES FROM THE ARTICLE "THE INFLUENCE OF ENVIRONMENTAL STABILITY AND UPWELLING VARIATION ON COPEPOD DIVERSITY IN THE HUMBOLDT CURRENT SYSTEM OFF CHILE"

Table 1: Number of occurrence records at species level per strata and zone in the study area. N=north; S=south. 79

Table 2: Dominant species of the HCS off Chile, occurring between 0 and 500 m depth and between 20°-40°S and 70°-78°S..... 88

Table 3: Two-way PERMANOVA results for models of species richness, Shannon-Wiener index, Hulbert index, species composition and its components turnover and nestedness. Significant permutation p-values below the 0.05 level are highlighted in bold. 95

Table 4: LMM for species richness (SR), Shannon-Wiener index (SW), Hurlbert index (HI), species composition (SC) and its components turnover (TO) and nestedness (NE). Statistics acronyms are df=degrees of freedom, logLik=log-likelihood, AICc=corrected Akaike information criterion, ΔAICc=delta AICc, R^2m=marginal R^2, R^2c=conditional R^2. Predictors' acronyms are: T_{mean}=mean temperature, S_{mean}=mean salinity, Chla=chlorophyll-a concentration, O_2=dissolved oxygen concentration, EKE=Eddy Kinetic Energy, T_{stab}=temperature stability, S_{stab}=salinity stability. The best fitting models are highlighted in bold. 99

INDEX OF FIGURES

Figure 1: South Pacific Ocean extent (blue area). Map projection is WGS 84 (EPSG 4326) 4

Figure 2: Map illustrating the Humboldt Current System extension off Chile (yellow band). Map projection is WGS 84 (EPSG 4326)..... 23

FIGURES FROM THE ARTICLE "BIODIVERSITY PATTERNS OF EPIPELAGIC COPEPODS IN THE SOUTH PACIFIC OCEAN: STRENGTHS AND LIMITATIONS OF CURRENT DATA BASES"

Figure 1: The South Pacific Ocean basin (red dashed area), its sampling coverage with georeferenced locations of the 393 cells (1° x 1°) which were generated (blue squares) from data spanning between 1993-2019. The major near-surface currents shown for the whole basin were obtained from Harvard Dataverse (http://doi:10.7910/dvn/tkgo2z). CHC=Cape Horn Current; EAC= East Australian Current; HCS=Humboldt Current System; SEC=South Equatorial Current; SPSG= South Pacific Subtropical Gyre; WWD=West Wind Drift; ACC= Antarctic Circumpolar Current. Map projection is WGS 84/PDC Mercator (EPSG 3832). 36

Figure 2: Richness patterns of Copepoda in the 0-200 m layer of the western and eastern side of the SPO for the period 1993-2019 based on species occurrence data obtained from OBIS portal. (a) Spatial distribution of alpha diversity considering the complete data cell with the curated data (i.e., 377 cells). (b) Inverse distance weighted (IDW) analysis for alpha diversity using cells with >10 species (i.e., only 77 cells from the total of 377 were selected). (c) Kriging interpolation for alpha diversity using cells with >10 species (i.e., only 77 cells from the total of 377 were selected). (d) Kriging interpolation for family richness. Transparent squares are the 1° sampled cells used for interpolation, whereas the grey dotted line delimits the South Pacific Ocean. Map projection is WGS 84/PDC Mercator (EPSG 3832) 41

Figure 3: Shannon-Wiener index of Copepoda in the western and eastern sides of the South Pacific Ocean. Transparent squares are the 1° sampled cells used for Kriging interpolation, whereas the grey dotted line delimits the South Pacific Ocean. *Estimates based on available data at species level. Map projection is WGS 84/PDC Mercator (EPSG 3832) 42

Figure 4: Getis-Ord G statistic of alpha diversity of Copepoda at the western and eastern sides of the SPO based on species occurrence data obtained from OBIS portal for the period 1993-2019. High and low values of richness are displayed in red and blue color, respectively. Color intensity denotes clusters' significance. Transparent squares are the 1° sampled cells used for Kriging interpolation, whereas the grey dotted line delimits the South Pacific Ocean. Map projection is WGS 84/PDC Mercator (EPSG 3832) 43

Figure 5: (a) Sample-size-based rarefaction (solid line segments) and extrapolation (dotted line segments) sampling curves for species richness with 95% confidence intervals (shaded areas) for Copepoda in the main surface current systems of the SPO. The symbols of each curve represent the reference samples. CHC=Cape Horn Current; EAC=East Australian Current; HCS=Humboldt Current System; SEC=South Equatorial Current; SPSG=South Pacific Subtropical Gyre; WWD=West Wind Drift. (b) Map of each main surface current system of the SPO 44

Figure 6: (a) Mean species composition and its components (b) turnover and (c) nestedness for Copepoda in the 0-200 m layer of the western and eastern sides of the SPO. Transparent squares are the 1° sampled cells used for Kriging interpolation, whereas the grey dotted line delimits the South Pacific Ocean. Map projection is WGS 84/PDC Mercator (EPSG 3832) 45

Figure 7: Predicted spatial variation in species composition of Copepoda at the western and eastern sides of the SPO based on a principal component analysis (PCA) of the Generalized Dissimilarity Modelling (GDM)-transformed environmental predictors. Colors represent gradients in species composition. Locations with similar colors indicate more similar expected composition. Dashed line at both sides of the antemeridian (180° longitude) delimits the South Pacific Ocean. Map projection is WGS 84/PDC Mercator (EPSG 3832) 46

FIGURES FROM THE ARTICLE "THE INFLUENCE OF ENVIRONMENTAL STABILITY AND UPWELLING VARIATION ON COPEPOD DIVERSITY IN THE HUMBOLDT CURRENT SYSTEM OFF CHILE"

Figure 1: Study area at the Humboldt Current System (HCS, represented by the sand color dotted area) delimiting the 2x2 degrees grid cells forming the total grid. Blue grids represent the sampled ones, whereas the red dots represent the sampling stations from where data was

obtained. The black dashed line at 30°S separates the north zone (NZ) and the south zone (SZ) of the HCS study area. Map projection is WGS 84 (EPSG 4326). 77

Figure 2: Alongshore surface wind speed (in m s^{-1}) from ERA5 reanalysis over the 1995-2011 period (a) Hovmöller diagram of the wind speed monthly climatology (b) latitudinal variation of the monthly wind standard deviation. 91

Figure 3: Mean Eddy Kinetic Energy (EKE in $cm^2\ s^{-2}$) computed from the daily outputs of the Glorys12 reanalysis over the 1995-2011 period. (a) surface EKE (b) vertical profile of the mean EKE averaged over the 20-30°S region (blue line) and the 30-40°S region (red line) (c) latitudinal variation of the mean EKE averaged from the coast to 78 °W and over 1° latitudinal bins, at different depths (0, 50, 100, 200, 300, 400 and 500 m)..... 93

Figure 4: Diversity indices for the study area, separated by zone (NZ=north zone; SZ=south zone) and bathymetric range..... 96

Figure 5: Getis-Ord Gi* statistic of species richness of Copepoda at each depth range and zone of the study area. A positive value for a standardized Z score suggests a hot spot, whereas a negative value indicates a cold spot..... 97

INDEX OF ANNEXES – SUPPLEMENTAL MATERIAL

ANNEX 1: SUPPLEMENTAL MATERIAL FOR THE ARTICLE "BIODIVERSITY PATTERNS OF EPIPELAGIC COPEPODS IN THE SOUTH PACIFIC OCEAN: STRENGTHS AND LIMITATIONS OF CURRENT DATA BASES"

Figure S1: Kriging interpolation analysis done for the western and eastern side of the SPO with 394 cells accounting for number of genera. Transparent squares are the 1° sampled cells used for Kriging interpolation, whereas the grey dotted line delimits the South Pacific Ocean. Map projection is WGS 84/PDC Mercator (EPSG 3832). 61

Figure S2: Maximum height of the spline function (hence the maximum value of the transformed predictors), indicating the stronger predictors of the observed dissimilarities for the Generalized Dissimilarity Modelling (GDM)-based spatial analysis. Their acronyms are: s = salinity, o2 = dissolved oxygen concentration, tmean = mean temperature, chla = chlorophyll-a concentration, mld = mixed layer depth, tstab= temperature stability, tsd = standard deviation of temperature. The spatial layers were generated and plotted with the predictors with heights over zero (i.e., s, o2, tmean and chla). 62

Figure S3: Spearman correlation matrices of environmental variables used in GAM models for (a) alfa diversity and (b) beta diversity. Positive correlations are displayed in red and negative correlations in blue color. Color intensity is proportional to the correlation coefficients. In the right side of the correlogram, the legend color shows the correlation

coefficients and the corresponding colors. Their acronyms are: Tmean = mean temperature, Tstab= temperature stability, Tsd = standard deviation of temperature, S = salinity, Chla = chlorophyll-a concentration, O2 = dissolved oxygen concentration, MLD = mixed layer depth. 63

Figure S4: Correlation between observed and predicted species richness. Pearson's r coefficient: 0.77 (p-value<0.01). Negative residuals (below the reference line) indicate knowledge shortfalls, whereas positive residuals (above the reference line) indicate underestimated species richness. 63

Figure S5: Correlation between observed and predicted species composition. Pearson's r coefficient: 0.84 (p-value<0.01). Negative residuals (below the reference line) indicate knowledge shortfalls, whereas positive residuals (above the reference line) indicate underestimated species composition. 64

Figure S6: Redundancy index obtained for the western and eastern side of the SPO. Values close to 1 indicate good sampling, whereas values close to 0 indicate poor sampling. Transparent squares are the 1° sampled cells used for Kriging interpolation, whereas the grey dotted line delimits the South Pacific Ocean. Map projection is WGS 84/PDC Mercator (EPSG 3832)..... 64

Table S1: Dominant copepod species in terms of occurrence for the main surface current systems of the South Pacific Ocean. CHC=Cape Horn Current; EAC=East Australian Current; HCS=Humboldt Current System; SEC=South Equatorial Current; SPSG=South Pacific Subtropical Gyre; WWD=West Wind Drift. 65

Table S2: Dominant copepod species of the South Pacific Ocean in terms of occurrence for all ranges values of beta diversity and its components turnover and nestedness. 66

Table S3: Analysis of map overlay and Pearson correlation between the richness of species, genera and families. 66

ANNEX 2: SUPPLEMENTAL MATERIAL FOR THE ARTICLE "THE INFLUENCE OF ENVIRONMENTAL STABILITY AND UPWELLING VARIATION ON COPEPOD DIVERSITY IN THE HUMBOLDT CURRENT SYSTEM OFF CHILE"

Figure S1: Spearman correlation matrix of environmental variables used in the Linear Mixed Models (LMM). Positive and negative correlations are displayed in blue and red color, respectively. Color intensity is proportional to the correlation coefficients, and the non-significant correlations are crossed out. The acronyms are: Temperature=mean temperature, Stab_T=temperature stability, Salinity=mean salinity, Stab_S=salinity stability

Chla=chlorophyll-a concentration, O2=dissolved oxygen concentration, POC=particulate organic carbon, pH=potential of hydrogen, EKE=Eddy Kinetic Energy. 126

Figure S2: Residual diagnosis inferred from a linear model (LM, left panels) and a linear mixed model (LMM, right panels) for (a) species richness, (b) Shannon-Wiener index, (c) Hurlbert index, (d) β-diversity and its additive components (e) turnover and (f) nestedness. Each panel show a QQ plot (quantile-quantile plot) between observed and expected values, and the variation of their residuals. Kolmogorov-Smirnov (KS) test p>0.05. 127

Figure S3: GLORYS12 EKE averaged between the coast and 78°W. 128

Table S1: Summary of common and exclusive species found in each zone and stratum of the study area. 129

Table S2: Coefficients obtained by linear mixed models used to evaluate the best predictors for species richness, Shannon-Wiener index, Hurlbert index, beta diversity (species composition) and its additive components turnover and nestedness. Predictors' acronyms are: Chla=chlorophyll-a concentration, EKE=Eddy Kinetic Energy, O_2=dissolved oxygen concentration, S=mean salinity, S_{stab}=salinity stability, T_{stab} = temperature stability, T=mean temperature. 133

RESUMEN

El zooplancton es un componente clave del ecosistema marino, principalmente por su papel como parte de la base de la vida en el océano, actuando como enlace trófico entre los productores primarios y otros niveles tróficos superiores, así como un componente del anillo microbiano y ejerciendo una función esencial en los ciclos biogeoquímicos. Además, debido a sus ciclos de vida relativamente cortos, responde rápidamente a las variaciones oceanográficas y ambientales asociadas con el cambio climático-oceanográfico. En general, el zooplancton ha sido ampliamente estudiado, especialmente los copépodos, que muestran una fuerte dependencia de sus tasas vitales con la temperatura y otros factores ambientales relacionados con el clima. En cuanto al impacto ambiental sobre el zooplancton, en el Océano Pacífico Sur existe una amplia variabilidad de la productividad superficial-oceánica y los regímenes físico-oceanográficos que dan forma a diferentes ambientes y condiciones tróficas dentro del océano costero y abierto; por lo tanto, estudiar los forzantes de la diversidad de especies de copépodos en esta región es útil para dilucidar cómo el zooplancton puede responder a un océano cambiante. El presente trabajo de tesis evaluó la diversidad del zooplancton en relación con la variación oceanográfica a gran escala en el Pacífico Sur.

En el primer capítulo, se utilizó una base de datos de 27 años (1993-2019) de ocurrencia de especies de copépodos planctónicos en el Océano Pacífico Sur, junto con variables oceanográficas asociadas, para evaluar los patrones espaciales de biodiversidad en los 200 m superiores del océano. El objetivo de este estudio fue identificar las regiones ecológicas y los predictores ambientales que explican dichos patrones. Se encontró que los puntos calientes y fríos de diversidad y los conjuntos de especies distintivos se encuentran

vinculados a las principales corrientes oceánicas y grandes regiones sobre la cuenca, con una creciente riqueza de especies en las áreas subtropicales de los lados este y oeste del Pacífico Sur. Los modelos espaciales señalan que los mejores predictores ambientales que contribuyen a la varianza de la diversidad y la composición de especies son la temperatura, la salinidad, la concentración de clorofila-a, la concentración de oxígeno y la autocorrelación residual. No obstante, se encontró que los patrones espaciales observados y los efectos ambientales derivados estaban fuertemente influenciados por la cobertura de muestreo en el espacio y el tiempo, lo que revela una cuenca altamente sub-muestreada.

En el segundo capítulo, demostramos la hipótesis de que la estabilidad ambiental es el mecanismo modulador clave de los patrones de diversidad de copépodos en el Sistema de la Corriente de Humboldt (SCH), utilizando una base de datos de 17 años (1995-2011) de ocurrencia de especies y datos ambientales en los 500 m superiores (divididos en cinco estratos verticales) para la zona de surgencia frente a Chile, distinguiendo dos regiones (norte y sur) con diferentes regímenes estacionales de surgencia impulsada por el viento. Estimamos índices de diversidad de copépodos y su distribución, segregados por regiones y estratos de profundidad. Los índices fueron asociados con variables oceanográficas forzadas por la intensidad de surgencia, junto con una estimación de la energía cinética turbulenta (EKE), como un proxy de la estabilidad ambiental. En la comunidad, encontramos 18 especies dominantes ampliamente distribuidas en el área de estudio. Algunas corresponden a especies exclusivas para el estrato de profundidad superior con diferencias en el número de especies exclusivas por región y profundidad. Los modelos lineales mixtos revelaron que los índices de diversidad diferían significativamente entre regiones y estratos, y su varianza se explicaba principalmente por la temperatura, la salinidad, la concentración de oxígeno, la estabilidad

de la temperatura y la energía cinética turbulenta (EKE). Tanto la estabilidad de la temperatura como la EKE fueron los predictores más eficientes de la diversidad de copépodos, lo que sugiere que la estabilidad climática-oceanográfica, forzada por la intensidad de surgencia, es el impulsor clave para promover y mantener la diversidad de copépodos en el SCH.

La tesis en su conjunto entrega resultados que permiten apoyar la hipótesis principal, concluyendo que la estructuración de comunidades de copépodos a una escala espacial extensa en el Pacífico Sur está fuertemente asociada a una zonación significativa sobre los ejes horizontales y verticales en los cuales la estabilidad (varianza) de parámetros ambientales, tales como la temperatura y energía cinética aparecen como factores claves en la modulación de estos patrones biogeográficos y de diversidad.

ABSTRACT

Zooplankton are a key component of the marine ecosystem, mainly due to their role as part of the foundation of life in the ocean acting as the trophic link between primary producers and the other upper-trophic levels, as well as a component of the microbial loop and their function in biogeochemical cycles. Moreover, due to their relatively short life cycles, they are known to rapidly respond to oceanographic and environmental variations associated with climate-oceanographic change. Zooplankton representatives have been widely studied, especially copepods, which exhibit a strong dependence of their vital rates with temperature and other climate-related environmental factors. Regarding environmental impact on zooplankton, in the South Pacific Ocean there is a broad range of surface-ocean productivity and physical-oceanographic regimes that shape different environments and trophic conditions within the coastal and open ocean; therefore, to study the drivers of their species diversity in these areas would be useful to elucidate how zooplankton may respond to a changing ocean. The present thesis work focused on zooplankton diversity in relation to large-scale oceanographic variation in the South Pacific while considering the vertical axis as well.

In the first chapter, a 27-years (1993–2019) database on species occurrence of planktonic copepods of the South Pacific Ocean was used, along with associated oceanographic variables, to examine their spatial patterns of biodiversity in the upper 200 m of the ocean. The aim of this study was to identify ecological regions and the environmental predictors explaining such patterns. It was found that hot and cold spots of diversity, and distinctive species assemblages were linked to major ocean currents and large regions over the basin,

with increasing species richness over the subtropical areas on the East and West sides of the South Pacific. While applying the spatial models, it was shown that the best environmental predictors for diversity and species composition were temperature, salinity, chlorophyll-a concentration, oxygen concentration, and the residual autocorrelation. Nonetheless, the observed spatial patterns and derived environmental effects were found to be strongly influenced by sampling coverage over space and time, revealing a highly under-sampled basin.

In the second chapter, we tested the hypothesis that environmental stability is the key modulating mechanism of copepod diversity patterns in the Humboldt Current System (HCS), by using a 17-years (1995-2011) database on species occurrence of copepods along with environmental data for the upper 500 m of the ocean (divided into five vertical strata) for the upwelling zone off Chile, distinguishing two regions (northern and southern) having different seasonal regimes of wind-driven upwelling. We estimated indices for copepod diversity and their distribution, segregated by regions and depth strata. The indices were then associated with oceanographic variables forced by upwelling intensity, along with an estimate of eddy kinetic energy (EKE), as a proxy of environmental stability. From the entire community, we found 18 dominant species widely distributed in the study area. Some were exclusive species for the upper depth stratum with differences in the number of exclusive species per region and depth. From Linear Mixed Models we found that the diversity indices significantly differed between regions and strata, and their variance was mainly explained by temperature, salinity, oxygen concentration, temperature stability, and eddy kinetic energy (EKE). Both temperature stability and EKE were the best predictors of copepods diversity,

suggesting that climate-oceanographic stability, forced by upwelling intensity, is the key driver for promoting and maintaining copepod diversity in the HCS.

The thesis provides findings that support the main hypothesis, concluding that the structuring of copepod communities on a large spatial scale in the South Pacific is strongly associated with a significant zonation on the horizontal and vertical axes in which the stability (variance) of environmental parameters, such as temperature and kinetic energy appear as key factors in the modulation of these biogeographic and diversity patterns.

1. INTRODUCTION

1.1. MARINE BIODIVERSITY AND ITS LARGE-SCALE PATTERNS

Biodiversity and its components' measurement at the ocean requires high exploration effort, moreover in open and deep sea (Costello and Chaudhary 2017). However, due to the growth of marine sciences and the development of new technologies, it has been documented that in the past decade the rate of discovery of marine species has been the highest than in any previous one (Appeltans et al. 2012). Globally, only 16 (Costello, Wilson, and Houlding 2012) to 25 (Mora et al. 2011) percent of named eukaryotic species are marine and despite it has been estimated that 19–23 (Costello et al. 2012) to 91 (Mora et al. 2011) percent of marine species are still awaiting description, it has been suggested that marine species will not increase their proportion of global species richness (Costello and Chaudhary 2017) due to the relatively less variable environment that the ocean displays (with fewer physical niches that isolate populations) and organisms' greater dispersal abilities (Costello et al., 2012).

Marine biodiversity spatial patterns and the factors related to them are relatively well studied, although there is little consensus about what factors or processes are the drivers of these patterns (Currie et al., 1999). Within the ocean, there are undersampled areas due to spatial biases in the distribution of sampling locations (Dornelas et al., 2018) that may affect sampling as well as taxonomic effort, producing a skew on the apparent latitudinal gradient (and thus vertical gradient) in marine species richness.

1.2. COPEPODA

Zooplankton are a key component of the marine ecosystem: they are the most widespread form of animal life on Earth, with the longest history of evolutionary continuity (Verity and Smetacek, 1996); and they are part of the foundation of life in the ocean acting as the trophic link between primary producers and the other upper-trophic levels (Lombard et al., 2019), as well as microbial loop (Valdés et al., 2018) and biogeochemical cycles (Hernández-León et al., 2019; Pérez-Aragón et al., 2011). Moreover, due to their relatively short life cycles (from one week to a few months), they are known to rapidly respond to oceanographic and environmental variations associated with climate change, such as fluctuations on temperature (Escribano et al., 2014), oxygenation (Ruz et al., 2018), acidification (Lewis et al., 2013; Thor and Dupont, 2015), stratification (Peterson and Bellantoni, 1987; Williams et al., 1994), primary production (Berline et al., 2012; Kiørbe and Nielsen, 1994), upwelling (Escribano et al., 2014; Medellín-Mora et al., 2016; Pino-Pinuer et al., 2014), circulation (Berline et al., 2012) and advection (Frederick et al., 2018).

Despite there are no global standard methodologies for their quantification (Lombard et al., 2019), due to their role as a key component of the marine ecosystem, zooplankton representatives have been widely studied, specially copepods. This taxon is among the ones having the biggest number of accepted species described and documented at the World Register of Marine Species (WoRMS) (Costello and Chaudhary, 2017), so that a thorough data base on their distribution (horizontal and vertical) is available for the South Pacific Ocean (OBIS, 2024). Copepods also exhibit a strong dependence in their vital rates and most of their ecological responses are related with temperature (Berline et al., 2012). Therefore,

within this context, to study the drivers of their species richness would be useful to elucidate how zooplankton may respond to a changing environment.

1.3. SOUTH PACIFIC OCEAN

The South Pacific Ocean represents the largest, but least known marine ecosystem of the world ocean. It has the greatest surface and seabed area, as well as the greatest volume, with a mean depth of 3993 m (Costello et al., 2010). It stretches from the Equator, including those islands of the Gilbert and Galápagos Groups which lie to the northward thereof, until the parallel of 60°S, and between South America and the northeastern limit of the East Indian Archipelago (from New Guinea to the Equator), along the southern, eastern and northern limits of the Bismarck and Solomon Seas, the southeastern and northeastern limits of the Coral Sea and the southern, eastern and northern limits of the Tasman Sea, going down the meridian of 146°55'E starting at the South East Cape, the southern point of Tasmania, until the parallel of 60°S (International Hydrographic Organization, 1953, 2002) (Figure 1). It has a highly varied topography that consists of oceanic ridges, guyots, trenches, and seamount chains that are formed by hotspot volcanoes under the Earth's surface. In the eastern side, the topography off western South America is complex, with a variable relief that shapes a narrow shelf (i.e., depth down to 200 m) off Colombia and Ecuador, which widens up to 1000 Km off Peru, and narrowing again towards northern and central Chile, where in some points it is virtually absent, dropping to a depth of 800 m at ca. 8 Km offshore at 30°S. Off Concepción (36°S), the shelf expands to widths between 20 and 60 Km; and, towards the southern part of Chile (from 42°S), the shelf becomes hundreds of Km wide, covered with scattered islands offshore the fjords (Strub et al., 1998). The offshore regions of the South Pacific Ocean are

divided into the Peru Basin between 0° and 15°S, and the Chile Basin south of 15°S, with the Carnegie Ridge leaving the coast near the Equator and stretching west to the Galápagos Islands that separates the Panama and Peru basins, and the Nazca ridge running southwest from the coast around 15°S separating the Peru and Chile basins (Strub et al., 1998).

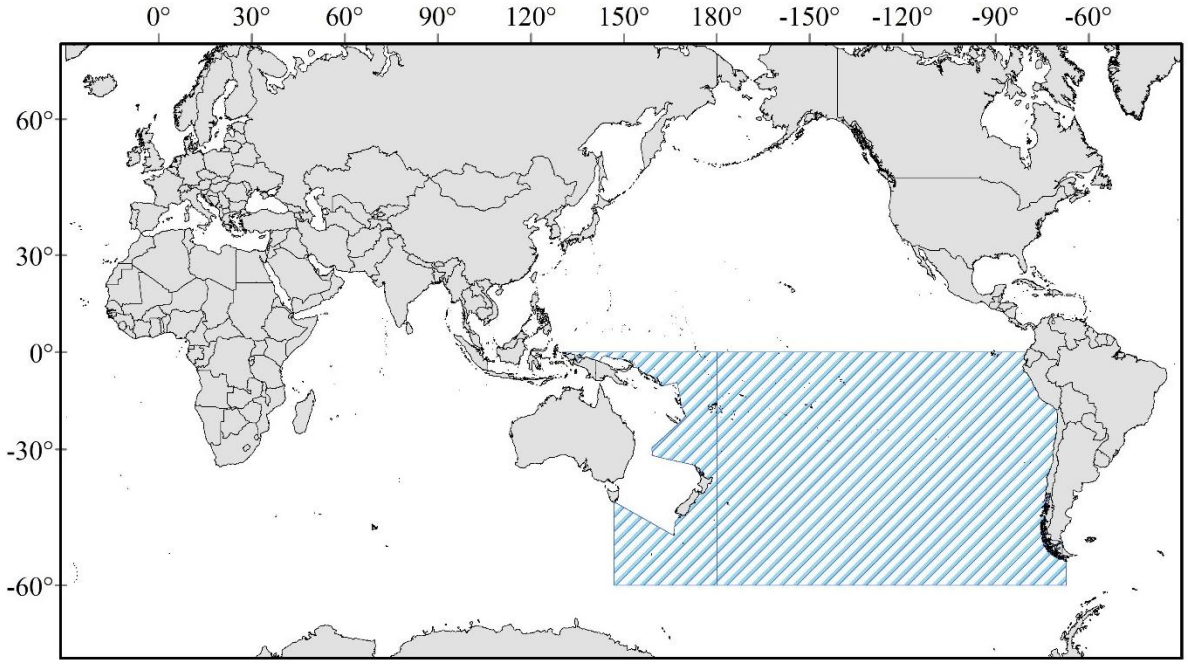

Figure 1: South Pacific Ocean extent (blue area). Map projection is WGS 84 (EPSG 4326).

The topography at the southwest Pacific Ocean boundary is very complex and has a major influence in the regional flow patterns (Ridgway and Dunn, 2003). The Tasman basin region is bounded by the Australian continent in the west, New Zealand at its southeast corner and the island archipelago of New Caledonia, Vanuatu and Fiji in the northeast (Ridgway and

Dunn, 2003). The bathymetry is dominated by several ridges that radiate northwards from the New Zealand continental land mass, with the largest of these ridges (Lord Howe Rise) diagonally bisecting the basin from the southeast to northwest reaching depths <1000 m along its crest (Ridgway and Dunn, 2003). The Norfolk Ridge stretches almost meridionally southward from New Caledonia, and is a sharper feature even though far more irregular (Ridgway and Dunn, 2003). The eastern entrance to the region, from 15° to 35°S, is protected by another double ridge system which lies immediately adjacent to the sheer wall of the Tonga Trench (Ridgway and Dunn, 2003). On the western boundary, a wide and deep abyssal plain narrows towards the north and pinching off at about 25°S (Ridgway and Dunn, 2003).

1.4. OCEANOGRAPHY AND CLIMATE VARIABILITY OF THE SOUTH PACIFIC BASIN

The general circulation in the South Pacific Ocean is dominated by the subtropical gyre, which manifests itself through elevated mean dynamic topography at its center (Schneider et al., 2007) (near 15° to 20°S; Reid, 1986). The westward flow of the South Pacific Subtropical Gyre, namely South Equatorial Current, terminates at its western boundary entering the Coral Sea as a series of jets between the Solomon Islands, Vanuatu and New Caledonia. At the east of the Great Barrier Reef between 15° and 22°S (Qu and Lindstrom, 2011), the South Equatorial Current bifurcates to form the North Queensland Current and the Gulf of Papua Current, as well as the southerly East Australian Current (Ganachaud et al., 2014), that is the predominant dynamical feature in the region (Ridgway and Dunn, 2003). To the south, the East Australian Current strengthens as it flows along the coast of Australia (Ganachaud et al., 2014). Southward of ~33°S, it starts to separate into filaments, forming the northwestward

South Pacific Subtropical Counter Current, the East Australian Current extension and the Tasman Front (Ganachaud et al., 2014) that consists of bands of zonal eastward outflow that occur as a series of current jets, where each follows different paths across the basin, with its main component occurring between 33° and 35°S (Ridgway and Dunn, 2003). The extension of the East Australian Current flowing towards the east along the Tasman Front seems to be a large component of subtropical water feeding into the South Pacific Subtropical Gyre circulation through the South Pacific Current, although it is more distinguishable starting out east of New Zealand as a combination of it with a narrow band of subtropical water flowing around the southern end of South Island that then flows around the northern end of North Island as the East Auckland Current and then southward as East Cape Current (Stramma et al., 1995). The South Pacific Current streams along the Sub-Tropical Front, associated to the Antarctic Circumpolar Current (West Wind Drift), that intersects the South American continent at ~45°S, where the Humboldt Current System domain starts (Montecino and Lange, 2009).

The Humboldt Current System is the largest of the four main Eastern Boundary Upwelling Systems (the other three are embedded in the California, Canary, and Benguela Currents) (García-Reyes et al., 2015). It is shaped by a broad equatorward eastern boundary current (Schneider et al., 2007) characterized by a flow of fresh, cooler Sub-Antarctic Surface Water along the eastern rim of the subtropical gyre (Montecino and Lange, 2009). Its domain extends from southern Chile (~45°S) to northern Peru and Ecuador (~4°S), where cool upwelled waters collide with warm tropical waters forming the Equatorial Front (Montecino and Lange 2009). It encompasses three well-defined upwelling subsystems: (1) a productive seasonal upwelling system in central-southern Chile; (2) a lower productivity and rather large

‘‘upwelling shadow” in northern Chile and southern Peru; and (3) the highly productive year-round Peru upwelling system (Montecino and Lange 2009). How these subsystems are inter-connected and/or dependent on each other remains uncertain (Montecino and Lange 2009).

In general, the high levels of productivity in the Eastern Boundary Upwelling Systems result from large-scale atmospheric pressure systems that favor along-shore equatorward winds, generating a wind driven flow that in combination with the Coriolis effect advects surface water offshore. As the water that replaces the offshore drift cannot be supplied by horizontal flow because of the coastal boundary, it is upwelled instead from the deeper layers, thus causing deeper, cooler, nutrient rich water with low pH, high CO_2 and low oxygen concentrations to reach into the coastal photic zone (Mann and Lazier 2013a), where they boost primary production (Anabalón et al. 2016) and efficiently convert it into secondary production and later into fish biomass (Strub et al. 1998).

In terms of atmospheric forcing, the South Pacific Subtropical Anticyclone or the South Pacific High, which spins counter-clockwise, is the most influential off the west coast of South America (Schneider et al. 2007; Strub et al. 1998) as well as being the dominant forcing of the subtropical gyre (Ancapichun and Garcés-Vargas 2015). However, it presents seasonal variation, abiding at its northern position (26°S, 86°W) during the late austral fall and winter, when it also is closer to the South American continent and its intensity is weaker; whereas, during austral spring and summer the South Pacific High moves southwest (37°S, 108 °W) and shows its maximum intensity (Ancapichun and Garcés-Vargas 2015). The latter (former) conditions generate stronger (weaker) Equatorward winds that favor (disfavor) coastal upwelling offshore central-south Chile (Montecino and Lange 2009). Also, a more poleward location of the South Pacific High during winter have caused more summer-like

hydrographic conditions on the continental shelf offshore central Chile, generating changes in the plankton community (Jacob et al. 2018; Schneider et al. 2017).

Subtropical ocean gyres are oligotrophic areas characterized by very low levels of nutrients in a stratified upper water column (euphotic zone, mixed layer), low biomass and low primary production. The mean sedimentation rates within the South Pacific Subtropical Gyre are among the lowest that occur at the Earth's surface (D'Hondt et al. 2009). It has also been on debate whether or not these areas may be subsided by westward mesoscale eddies (von Dassow and Collado Fabbri 2014), that are involved in the offshore advection of nutrient-rich waters and plankton from the coastal upwelling zone off Chile, potentially enhancing cross-shelf exchanges and sustaining phytoplankton growth in the slope area (Morales et al., 2017), that may explain the higher mean sedimentation rates found at the eastern-most sites of the gyre (D'Hondt et al., 2009).The South Pacific Subtropical Gyre is dominated by heterotrophic bacterioplankton (up to 83 percent of total particulate organic carbon), whereas its phototrophic biomass is dominated by picoplankton (size fraction between 0,2 and 3 µm diameter), that contributes to the 53 percent of total phytoplankton biomass (von Dassow and Collado Fabbri, 2014). Throughout the gyre between 0–50 m depths, heterotrophs account for up to 75–80 percent of all eukaryotic cells, whereas in deeper euphotic zone communities, where photosynthetic cells dominate, mixotrophs appear to be important or dominant among chlorophyll-containing cells; leading to a vertical biomass distribution consisting of low concentrations near the surface with very deep maxima, except in the case of bacterioplankton and particulate organic matter, that exhibit more homogeneous vertical distributions in the surface, decreasing below the euphotic zone (von Dassow and Collado Fabbri, 2014). The deep chlorophyll maximum (DCM) is a permanent feature in the sub-

tropical oligotrophic basins and a typical occurrence in temperate waters after spring bloom conditions (Mann and Lazier, 2013b), and for this system it has been located mostly below 100 m and centered at ~150 m depth (von Dassow and Collado Fabbri, 2014).

Eddies are of importance when studying ocean circulation and dynamics as they determine vertical mixing in the ocean (Ivanov and Ginzburg, 2002), nutrient or food retention (Chang et al., 2018) and thus may have an effect on different organisms. They are classified by scale, between synoptic, mesoscale and submesoscale eddies, with diameters of hundreds of kilometers, between 20–100 kilometers and few hundreds of meters to tens of kilometers, respectively (Kostianoy et al., 2018).These structures may be of importance for zooplankton distribution, as they can concentrate in cyclonic cores showing significantly higher populations than surrounding waters, potentially having implications for the biological pump as well as biogeochemical fluxes since zooplankton have high feeding rates in eddy cores or high-turbulence areas due to food enrichment; therefore increasing their growth (Chang et al., 2018; Saito et al., 2014), fecal production (Goldthwait and Steinberg, 2008; Riquelme-Bugueño et al., 2015) and lipid accumulation (Saito et al., 2014), which thus enhances their survival rates and may favor their ampler distribution from surface into deeper waters (Zhong et al., 2017) as well as from coastal into offshore waters (Haury et al., 1986).

1.5. VERTICALLY LAYERED (3-D) OCEAN STUDIES AND DIVERSITY PATTERNS

The ocean has been structured vertically in terms of density and depth. Regarding density, it has been divided, excluding poles, into three horizontal depth zones: mixed layer, pycnocline and deep layer. Regarding depth, the ocean has been divided into five main zones or layers,

namely epipelagic, mesopelagic, bathypelagic, abyssopelagic and hadalpelagic zones, that are within the depth ranges of 200–0 m, 1000–200 m, 4000–1000 m, 6000–4000 m and below 6000 m, respectively.

Most of the biogenic material exported from the euphotic zone and ocean margins (Bauer and Druffel, 1998) is remineralized within the mesopelagic zone (Jahnke et al., 1990; Jahnke and Jahnke, 2000). Nutrient supply (Pichevin et al., 2009) as well as the structure of the metazoan and planktonic food webs exert control on the vertical transport (Angel, 1982), cycling (Roman and McCarthy, 2010) and composition of the particulate (Angel, 1982) and dissolved (Pérez-Aragón et al., 2011) organic matter, as well as its coupling with microbes (Valdés et al., 2018; Valdés et al., 2017). At the bathypelagic zone, which includes all ocean depths below 1000 m, residence time is on the centennial (Rowe et al., 1991; Stuiver et al., 1983) scale, thus being slowly ventilated and circulated (van Aken, 2007) as well as presenting biogeochemical signals that suggest the lateral transport of organic material originated in ocean margins (Bauer and Druffel, 1998; Boetius et al., 1996; R A Jahnke et al., 1990), hence integrating unique metabolisms (Tian et al., 2018) over a large temporal and spatial range. The deep sea is an environment defined by depths beyond the continental shelf (Roberto Danovaro et al., 2014) (ca. 200 m) that comprises most of the ocean, with only 11% of the its area and <1% of its volume being shallower than 1000 m depth (Costello et al., 2010). More specifically, 75% of the area and 90% of the volume of the ocean is between 3000 and 6000 m (Costello et al., 2010). Thus, deep oceans are ecosystems that, due to its inaccessibility, have relatively few documentations in relation to their biology and ecology, as well as the role they may play on the cycling of biogeochemical compounds. This environment is considered to exhibit extreme conditions to marine life, as the organisms

inhabiting it are surrendered to pressure, low temperature and no light (thus no diel nor seasonal rhythms) plus a slow rain of sinking particles (Havermans and Smetacek, 2018). Nowadays, a much greater degree of complexity and variation of this ecosystem has been documented (Danovaro et al., 2002; Danovaro et al., 2008, 2016; Gambi et al., 2003; Thatje et al., 2010; Thatje and Robinson, 2011), highlighting the necessity of organizing this relatively new knowledge within a framework of more dynamic interactions.

Excepting hydrostatic pressure, physical characteristics of deep sea and trenches are not different and actually reflect those of shallower depths (Jamieson et al., 2010), whereas spatial and temporal patterns of food supply varies between systems, showing differences of quantity as well as quality of food (Boetius et al., 1996; Kitahashi et al., 2014; Luo et al., 2017). Therefore, within the context of climate change (Cohen et al., 2018; Francis et al., 2018; Gentemann et al., 2017; Hobday et al., 2018; Jordan et al., 2018; Kretschmer et al., 2018; Levitus et al., 2000; Oliver et al., 2018), it is important to better understand how the interplay of biological and biogeochemical processes in the open and deep ocean function, as they have direct connection to the processes occurring at surface through the biological pump (R. Danovaro et al., 2003), and thus may have an impact on the CO_2 budget and finally on circulation of water masses (Toggweiler and Key, 2001) and climate (Falkowski et al., 1998), that will consequently have an effect on marine biodiversity patterns.

Marine biodiversity has shown variations along time series (Dornelas et al., 2014) as well as geological time scales (Renema et al., 2008); however, its current decline is evident (Monastersky, 2014; Pereira et al., 2010). Therefore, a better understanding of the spatial and temporal biodiversity patterns is crucial for its preservation (Dornelas et al., 2018). And, in order to improve that knowledge, the consideration of the third dimension of depth on the

spatial determination of marine biodiversity patterns should be addressed, as in the ocean realm, which is the most widespread suite of habitats of the planet, organisms are distributed within its volume and not its area (Boero et al., 2019).To do so, a more coherent structure of the water column should be developed, by considering ecologically functional compartments characterized by certain biotic and abiotic parameters that occur within specific ranges, to which plankton associate according their biological traits.

Despite the lack of studies along the length and breadth as well as the depth of water column pursuing to elucidate this issue for zooplankton as of yet, patterns of species diversity have been however documented at the terrestrial environment (Currie, 1991; McCain, 2009; McCain and Grytnes, 2010; Rapoport, 1975), and along depth for pelagic fishes (Smith and Brown, 2002) as well as benthic and demersal species (Pineda and Caswell, 1998); and, hypotheses or explanations have been tried to be established in order to explain these diversity patterns. Among them, environmental factors (Gaston et al., 1998) such as temperature (Allen et al., 2007; Smith and Brown, 2002), productivity (Levin et al., 2001; Smith and Brown, 2002), pressure (Brown et al., 2017; Brown and Thatje, 2011; Mestre et al., 2013; Thatje et al., 2010) as well as geometric constrains over habitat (Colwell et al., 2004; Colwell and Lees, 2000; Gaston et al., 1998; Smith and Brown, 2002; Zeppilli et al., 2016) are discussed as the primary causes of diversity.

1.6. TEMPERATURE IN THE OCEAN

Two of the most important properties of seawater are temperature and salinity (concentration of dissolved salts), for together they control its density, which is the major factor governing the vertical movement of oceanwaters (Suckow et al., 1995). Temperature depends on the part of solar radiation that reaches the surface, i.e., insolation; and, the intensity of insolation depends primarily on the angle at which the Sun's rays strike the surface; therefore, the distribution of temperature over the surface of the Earth varies with latitude and season, because of the tilt of the Earth's axis with respect to its orbit round the Sun (Suckow et al., 1995). In polar regions, the density of surface waters increases by direct cooling or by the formation of sea-ice, whereas at lower latitudes, dense saline water is produced by excess evaporation, which may be aided by strong winds (Suckow et al., 1995). The range of temperature in the oceans is about 40°C (or about 30 °C if shallow and restricted seas are not included), and its buffering effect depends on the continuous exchange of heat and water between ocean and atmosphere, mainly by means of the hydrological cycle (Suckow et al., 1995). Temperature decreases with depth, as most solar energy is absorbed within a few meters of the ocean surface, directly heating the surface waters and providing the energy for photosynthesis by marine plants and algae (Suckow et al., 1995). All of the infrared radiation is absorbed within about a meter of the surface, and nearly half of the total incident solar energy is absorbed within 10 cm of the surface (Suckow et al., 1995). Penetration will also depend on the clarity or transparency of the water, which in turn depends on the amount of suspended matter in it (Suckow et al., 1995). Turbulent mixing by winds and waves is the main mechanism that establishes a mixed surface layer that can be as thick as 200–300 m or even more at mid-latitudes in the open oceans in winter, and as little as 10 m thick or less in

sheltered coastal waters in summer (Suckow et al., 1995). At the region between 200–300 m and 1000 m depth, there is a steep temperature gradient where the temperature declines rapidly throughout much of the ocean, known as the permanent thermocline, beneath which, from about 1000 m to the ocean floor, there is virtually no seasonal variation and temperature decreases gradually to between about 0°C and 3°C (Suckow et al., 1995). This narrow range is maintained throughout the deep oceans, both geographically and seasonally, because it is determined by the temperature of cold, dense water that sinks from the polar regions and flows towards the Equator (Suckow et al., 1995).

1.7. STATE OF THE ART ON BIOGEOGRAPHY AND DIVERSITY PATTERNS OF PLANKTON

Regarding global patterns of plankton species richness, many hypotheses have attempted to explain its latitudinal gradients, although for most of them their support is provided by post hoc analyses rather than testing them (Currie et al., 1999), and a general consensus on the mechanisms that originate such relationships is lacking. However, efforts have been done in order to test hypotheses as well as identifying the greater factors influencing richness; and, among all of them, temperature is the factor showing the greatest correlation (Allen et al., 2002; Brown et al., 2004; Currie et al., 1999; Rohde, 1992; Rombouts et al., 2009; Roy et al., 2002; Tittensor et al., 2010), supporting the species-energy hypothesis, which proposes that the latitudinal biodiversity gradient has somehow been generated and maintained as a direct consequence of greater energy availability towards the equator (Allen et al., 2007). Energy refers to solar radiation, which is a form of kinetic energy essential to life because it is used by plants to photosynthesize reduced carbon compounds that once they are formed represent

the potential energy, which is the second basic form of energy defined as energy stored in an object, and that fuels virtually all biochemical reactions in the biosphere (Allen et al., 2007). Metabolism is the process of transforming kinetic energy to potential forms (and vice versa) through a complex network of biochemical reactions catalyzed by enzymes that regulates the concentrations of substrates and products, as well as the rates of reactions (Allen et al., 2007; Brown et al., 2004). The metabolic rate of an organisms is the fundamental biological rate, because it is the rate of energy uptake, transformation, and allocation for fitness-enhancing processes of survival, growth, and reproduction (Brown et al., 2004). Most organisms exhibit phenotypic plasticity in the expression of metabolism; however, temperature is one of the primary factors regulating it (Allen et al., 2007; Brown et al., 2004), leading to the hypothesis that kinetic and potential forms of energy both help regulate biodiversity through their effects on speciation rates (Allen et al., 2007).

Copepoda is a monophyletic taxon (Khodami et al., 2017; Spears and Abele, 2011) with over 10000 non- and parasitic species inhabiting a wide range of habitats, from north to south, from high altitude lakes to deep sea. Although their fossil history is relatively poor (Blanco-Bercial et al., 2011; Lange and Schram, 1999), the oldest register suggests they originate from the Cambrian period (542–488 million years ago) (Selden et al., 2010), having phylogenetic trees recording their origin in the benthos (Rigby and Milsom, 1996), from where they radiated in response to the increasing oxygenation and habitat diversity (Bradford-Grieve, 2002) maintaining their basic body shape despite their genetic variation, thus suggesting strong environmental constraints on their morphology (Verity and Smetacek, 1996), which has been pointed as one of the main features accounting for their numerical dominance in the pelagic realm (Kiørboe, 2011).

Studies on copepods' diversity and its fluctuations with environmental forcers have been performed (Hooff and Peterson, 2006; Rombouts et al., 2009); however, despite their importance and the relatively high amount of data available on their distribution, open ocean studies on their biogeography patterns are scarce, especially at the South Pacific Ocean. As of yet, a study performed over a large latitudinal range for copepods richness had shown maxima around subtropical areas for the Northern Hemisphere and a tropical-subtropical plateau at the Southern Hemisphere (Rombouts et al., 2009); and, similar patterns have been found for other planktonic groups, such as euphausiids (Tittensor et al., 2010), tintinnid cilliates (Dolan et al., 2006), foraminifera (Rutherford et al., 1999; Tittensor et al., 2010); as well as benthic marine invertebrates such as prosobranch gastropods (Roy et al., 2002); and higher trophic level organisms such as fishes (Tittensor et al., 2010; Worm et al., 2005), sharks (Tittensor et al., 2010), squids (Tittensor et al., 2010) and cetaceans (Tittensor et al., 2010). This spatial pattern among taxonomically distant species groups suggests the existence of a common underlying mechanism that supports their similar distribution (Rombouts et al., 2010; Worm et al., 2005), that may be related to the kinetic energy or temperature hypothesis, that is, that higher metabolic rates or relaxed thermal constraints promote diversity (Tittensor et al., 2010). Another focus has been put on functional traits seeking to identify and understand the underlying ecophysiology of the biogeography of plankton traits, rather than of plankton species, thus revealing the mechanisms that regulate community ecology (Barton et al., 2013). For zooplankton, the main traits are body size, ontogeny and feeding behavior, that are directly or indirectly related to temperature (Barton et al., 2013).

1.8. CONCEPTUAL FRAMEWORK, SCIENTIFIC QUESTIONS AND PROPOSED HYPOTHESIS

Biogeographic patterns can be explained on the basis of evolutionary (Bradford-Grieve, 2002; Rigby and Milsom, 1996) processes and spatial correlations (Braga et al., 1999) which are considered as the historical context for observed spatial distribution. However, over an ecological time scale, environmental factors can play a fundamental role in structuring spatial patterns, in particular in plankton groups with limited migration capacity and short life cycles. In this case, species distribution and the structure of species assemblages may obey to some physical processes (e.g. large-scale circulation, currents, eddies, fronts) and also the effect of local conditions, such as the temperature, food resources, oxygen, or others, favoring differential reproduction, mortality and growth. In this sense, temperature plays a fundamental ecological role in the marine ecosystem. It controls physiological rates (Pörtner, 2002), metabolism (Pörtner, 2002), reproduction (Escribano et al., 2014), mortality (Elliott and Tang, 2011) and community structure (Hooff and Peterson, 2006; Sorte et al., 2011), even at large spatial scales (Beaugrand et al., 2010; Mackas et al., 2007; Rombouts et al., 2010). Because of this role it may be thought that temperature can also influence the distribution of organisms in the ocean. This also because temperature can substantially vary in the three dimensions in the ocean and thus displaying a gradient in the water column structure that is thought to generate the large scale spatial trends on different organisms' distribution across the global ocean. Over the meridional axis temperature exhibits a strong gradient from the equator to the poles, while a similar gradient is commonly present from coastal areas to central gyres. The vertical axis also has a strong temperature gradient from the upper mixed layer down to the deep cold waters. Therefore, on the basis of the presence

of temperature gradients in the ocean and a variable distribution of organisms, this study will address the following main scientific questions:

What is the spatial conformation of the species diversity of zooplankton (Copepoda) in the South Pacific Ocean?

What are the main environmental drivers that shape the geographical structure of that diversity?

¿Is temperature the most important environmental driver structuring, shaping and maintaining the horizontal and vertical zonation and so that the biogeographic patterns of zooplankton in the ocean?

2. OBJECTIVES AND HYPOTHESIS

2.1 GENERAL OBJECTIVE

The study aimed to determine the factors/processes that structure the zooplankton community(ies) of the South Pacific Ocean allowing a mapping of the diversity patterns of copepods in this region with the aim of defining functional/ecological compartments over the horizontal and vertical axes in the upper ocean.

2.2 HYPOTHESIS

Considering the background given previously, and although the thesis addressed several issues related to biogeographic patterns of zooplankton in the South Pacific Ocean at different scales (basin and regional), the fundamental hypothesis underlying the study can be stated as:

H1: The zooplankton diversity patterns of the ocean are horizontally and vertically structured in ecological significant zones within which the interactions between the physical-chemical environment and the organisms are the key drivers for ecological zonation, and so determining the biogeographic and diversity patterns.

2.3. SPECIFIC OBJECTIVES

1) Characterizing species diversity patterns of the key invertebrate ectothermic taxon Copepoda, as a major component of marine zooplankton.

2) Evaluating how susceptible their biodiversity patterns are to be affected by fundamental environmental factors in the ocean, such as temperature gradients horizontally as well as vertically.

3) Defining ecological or functional compartments at the ocean over the vertical plane by using physical and ecological data.

3. MATERIALS AND METHODS

3.1 STUDY AREA

3.1.1. South Pacific Ocean (Chapter 1)

The SPO possesses the greatest surface and seabed area, as well as the greatest volume, with a mean depth of 3993 m (Costello et al., 2010). The ocean stretches from the Equator—including the islands of the Gilbert and Galápagos Groups, which lie to the northward thereof—until the parallel of 60˚S, and between South America and the northeastern limit of the East Indian Archipelago (from New Guinea to the Equator), along the southern, eastern and northern limits of the Bismarck and Solomon Seas; the southeastern and northeastern limits of the Coral Sea; and the southern, eastern and northern limits of the Tasman Sea, going down the meridian of 146˚ 55'E starting at the South East Cape, the southern point of Tasmania, up to the parallel of 60˚S (International Hydrographic Organization, 1953, 2002) (Figure 1).

3.1.2. The Humboldt Current System (Chapter 2)

The Humboldt Current System (HCS) (Figure 2) extends from southern Chile (~42-45°S) to northern Peru and Ecuador (~4°S) (Montecino and Lange, 2009; Thiel et al., 2007), being the largest of the four main Eastern Boundary Upwelling Systems—as the other three are embedded in the California, Canary, and Benguela Currents (García-Reyes et al., 2015). It represents the equatorward-flowing, eastern portion of the basin-scale South Pacific

Subtropical Gyre, that in terms of atmospheric forcing is mainly influenced by the South Pacific Subtropical Anticyclone or the South Pacific High (Ancapichun, Garcés-Vargas, 2015; Thiel et al., 2007), that presents seasonal variation, abiding at its northern position (26°S, 86°W) during the late austral fall and winter, and moving southwest (37°S, 108 °W) during austral spring and summer (Ancapichun, Garcés-Vargas, 2015). The latter (former) conditions generate stronger (weaker) Equatorward winds that favor (disfavor) coastal upwelling offshore central-south Chile (Montecino and Lange, 2009). Then, off Chile, the HCS transitions from highly seasonal with maximum upwelling-favorable winds and biological productivity in austral summer between 30°S and 40°S into permanent upwelling off northern Chile (Montecino and Lange, 2009). Also, the HCS is characterized by the presence of an Oxygen Minimum Zone (OMZ) caused by the shoaling of the oxygen-poor Equatorial Subsurface Water (ESSW) due to the upwelling events, resulting in low concentrations of dissolved oxygen near the surface (Morales et al., 1999). Therefore, the distribution of the OMZ along the water column in the HCS obeys latitudinal shifts in the upwelling regimes, with a shallower annual average depth of the upper OMZ in northern Chile (permanent upwelling) compared to central south Chile (seasonal upwelling) (Yáñez et al., 2012).

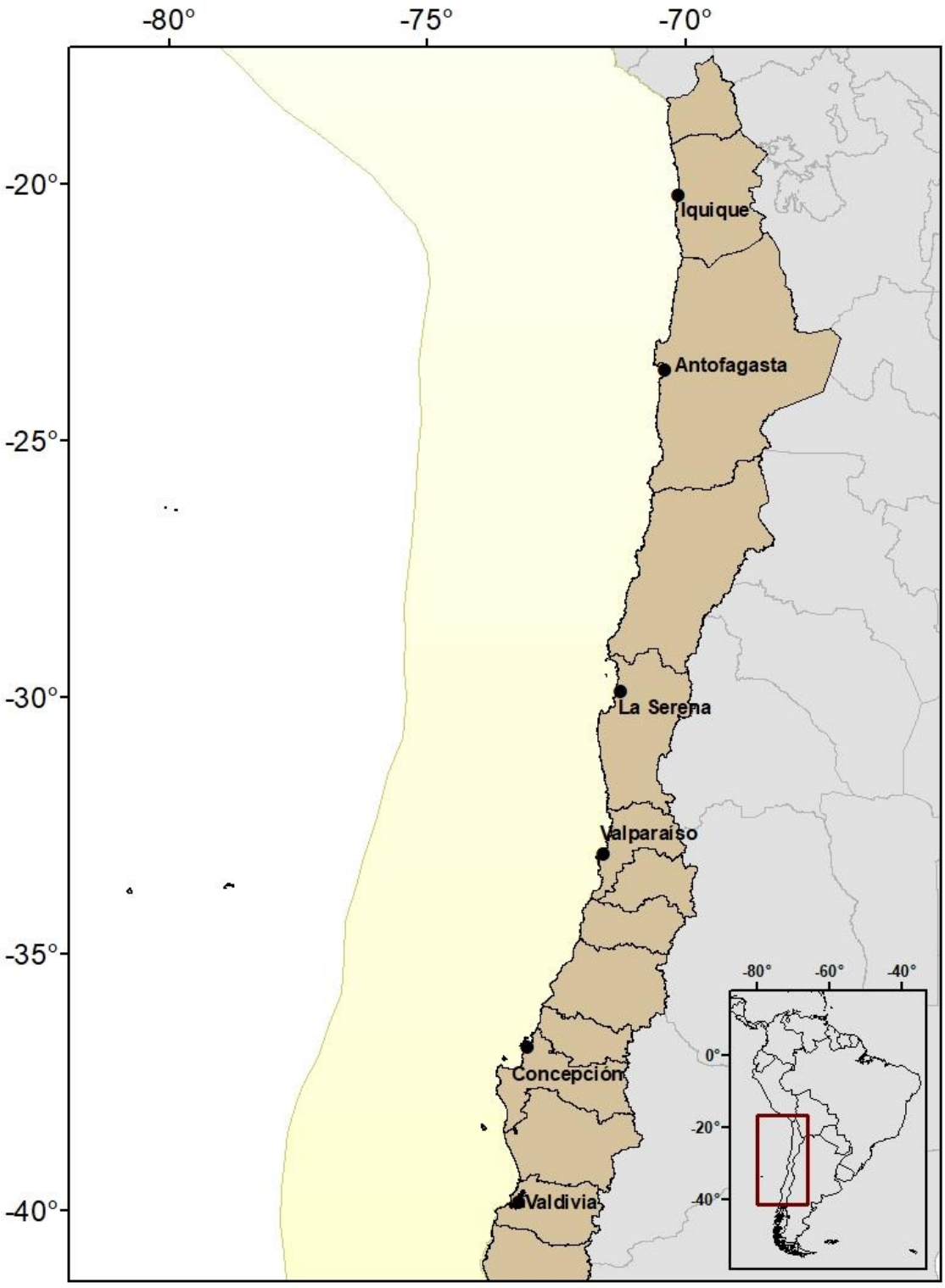

Figure 2: Map illustrating the Humboldt Current System extension off Chile (yellow band). Map projection is WGS 84 (EPSG 4326).

3.2. ENVIRONMENTAL DATA

For the first chapter, the oceanographic variables used for analyses were obtained from Copernicus Marine Environment Monitoring Service (CMEMS, https://marine.copernicus.eu) to a resolution of 1 x 1 degree and 0.25 x 0.25 degrees. From this data base, we obtained sea surface temperature (Desportes et al., 2021), salinity (Desportes et al., 2021), total chlorophyll-a concentration (Le Galloudec et al., 2021), dissolved oxygen concentration (Le Galloudec et al., 2021), and mixed layer depth (Guinehut, 2021). The resolution selected to analyze our data was 1 degree; hence, the environmental variables with a resolution of 0.25 degrees were resampled into a 1-degree resolution using QGIS 3.10 (QGIS, 2022). All data were averaged for the 0–200 m depth range, as well as from years 1993 to 2019. For temperature data, two additional variables were generated: temperature stability and standard deviation of temperature, which were calculated based on temperature data in temporal lags of two years, with the package climateStability (Owens and Guralnick, 2019) implemented in R software (R Core Team, 2021). “Deviation” of temperature is defined as the mean standard deviation between time slices over time elapsed, which was calculated at the beginning and end of each of the two years temporal lags and dividing this result by the length of the interval to quantify deviation over time for each time slice, to finally average the result across all time slices. Later, “stability” was obtained when taking the inverse of the deviation and scaling it between 0 and 1 (Owens and Guralnick, 2019). Therefore, a total of seven variables were included in the analyses, and are available in Zenodo repository: https://doi.org/10.5281/zenodo.8257222 (version 1).

For the second chapter, eight oceanographic and two atmospheric variables were selected for the analyses. The oceanographic variables were obtained from Copernicus Marine Environment Monitoring Service (CMEMS, https://marine.copernicus.eu) to a resolution of 1 x 1 degree and 0.25 x 0.25 degrees, namely: mean temperature (Desportes et al., 2021), salinity (Desportes et al., 2021), total chlorophyll-a concentration (Le Galloudec et al., 2021), dissolved oxygen concentration (Le Galloudec et al., 2021), pH (Le Galloudec et al., 2021), geostrophic eastward sea water velocity (ugo) (Guinehut, 2021), geostrophic northward sea water velocity (vgo) (Guinehut, 2021) and particulate organic carbon (POC) (Sauzède et al., 2023). And, the atmospheric variables of eastward and northward components of the wind at a height of 10 meters above the surface of the Earth (u10 y v10, respectively) (Hersbach et al., 2024), were obtained from the Copernicus Climate Change Service (C3S) Climate Data Store (CDS, https://cds-beta.climate.copernicus.eu/) to a resolution of 0.25 x 0.25 degrees. All variables were retrieved within the time range from 1995 and 2011, excepting POC—which registers start from 1998, and averaged between those years, as well as for each depth range both at the north and south zones of the study area (i.e., 100-0 m, 200-100 m, 300-200 m, 400-300 m, 500-400 m). Finally, all environmental variables were resampled to a resolution of 2 degrees using QGIS 3.10 (QGIS, 2022), and each grid-cell with environmental data was linked with ecological data. The environmental variables included in the analyses are available in a Zenodo repository: https://doi.org/10.5281/zenodo.xxxx (version 1).

3.3. ECOLOGICAL DATA - OBIS

As to assess the objectives and test the hypothesis for each chapter, Copepoda was considered as a model taxon, having ectothermal species for which more complete registers have been done for the region and are available through OBIS (*Ocean Biodiversity Information System (OBIS)*, 2024), that is a global open-access data and information clearing-house on marine biodiversity for science, conservation and sustainable development that pursues to build and maintain a global alliance that collaborates with scientific communities to facilitate free and open access to, and application of, biodiversity and biogeographic data and information on marine life. It is organized with more than 20 OBIS nodes around the world, connecting 500 institutions from 56 countries that have collectively provided over 45 million observations of nearly 120000 marine species, from bacteria to whales, from the surface to 10,900 meters depth, and from the tropics to the poles. OBIS emanated from the Census of Marine Life (2000-2010) and was adopted as a project under IOC-UNESCO's International Oceanographic Data and Information (IODE) programme in 2009. Over time, OBIS has been cited on different publications, with a peak of 206 in 2022, including articles from renowned peer-reviewed scientific journals, such as Nature and Science. The Department of Oceanography of the University of Concepción is running a Regional OBIS Node (RON) that is focused on the Eastern South Pacific (Unesco/IODE/OBIS/ESPOBIS, the Eastern Southern Pacific-Oceanographic Biodiversity Information System and Programa de Biodiversidad Marina, 2024001000PG, Universidad de Concepción) and aims to gather and tabulate information on biodiversity from different researchers and institutions. With the data collected, predictive models of copepods biodiversity were generated, based on biogeographic information including environmental parameters as well as data on copepods'

biodiversity patterns. The different sources of information were compiled in a spatial data base, through ArcMap 10.4.1 software (ESRI 2016), and QGIS 3.10 (QGIS.org, 2022) for the generation of predictive and explicative models of species diversity.

For both chapters, species occurrence records were obtained from OBIS data base. For the first chapter, the robis (Provoost and Bosch, 2021) and devtools (Wickham et al., 2021) packages implemented in the R Core Team (2021) were used for obtaining all occurrences between 0–200 m of the SPO, from 1993 to 2019. For the second chapter, species occurrence records were downloaded using the Mapper tool (http://https://mapper.obis.org/), obtaining data for five strata of 100 m each between 500-0 m depth within the study area previously described, within the time range from 1995 to 2011. Following the retrieval of the data, records without information on the geographic coordinates, coordinates equal to zero, or records located inside continents were eliminated, while selecting only records at level of species and excluding duplicate records. This procedure allowed to compile data to estimate species diversity, but also resulted in a drastic reduction of information since many records are reported for genera or higher taxonomic levels (e.g. families), and in some cases without clear or wrong georeference. Taxonomy was revised and updated using the WoRMS portal (http://www.marinespecies.org) through the *match_taxa* function of 'robis' package (Provoost and Bosch, 2021) implemented in R software (R Core Team, 2021). After we had cleaned and curated the data, a total of 22345 and 7013 records of Copepoda were selected for working on the first and second chapter, respectively. The data on occurrences of Copepoda species are available in different Zenodo repositories: https://doi.org/10.5281/zenodo.8257222 (version 1) for the first chapter and https://doi.org/10.5281/zenodo.xxxxxx (version 1) for the second chapter. Finally, diversity

indexes (see below) were generated based on biogeographic information of copepod biodiversity patterns at 1 and 2 degrees resolution and totaling 393 1-degree cells and 13 2-degrees cells for the first and second chapter, respectively.

3.4 SPATIAL ANALYSES

Biodiversity hotspots were determined based on spatial-statistical criteria to describe biodiversity patterns for the 0–200 m depth water column of the SPO in the first chapter, and for five 100 m strata in the HCS in the second chapter. It was specifically aimed to detect cells or groups of cells (i.e., spatial clusters) with species richness greater than the richness expected in a random distribution. Spatial hotspots were defined in ArcMap 10.4.1 (ESRI 2016) software using the High/Low Clustering (Getis-Ord G*) statistic (Getis and Ord, 1992), which identifies spatial concentrations of an entity (in this case species richness per cell) or areas that contain higher/lower values than expected by chance for a given study area. For a hot spot, the observed G* index indicated high values of richness clustered in the study area; whereas for a cold spot, the observed G* index indicated that low values of richness were clustered in the study area.

Species richness (alpha diversity) is the absolute number of species living in a given area, giving equal weight to all resident species (Swingland, 2013). Species composition (namely beta diversity) can be viewed as a measure that compares inventory diversity at two different scales (alpha and gamma diversity). Beta diversity is also a measure of similarity between sites (Koleff et al., 2003), and thus reflects the differences between local biological communities within a region. These differences arise from two phenomena which should be distinguished when understanding how biological diversity is distributed: nestedness and

spatial turnover (Baselga and Gómez-Rodríguez, 2019). Nestedness of species occurs when the biota of sites with smaller numbers of species are subsets of the biota at richer sites. Contrary to nestedness, spatial turnover implies the replacement of some species by others as a consequence of environmental sorting or historical and spatial constraints (Qian et al., 2005). We therefore calculated alpha diversity as species richness and beta diversity as species composition while distinguishing between turnover and nestedness. Alpha diversity was calculated in Biodiverse 3.1 software (Laffan et al., 2010), whereas beta diversity was estimated using the packages betapart (Baselga and Orme, 2012), CommEcol (Sanches Melo, 2021) and letsR (Vilela and Villalobos, 2015) in R software (R Core Team, 2021).

As biodiversity index, we used the Shannon-Wiener index which was calculated in Biodiverse 3.1 software (Laffan, 2022).

We generated a biological-environmental spatial database, wherein each grid cell had the biogeographic information of copepod diversity indices together with oceanographic data from the selected environmental variables. We employed Generalized Additive Models (GAMs) in the first chapter, and Linear Mixed Models (LMMs) in the second chapter to evaluate the relationship between copepod diversity indices and the environmental predictors in the SPO and the HCS, respectively.

The model selection was done through Bayesian Information Criterion (BIC) in the first chapter, and through the corrected Akaike Information Criterion (AICc) in the second chapter. The best model was the one providing the minimum delta BIC and AIC. The analyses were conducted through the package MuMIn (Bartoń, 2022), in R software (R Core Team, 2021).

4. RESULTS

4.1 Chapter 1: "Biodiversity patterns of epipelagic copepods in the South Pacific Ocean: Strengths and limitations of current data bases". Scientific article published in PLOS ONE, https://doi.org/10.1371/journal.pone.0306440.

Abstract

Basin-scale patterns of biodiversity for zooplankton in the ocean may provide valuable insights for understanding the impact of climate change and global warming on the marine ecosystem. However, studies on this topic remain scarce or unavailable in vast regions of the world ocean, particularly in large regions where the amount and quality of available data are limited. In this study, we used a 27-year (1993–2019) database on species occurrence of planktonic copepods in the South Pacific, along with associated oceanographic variables, to examine their spatial patterns of biodiversity in the upper 200 m of the ocean. The aim of this study was to identify ecological regions and the environmental predictors explaining such patterns. It was found that hot and cold spots of diversity, and distinctive species assemblages were linked to major ocean currents and large regions over the basin, with increasing species richness over the subtropical areas on the East and West sides of the South Pacific. While applying the spatial models, we showed that the best environmental predictors for diversity and species composition were temperature, salinity, chlorophyll-a concentration, oxygen concentration, and the residual autocorrelation. Nonetheless, the observed spatial patterns and derived environmental effects were found to be strongly influenced by sampling coverage over space and time, revealing a highly under-sampled basin.

Our findings provide an assessment of copepods diversity patterns and their potential drivers for the South Pacific Ocean, but they also stress the need for strengthening the data bases of planktonic organisms, as they can act as suitable indicators of ecosystem response to climate change at basin scale.

Resumen

Los patrones de biodiversidad a escala de cuenca para el zooplancton en el océano pueden brindar información valiosa para comprender el impacto del cambio climático y el calentamiento global en el ecosistema marino. Sin embargo, los estudios sobre este tema siguen siendo escasos o no están disponibles en vastas regiones del océano mundial, en particular en grandes regiones donde la cantidad y la calidad de los datos disponibles son limitadas. En este estudio, utilizamos una base de datos de 27 años (1993-2019) de ocurrencia de especies de copépodos planctónicos en el Pacífico Sur, junto con variables oceanográficas asociadas, para examinar sus patrones espaciales de biodiversidad en los 200 m superiores del océano. El objetivo de este estudio fue identificar las regiones ecológicas y los predictores ambientales que explican dichos patrones. Se encontró que los puntos calientes y fríos de diversidad y los conjuntos de especies distintivos estaban vinculados a las principales corrientes oceánicas y a las grandes regiones de la cuenca, con una creciente riqueza de especies en las áreas subtropicales de los lados este y oeste del Pacífico Sur. Al aplicar los modelos espaciales, demostramos que los mejores predictores ambientales de la diversidad y la composición de especies fueron la temperatura, la salinidad, la concentración de clorofila-a, la concentración de oxígeno y la autocorrelación residual. No obstante, se encontró que los patrones espaciales observados y los efectos ambientales derivados estaban

fuertemente influenciados por la cobertura de muestreo en el espacio y el tiempo, lo que revela una cuenca con un nivel de muestreo muy bajo.

Nuestros hallazgos brindan una evaluación de los patrones de diversidad de copépodos y sus posibles forzantes para el Océano Pacífico Sur, pero también enfatizan la necesidad de fortalecer las bases de datos de organismos planctónicos, ya que pueden actuar como indicadores adecuados de la respuesta del ecosistema al cambio climático a escala de cuenca.

PLOS ONE

RESEARCH ARTICLE

Biodiversity patterns of epipelagic copepods in the South Pacific Ocean: Strengths and limitations of current data bases

Manuela Pérez-Aragón[1,2☯], **Ruben Escribano**[2,3☯*], **Reinaldo Rivera**[2☯], **Pamela Hidalgo**[2,3☯]

1 Doctoral Program of Oceanography, Facultad de Ciencias Naturales y Oceanográficas, Universidad de Concepción, Concepción, Chile, **2** Instituto Milenio de Oceanografía (IMO), Universidad de Concepción, Concepción, Chile, **3** Department of Oceanography, Facultad de Ciencias Naturales y Oceanográficas, Universidad de Concepción, Concepción, Chile

☯ These authors contributed equally to this work.
* rescribano@udec.cl

Citation: Pérez-Aragón M, Escribano R, Rivera R, Hidalgo P (2024) Biodiversity patterns of epipelagic copepods in the South Pacific Ocean: Strengths and limitations of current data bases. PLoS ONE 19(7): e0306440. https://doi.org/10.1371/journal.pone.0306440

Editor: Hans G. Dam, University of Connecticut, UNITED STATES OF AMERICA

Received: April 20, 2023

Accepted: June 18, 2024

Published: July 11, 2024

Data Availability Statement: All data used in this study on occurrences of Copepoda species and environmental variables are fully available in Zenodo repository https://doi.org/10.5281/zenodo.8257222.

Funding: This work was funded by the Instituto Milenio de Oceanografía (IMO) through the Agencia Nacional de Investigación Científica y Tecnológica de Chile (ANID) Grant IC_120019. The funders had no role in study design, data collection

Abstract

Basin-scale patterns of biodiversity for zooplankton in the ocean may provide valuable insights for understanding the impact of climate change and global warming on the marine ecosystem. However, studies on this topic remain scarce or unavailable in vast regions of the world ocean, particularly in large regions where the amount and quality of available data are limited. In this study, we used a 27-year (1993–2019) database on species occurrence of planktonic copepods in the South Pacific, along with associated oceanographic variables, to examine their spatial patterns of biodiversity in the upper 200 m of the ocean. The aim of this study was to identify ecological regions and the environmental predictors explaining such patterns. It was found that hot and cold spots of diversity, and distinctive species assemblages were linked to major ocean currents and large regions over the basin, with increasing species richness over the subtropical areas on the East and West sides of the South Pacific. While applying the spatial models, we showed that the best environmental predictors for diversity and species composition were temperature, salinity, chlorophyll-a concentration, oxygen concentration, and the residual autocorrelation. Nonetheless, the observed spatial patterns and derived environmental effects were found to be strongly influenced by sampling coverage over space and time, revealing a highly under-sampled basin. Our findings provide an assessment of copepods diversity patterns and their potential drivers for the South Pacific Ocean, but they also stress the need for strengthening the data bases of planktonic organisms, as they can act as suitable indicators of ecosystem response to climate change at basin scale.

Introduction

Spatial patterns of biodiversity in the marine environment have long been documented [1, 2]; however, factors and processes controlling such patterns remain unclear [3]. In the framework

and analysis, decision to publish, or preparation of the manuscript.

Competing interests: The authors have declared that no competing interests exist.

of conservation purposes and preserving ocean biodiversity, it becomes clear that the variation in the biogeographic regions from time series observations [4], as well as from geological time scale analyses [5], requires a better understanding of underlying mechanisms driving the spatial and temporal biodiversity patterns [6].

Zooplankton are a significant component of the marine ecosystem; they are the most widespread form of animal life on Earth, with the longest history of evolutionary continuity [7]. These organisms are also the foundation of life in the ocean, acting as the trophic link between primary producers and upper trophic levels [8], being important components of marine biogeochemical cycles [9]. They are also known to rapidly respond to oceanographic and environmental variations, such as fluctuations on temperature [10], oxygenation [11], acidification [12, 13], stratification [14, 15], primary production [16, 17], upwelling [10, 18, 19], circulation [17] and advection [20], thus providing themselves essential environmental sensors for a changing ocean.

Copepods are the taxon with the largest amount of accepted species described and documented in the World Register of Marine Species (WoRMS) [21]. It is also a well-represented taxonomic group in several data bases for marine species, such that a relatively thorough database on their distribution (horizontal and vertical) is available for the South Pacific Ocean [22]. Most copepod data bases only report species occurrences, or at higher taxonomic levels, and with emphasis on Calanoid copepods. Even that, such data can facilitate studies on the drivers controlling copepods species richness, how they are spatially structured, and the way they might respond to a changing environment. However, the study of large-scale copepod diversity patterns and their fluctuations driven by environmental forces have been scarcely conducted [23–25]. Moreover, open ocean studies on biogeography patterns of copepods are especially scarce in the Southern Hemisphere. For the vast South Pacific Ocean (SPO), that represents the largest yet the least-known marine ecosystem in the world, available data on copepods are mostly compiled in the Ocean Biodiversity Information System (OBIS) Portal [26]. An important task, however, to use these data sets for studies on copepods distribution and diversity, is the assessment of their quality in terms of resolution and coverage, both in time and space.

With respect to global distribution of plankton species richness, efforts have been made to test hypotheses explaining spatial patterns [23, 27]. For instance, the species-energy hypothesis [28, 29], stating that available energy can regulate species diversity, has been widely supported [30], but how diversity becomes linked to available energy is matter of debate [23]. In the same context, the best predictor of plankton diversity in the ocean appears to be temperature, exhibiting the greatest correlation or highest explanatory power as reported in many works [3, 23, 25, 30–35], although, when analyzing latitudinal patterns of copepod diversity in the Atlantic Ocean, Woodd-Walker et al. (2002) [36] found that species diversity was fundamentally related to variability in seasonality from the equator to polar regions rather than to temperature. The explanation was that more stable conditions and continuous primary production at low latitude can promote a higher diversity, while a highly variable and strongly seasonal cycle of primary production in high latitudes can favor the dominance of fewer species. In any case, the positive correlation between sea temperature and diversity of zooplankton continues to be a key issue for predicting large-scale spatial variability of plankton communities [37, 38]. Temperature is one of the two most important properties of seawater controlling its density and thus governing the dynamics and circulation of the water masses [39]. Temperature also plays a key role in the range of distribution of various marine organisms [34, 40]. For instance, copepods exhibit a strong dependence in their vital rates with temperature [17], since they are ectotherms, so that their population dynamics is strongly influenced by this factor, with major implications on their species composition and diversity patterns [18, 41].

Over a large-scale domain (e.g., a basin-scale), the role of temperature or other environmental correlates as biogeographic predictors for copepods is still unclear for the South Pacific region. The remaining questions are: do copepod species exhibit significant clustering or distinctive spatial assemblies? and, what are the most plausible environmental correlates to predict the diversity distribution of copepods at a basin scale? Lastly, is temperature alone the best predictor of such spatial structures, and whether such structures and biogeographic patterns replicate those observed in the North Pacific or Atlantic Ocean? In this study, we addressed these questions using a long-term (1983–2019) data base on occurrence of copepod species, extracted from the OBIS Portal, allowing us to further evaluate the robustness of these compiled data on species records of epipelagic copepods. For this, we assessed the diversity patterns of planktonic Copepoda and their relationship with oceanographic conditions in the upper 200 m of the western and eastern sides of the SPO to identify biogeographic regions and the presence of hot and cold spots of diversity. We aimed at testing the hypothesis that water temperature is the best predictor explaining spatial diversity patterns of planktonic copepods at basin scale in the SPO. Ultimately, our study will provide a first assessment of copepods diversity for the entire basin, helping us to gain insights into how such patterns may vary under ongoing ocean warming and, also allowing us to evaluate the robustness of current data bases for plankton organisms in this large ocean basin.

Materials and methods

Study area

The SPO possesses the greatest surface and seabed area, as well as the greatest volume, with a mean depth of 3993 m [42]. The ocean stretches from the Equator—including the islands of the Gilbert and Galápagos Groups, which lie to the northward thereof—until the parallel of 60˚S, and between South America and the northeastern limit of the East Indian Archipelago (from New Guinea to the Equator), along the southern, eastern and northern limits of the Bismarck and Solomon Seas; the southeastern and northeastern limits of the Coral Sea; and the southern, eastern and northern limits of the Tasman Sea, going down the meridian of 146˚ 55'E starting at the South East Cape, the southern point of Tasmania, up to the parallel of 60˚S [43, 44] (Fig 1). The general circulation in the SPO and major current systems are illustrated in Fig 1.

Data sources—Copepoda species and quality control procedures

Species occurrence records were obtained from the Ocean Biodiversity Information System, OBIS [22] (http://www.iobis.org) data base, using the robis [45] and devtools [46] packages implemented in the R Core Team (2021). The data were obtained for all occurrences between 0–200 m of the SPO, from 1993 to 2019. Following the retrieval of the data, we eliminated records without information on the geographic coordinates, coordinates equal to zero, or records located inside continents. We selected only records at level of species and excluded duplicate records. This procedure allowed us to compile data to estimate species diversity, but also resulted in a drastic reduction of information since many records are reported for genera or higher taxonomic levels (e.g. families), and in some cases without clear or wrong georeference. Taxonomy was revised and updated using the WoRMS portal (http://www.marinespecies.org) through the *match_taxa* function of robis package [45] implemented in R software (R Core Team, 2021). After we had cleaned and curated the data, a total of 22345 records of Copepoda were selected. The data on occurrences of Copepoda species are available in a Zenodo repository: https://doi.org/10.5281/zenodo.8257222 (version 1). Finally, diversity indexes (see below) were generated based on biogeographic information of copepod biodiversity patterns,

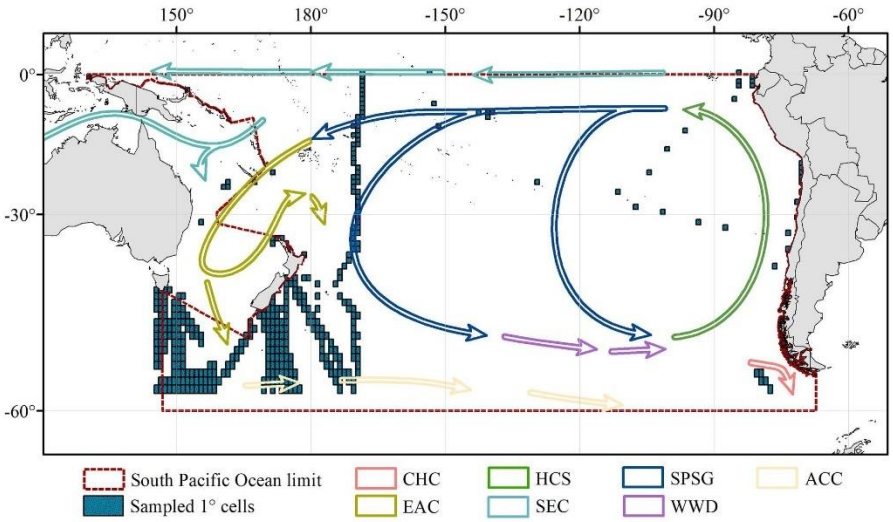

Fig 1. The South Pacific Ocean basin (red dashed area), its sampling coverage with georeferenced locations of the 393 cells (1˚ x 1˚) which were generated (blue squares) from data spanning between 1993–2019. The major near-surface currents shown for the whole basin were obtained from Harvard Dataverse (https://doi.org/10.7910/dvn/tkgo2z). CHC = Cape Horn Current; EAC = East Australian Current; HCS = Humboldt Current System; SEC = South Equatorial Current; SPSG = South Pacific Subtropical Gyre; WWD = West Wind Drift; ACC = Antarctic Circumpolar Current. Map projection is WGS 84/PDC Mercator (EPSG 3832).

https://doi.org/10.1371/journal.pone.0306440.g001

implemented in QGIS 3.10 (QGIS, 2022) at 1 degree resolution, totaling 393 cells (Fig 1). However, for all the spatial analyses, the basin was divided into two sections where more data were available. i.e., eastern and western side, excluding a longitudinal band containing cells between -110˚ and -170˚, that had low data coverage (only 16 cells available for that area) and could skew spatial patterns results. Therefore, 377 cells were considered for the analyses. Moreover, when representing alpha diversity patterns through kriging and an inverse distance weighted technique, all sampling cells containing less than 10 species were excluded, assuming they underestimated the species records and hence introduced biases in the patterns. Therefore, for those analyses, only 77 cells were considered.

Data sources—Environmental database and processing

The oceanographic variables used for analyses were obtained from Copernicus Marine Environment Monitoring Service (https://marine.copernicus.eu) to a resolution of 1 x 1 degree and 0.25 x 0.25 degrees. From this data source, we obtained sea surface temperature [47], salinity [47], total chlorophyll-a concentration [48], dissolved oxygen concentration [48], and mixed layer depth [49]. The resolution selected to analyze our data was 1 degree; hence, the environmental variables with a resolution of 0.25 degrees were resampled into a 1-degree resolution using QGIS 3.10 (QGIS, 2022). All data were averaged for the 0–200 m depth range, as well as from years 1993 to 2019. For temperature data, two additional variables were generated: temperature stability and standard deviation of temperature, which were calculated based on temperature data in temporal lags of two years, with the package climateStability [50] implemented

in R software (R Core Team, 2021). "Deviation" of temperature is defined as the mean standard deviation between time slices over time elapsed, which was calculated at the beginning and end of each of the two years temporal lags and dividing this result by the length of the interval to quantify deviation over time for each time slice, to finally average the result across all time slices. Later, "stability" was obtained when taking the inverse of the deviation and scaling it between 0 and 1 [50]. Therefore, a total of seven variables were included in our analyses and are available in Zenodo repository: https://doi.org/10.5281/zenodo.8257222 (version 1). These environmental variables were preprocessed by standardizing them subtracting their mean and dividing them by their standard deviation for later performing variable selection by using Random Forests through the package VSURF [51] implemented in R software (R Core Team, 2021). This is a two-stage strategy based on a preliminary ranking of the explanatory variables using the random forests permutation-based score of importance [52]. We selected a subset of important variables from the second or the "interpretation" step according to the reduction of the out-of-bag error by adding them into the decision training models. These variables were later used for analysis of predictive models of species richness and species composition. Further, for the selected environmental variables, we calculated the Spearman rank-order correlation coefficient matrix to visualize their degree of association as well as check for redundancy.

Spatial analyses

To analyze the species composition and its spatial distribution, the most dominant species (most recurrent) were extracted from the data bases and then associated with major current systems of the SPO, assuming they were representing distinctive species assemblages from these currents. Also, for beta diversity and its components, turnover and nestedness, a presence-absence matrix (PAM) was generated through the package fuzzySim in R software (R Core Team, 2021) [53] from the list of species that occurred for each range of values. This PAM was later matrix plotted in PAST software [54], from which we selected visually the dominant species, i.e., the ones occurring in all ranges of values for each component.

Biodiversity hotspots were determined based on spatial-statistical criteria to describe biodiversity patterns for the 0–200 m depth water column. It was specifically aimed to detect cells or groups of cells (i.e., spatial clusters) with species richness greater than the richness expected in a random distribution. First, the evaluation of whether copepods depict spatial autocorrelation using Moran's I statistic was conducted. Second, spatial hotspots were defined in ArcMap 10.4.1 (ESRI 2016) software using the High/Low Clustering (Getis-Ord G*) statistic [55], which identifies spatial concentrations of an entity (in this case species richness per cell) or areas that contain higher/lower values than expected by chance for a given study area. For a hot spot, the observed G* index indicated high values of richness clustered in the study area; whereas for a cold spot, the observed G* index indicated that low values of richness were clustered in the study area.

Species richness (alpha diversity) is the absolute number of species living in a given area, giving equal weight to all resident species [56]. Species composition (namely beta diversity) can be viewed as a measure that compares inventory diversity at two different scales (alpha and gamma diversity). Beta diversity is also a measure of similarity between sites [57], and thus reflects the differences between local biological communities within a region. These differences arise from two phenomena which should be distinguished when understanding how biological diversity is distributed: nestedness and spatial turnover [58]. Nestedness of species occurs when the biota of sites with smaller numbers of species are subsets of the biota at richer sites. Contrary to nestedness, spatial turnover implies the replacement of some species by others as a consequence of environmental sorting or historical and spatial constraints [59]. An application of knowing these components of beta diversity is the attempt to use differences between

communities to determine biogeographical regions, as a community that is a subset of a larger one (nestedness) has no exclusive species, and thus such difference should not be taken into account to delimit regions; whereas by using indexes not affected by nestedness it is possible to delimit regions with unique biological communities [58]. We therefore calculated alpha diversity as species richness and beta diversity as species composition while distinguishing between turnover and nestedness. Alpha diversity was calculated in Biodiverse 3.1 software [60], whereas beta diversity was estimated using the packages betapart [61], CommEcol [62] and letsR [63] in R software (R Core Team, 2021), and using the following equation:

$$\beta sor = \beta sim + \beta sne \equiv \frac{b+c}{2a+b+c} = \frac{b}{b+a} + \left(\frac{c-b}{2a+b+c}\right)\left(\frac{a}{b+a}\right), \quad (1)$$

where βsor is Sørensen dissimilarity, βsim is Simpson dissimilarity (i.e., turnover component of Sørensen dissimilarity), βsne is the nestedness component of Sørensen dissimilarity, a is the number of shared species between two cells, b the number of species unique to the poorest site, and c the number of species unique to the richest site.

As biodiversity index, we used the Shannon-Wiener index which was calculated in Biodiverse 3.1 software [62], according to Eq 2 [64] in the following way:

$$H = -\sum_{i=1}^{n} p_i \cdot ln\, p_i \quad (2)$$

where p_i is the number of samples (in this case, occurrences) of the i species as a proportion of the total number of occurrences in the neighborhoods (1˚ x 1˚ sampling cells). This proportion is estimated as:

$$p_i = \frac{n_i}{N} \quad (3)$$

where n_i is the number of records of the i species and N is the total number of records at species level in the sampled cell.

In order to account for the low sampling coverage and explore whether cells with low values of richness were causing biases in the analyses, we discarded the cells with values of alpha diversity < 10, and later performed the spatial analysis using an inverse distance weighted (IDW) technique that interpolates a raster surface from points, limiting to the range of the values used to interpolate and giving more (or less) weight where there is more (or less) data. In addition, to explore further at higher taxonomic levels, we performed the same analysis considering genus and family levels. Both analyses were plotted through Kriging interpolation using ArcMap 10.4.1 software (ESRI 2016).

Since species richness in a sample is highly dependent on sample size or sampling efforts [65], and the ocean has under-sampled areas due to spatial biases in the distribution of sampling locations [6], a skew on the apparent patterns of marine species richness can be produced. Hence, redundance statistics were used to count the total number of species, and an assessment of sample completeness was done for species richness through the R package iNEXT, which provides functions to compute and plot the seamless rarefaction and extrapolation sampling curves [65]. This latter analysis was performed for each main surface current system of the SPO, namely: Cape Horn current, East Australian Current, Humboldt Current System, South Equatorial Current, South Pacific Subtropical Gyre, and West Wind Drift, to evaluate whether some areas had a greater or lower coverage than others. The previously mentioned main surface current systems were downloaded from Harvard Dataverse [66].

We generated a biological-environmental spatial database, wherein each cell had the biogeographic information of copepod alpha and beta diversity together with oceanographic data

from the selected environmental variables. We employed Generalized Additive Models (GAMs) to evaluate the relationship between copepod alpha and beta diversity in the 0–200 m layer of the South Pacific Ocean and the environmental predictors while considering spatial autocorrelation in our analyses. Spatial correlation is a pattern in which observations are related to one another by the geographic distance between the observation, with locations close to each other exhibiting more similar values than those further apart, thus violating the assumption of independent and identically distributed errors, which can inflate type I errors [67]. This can lead to the selection of unimportant explanatory variables and poorly estimated parameters, moreover in ecology, as autocorrelation is a general property of ecological variables measured over geographic space [67]. Therefore, to take spatial autocorrelation into account, we used the residuals autocovariate (RAC) approximation [67] by including autocorrelation in the GAMs by adding another term to it that represents the influence of neighboring observations on the dependent variable at a particular location. Subsequently, the residuals of the auto-covariables were used as a new predictive variable in the models. The calculations of GAM+RAC were performed with the spdep package [68, 69] implemented in R software (R Core Team, 2021).

The model selection was done through Bayesian Information Criterion (BIC), that is based on information theory but within a Bayesian context and imposes a greater penalty for the number of parameters compared to the Akaike information criterion [70]. The best model is the one that provides the minimum BIC, denoted by BIC*, and delta BIC can be computed as: $\Delta BIC = BIC_m - BIC^*$. This implies that for given M models, the magnitude of the delta BIC can be interpreted as evidence against a candidate model being the best model [70]. As a rule, values of ΔBIC less than 2 are not worth more than a mention, values between 2 and 6 indicate that evidence against the candidate model is positive, values between 6 and 10 indicate that evidence against the candidate model is strong, and values greater than 10 indicate that evidence against the candidate model is very strong [70]. The analyses were conducted through the package MuMIn [71], in R software (R Core Team, 2021).

Beta diversity was evaluated at each side of the SPO using Generalized Dissimilarity Modelling (GDM)-based spatial analysis technique, which involves mapping the first three axes derived from a principal component analysis (PCA) performed on the set of transformed predictor layers [72]. It first formulates the relationship between biological dissimilarity and spatial distance by transforming each predictor variable through l-spline basis functions considering a term called 'predicted ecological distance' in a negative exponential function, with the assumption that dissimilarity between site-pairs increases monotonically from 0 to 1 and in a saturating manner with predicted ecological distance. Based on the maximum height of the spline function (and hence, the maximum value of the transformed predictor), which shows the importance of the predictor in explaining dissimilarities, only the predictors with maximum height over zero were selected for the generation and plotting of the spatial layers. A RGB (RedGreenBlue) color palette dimension was assigned to each of the three axes of the PCA, and they were mapped by combining them, finally enabling the visualization of areas predicted to have more similar species composition (shown as similar colors) or less similar species composition (shown as different colors). The GDM analysis was performed using the package gdm [73] in R software (R Core Team, 2021) and its plotting was done through Kriging interpolation using ArcMap 10.4.1 (ESRI 2016) software.

Results

Diversity patterns

For the South Pacific Ocean, a total of 178 species were reported at the upper 200 m water column of its basin. Regarding the main species present at each main surface current system, we

searched the dominant ones in terms of their occurrence along the whole period for each of the major current systems defined above. Most of the dominant species in the SPO were representatives of the Order Calanoida (S1 Table), except for the cyclopoid *Oithona similis*, which was the dominant species in the CHC, along with *Calanus simillimus* and *Pleuromamma robusta*. In the EAC, *O. similis* and *C. simillimus* were the dominant species accompanied by *Neocalanus tonsus*. In the SPSG *Calocalanus kristalli*, *Paracalanus parvus*, and *Calocalanus plumulosus* dominated; in the WWD *Calocalanus kristalli*, *Paracalanus parvus* and *Calocalanus plumulosus* were the most recurrent species; in the HCS *Paracalanus indicus*, *Oithona similis* and *Acartia tonsa* prevailed; and finally in the SEC *Paracalanus parvus*, *Calocalanus kristalli* and *Calocalanus plumulosus* were the most dominant ones (S1 Table).

For beta diversity and its components turnover and nestedness, the list of dominant species is shown in S2 Table. The dominant species for the mean beta diversity were the Calanoids *Acartia longiremis*, *Calocalanus kristalli*, *Calocalanus pavo*, and *Paracalanus parvus*, whereas turnover had similar dominant species, except by the substitution of *C. pavo* by *C. plumulosus*. Finally, nestedness resulted in a different species assemblage represented by *Calocalanus pavo*, *Euterpina acutifrons*, *Lucicutia flavicornis*, and *Mecynocera clausi*.

The spatial distribution of alpha diversity considering the complete data set with the curated data (i.e., 377 cells, excluding the -110˚–-170˚ longitudinal band) is shown in Fig 2A. The removal of cells with values of alpha diversity < 10, left 77 cells located at the eastern and western sides of the SPO, that were used for the inverse distance weighted (IDW) technique analysis (Fig 2B), and for the Kriging interpolation (Fig 2C). Those results showed a similar tendency as the ones obtained with Kriging interpolation done to explore the outcome of this approach by using the complete dataset (393 cells, without excluding the -110˚–-170˚ longitudinal band), i.e., showing lower values of diversity at the western side of the SPO with a peak in the tropical and temperate zone, decreasing towards higher latitudes, whereas the eastern side showed higher values peaking at the temperate area that decreased towards the Equator and from the coastal towards the oceanic zone (Fig 2B and 2C). When considering family level, the number of cells increased to 399, and the Kriging interpolation presented a pattern with more families observed towards the eastern tropical and equatorial zone, with lower values towards the temperate, subpolar, and western area; whereas its western side showed higher values of families towards the continent with peaks in equatorial and temperate areas, and decreasing towards the open ocean (Fig 2D).When considering genus level, the number of cells increased to 394, and the Kriging interpolation presented a similar pattern to that observed at species level for eastern alpha diversity in Fig 2A and 2B, with clearer peaks in northern Chile and off Ecuador; whereas its western side showed higher values of genus towards the continent with peaks in equatorial and temperate areas, and decreasing towards the open ocean (S1 Fig).

The Shannon-Wiener index of diversity for pelagic copepods exhibited a pattern that varied from that of alpha diversity. For the eastern and western sides of the basin, the higher values were within the moderate range (2.4 and 2.9, respectively), showing different spatial patterns. At the eastern side of the SPO, greater diversity is observed on a coastal band from the temperate zone towards the equator, with decreasing values towards the open ocean (Fig 3). At the western side, higher diversity was observed from subtropical areas towards temperate and subpolar zones, while also showing decreasing values towards the open ocean (Fig 3).

To identify the extreme areas in terms of diversity, we used the High/Low Clustering (Getis-Ord G) statistical analysis. This method yielded patterns consistent with those of diversity (in terms or species richness) and allowed us to identify most of the hot spots (high values of richness) present in western temperate-subpolar areas off Australia, and in the equatorial area off Peru and Ecuador, decreasing towards the south and into the open ocean (Fig 4).

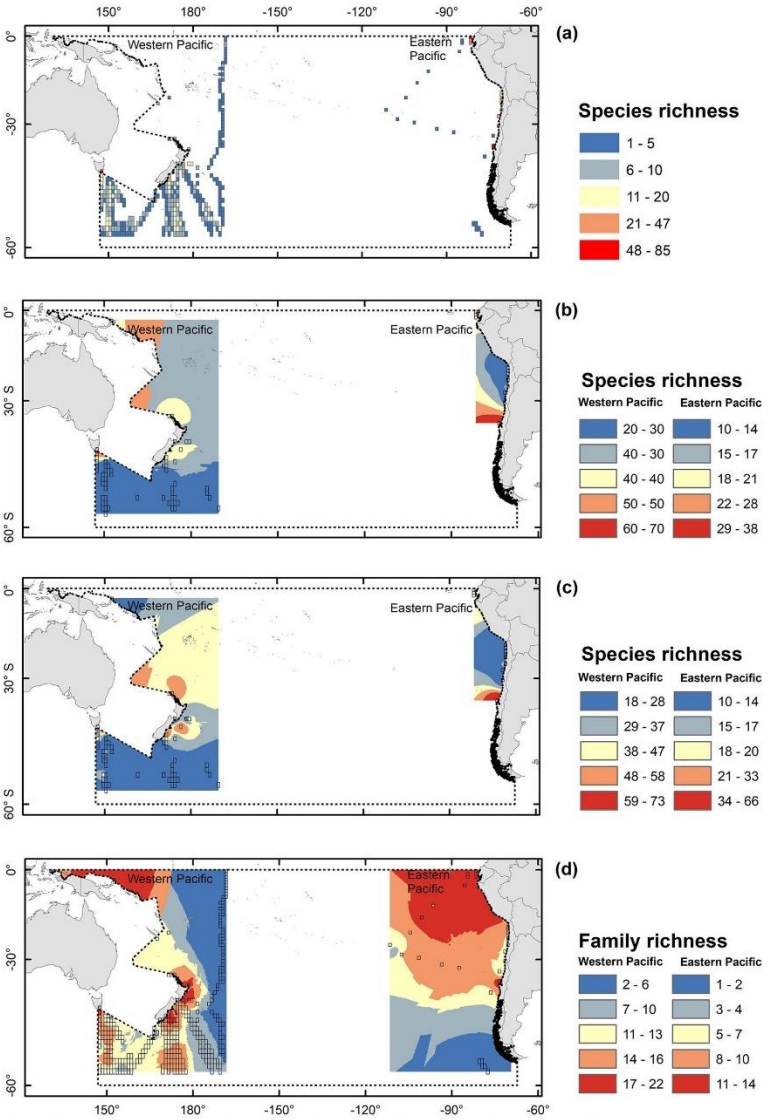

Fig 2. Richness patterns of Copepoda in the 0–200 m layer of the western and eastern side of the SPO for the period 1993–2019 based on species occurrence data obtained from OBIS portal. **(a)** Spatial distribution of alpha diversity considering the complete data cell with the curated data (i.e., 377 cells). **(b)** Inverse distance weighted (IDW) analysis for alpha diversity using cells with >10 species (i.e., only 77 cells from the total of 377 were selected). **(c)** Kriging interpolation for alpha diversity using cells with >10 species (i.e., only 77 cells from the total of 377 were selected). **(d)** Kriging

interpolation for family richness. Transparent squares are the 1˚ sampled cells used for interpolation, whereas the grey dotted line delimits the South Pacific Ocean. Map projection is WGS 84/PDC Mercator (EPSG 3832).

https://doi.org/10.1371/journal.pone.0306440.g002

The expected number of species, as a function of sampling units for different defined regions can illustrate the actual level of sampling coverage (Fig 5). As shown by species rarefaction curves, the sampling effort (samples per sampling units) varied extensively within and between regions, and no saturated curves were found in any of the regions, indicating a rather low coverage to assess the whole copepod community (Fig 5A). The distribution of the defined regions or current systems are illustrated in Fig 5B.

The spatial variability in diversity among potential distinct assemblies can be reflected in beta diversity, which may also indicate the degree to which such communities differ from each other. Beta diversity of copepods in the eastern SPO was higher in its equatorial-tropical area, with another area showing higher values at is temperate zone (Fig 6A); whereas the western side of the SPO had higher values of beta diversity expanding from tropical to subpolar areas (Fig 6A). This beta diversity (Fig 6A; mean beta = 0.579) was better explained by mean turnover (Fig 6B; mean turnover = 0.295) rather than mean nestedness (Fig 6C; mean nestedness = 0.284). The turnover rate at the eastern side of the SPO was higher in its equatorial-tropical area, with another area showing higher values at is temperate zone (Fig 6B); whereas the western side of the SPO had higher values of turnover expanding form tropical to subpolar areas (Fig 6B). Nestedness was found to be higher at the open ocean in the eastern side, with a higher values patch associated to the coastal area in the temperate zone (Fig 6C); whereas at the western side, it showed higher values in more oceanic areas at the temperate and subpolar zones (Fig 6C).

When applying the GDM-based spatial analysis to assess species composition, we found that salinity was the strongest predictor of the observed dissimilarities, followed by oxygen concentration, mean temperature and chlorophyll-a concentration. In contrast, mixed layer depth, temperature stability and standard deviation of temperature were the least important predictors, (S2 Fig). The spatial layers were generated and plotted with the best predictors and showed three clear latitudinal bands of similar color that kept almost the same distribution

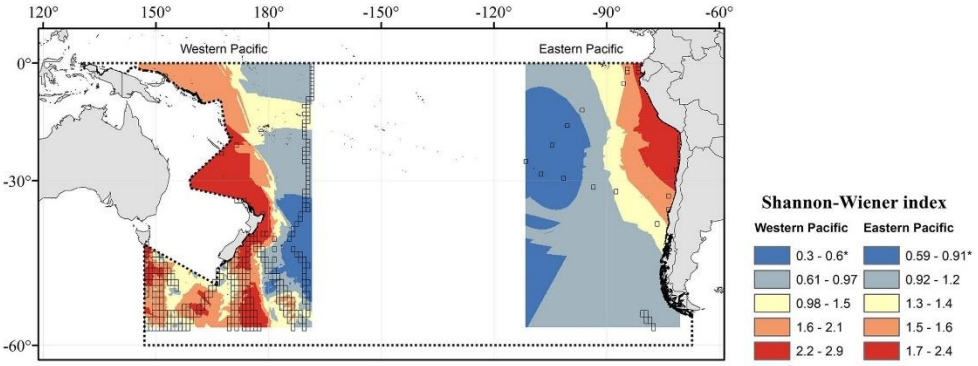

Fig 3. Shannon-Wiener index of Copepoda in the western and eastern sides of the South Pacific Ocean. Transparent squares are the 1˚ sampled cells used for Kriging interpolation, whereas the grey dotted line delimits the South Pacific Ocean. *Estimates based on available data at species level. Map projection is WGS 84/PDC Mercator (EPSG 3832).

https://doi.org/10.1371/journal.pone.0306440.g003

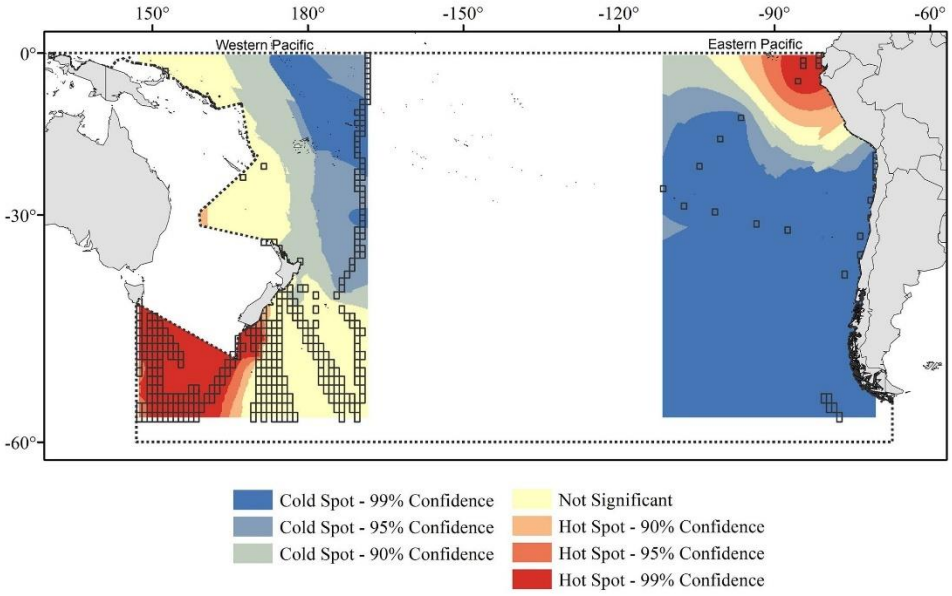

Fig 4. Getis-Ord G statistic of alpha diversity of Copepoda at the western and eastern sides of the SPO based on species occurrence data obtained from OBIS portal for the period 1993–2019. High and low values of richness are displayed in red and blue color, respectively. Color intensity denotes clusters' significance. Transparent squares are the 1˚ sampled cells used for Kriging interpolation, whereas the grey dotted line delimits the South Pacific Ocean. Map projection is WGS 84/PDC Mercator (EPSG 3832).

https://doi.org/10.1371/journal.pone.0306440.g004

when extracting the -110˚–-170˚ longitudinal band, indicating a more similar expected composition of Copepoda or the existence of distinctive species assemblies (communities) with a variable degree of mix; however, they covered large areas over each side of the basin, indicating the existence of different communities (Fig 7). These distinct communities can also be defined in terms of their dominant species which are shown in S2 Table. Some of these dominant species are shared between current systems, although their presence also reflects a wide distribution over the SPO basin.

Data coverage, biogeographic patterns, and dominant species

This assessment was carried out in association with the major current systems illustrated in Fig 1. The general circulation of the SPO is dominated by the subtropical gyre, that has an elevated mean dynamic topography at its center [74] (near 15˚ to 20˚S [75]). The South Equatorial Current represents the westward flow of the South Pacific Subtropical Gyre, that terminates entering the Coral Sea and bifurcating at the east of the Great Barrier Reef between 15˚ and 22˚S [76] to form the southerly East Australian Current [77], that strengthens as it flows along the coast of Australia [77]. Southward of ~33˚S, it begins to separate into filaments, forming the East Australian Current extension and the Tasman Front [77] that consists of a series of current jets flowing eastward, mainly between 33˚ and 35˚S [78]. These appears to be a large component of subtropical water feeding into the South Pacific Subtropical Gyre

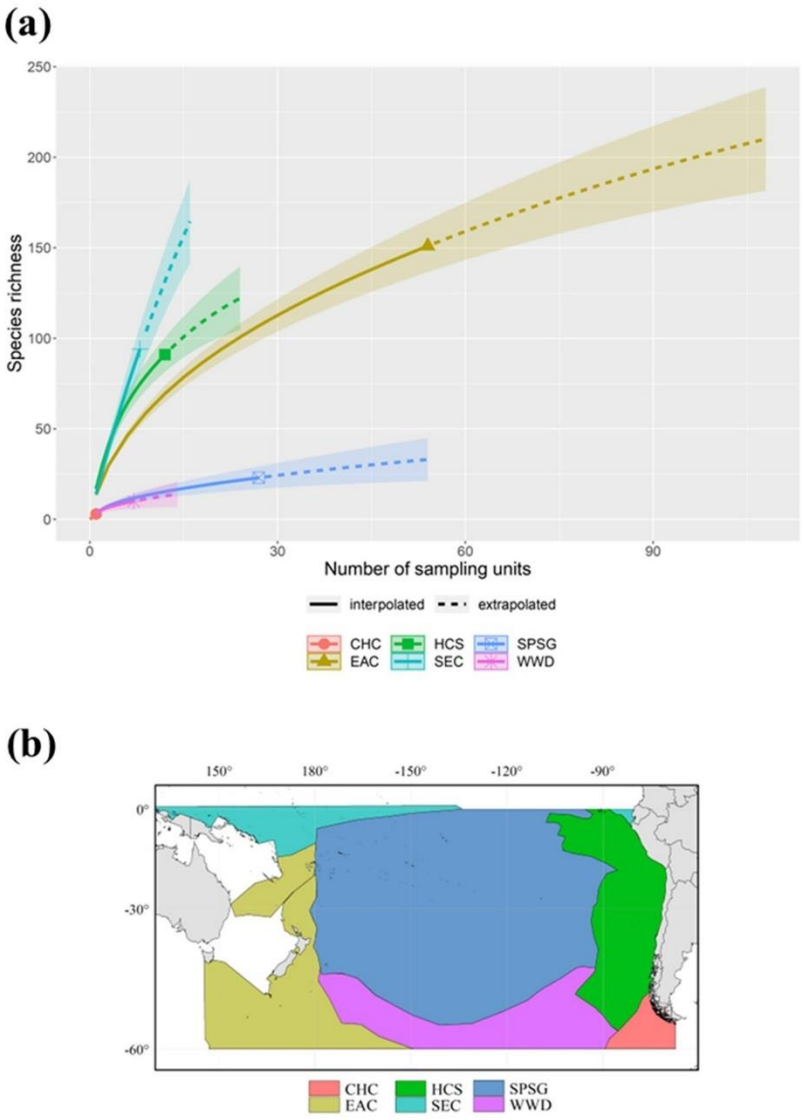

Fig 5. **(a)** Sample-size-based rarefaction (solid line segments) and extrapolation (dotted line segments) sampling curves for species richness with 95% confidence intervals (shaded areas) for Copepoda in the main surface current systems of the SPO. The symbols of each curve represent the reference samples. CHC = Cape Horn Current; EAC = East Australian Current; HCS = Humboldt Current System; SEC = South Equatorial Current; SPSG = South Pacific Subtropical Gyre; WWD = West Wind Drift. **(b)** Map of each main surface current system of the SPO.

https://doi.org/10.1371/journal.pone.0306440.g005

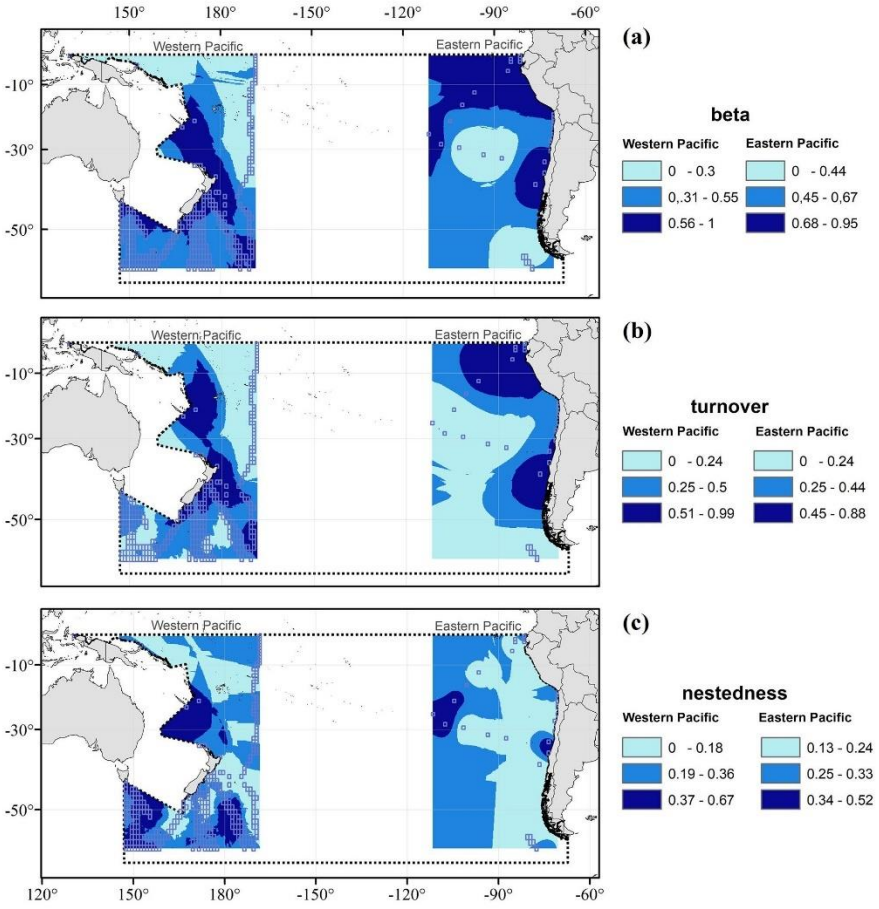

Fig 6. (a) Mean species composition and its components (b) turnover and (c) nestedness for Copepoda in the 0–200 m layer of the western and eastern sides of the SPO. Transparent squares are the 1˚ sampled cells used for Kriging interpolation, whereas the grey dotted line delimits the South Pacific Ocean. Map projection is WGS 84/PDC Mercator (EPSG 3832).

https://doi.org/10.1371/journal.pone.0306440.g006

circulation along the Sub-Tropical Front associated with the West Wind Drift, that streams equatorward of the Subantarctic Front associated with the Antarctic Circumpolar Current (ACC) [79, 80] and intersects the South American continent at ~45˚S, where the Cape Horn Current and Humboldt Current System begin towards the south and the north, respectively [81, 82]. The latter is the largest of the four main Eastern Boundary Upwelling Systems—as the other three are embedded in the California, Canary, and Benguela Currents [83]—and is shaped by a broad current of fresh, cooler Sub-Antarctic Surface Water along the eastern rim of the subtropical gyre [81], extending from southern Chile (~45˚S) to northern Peru and

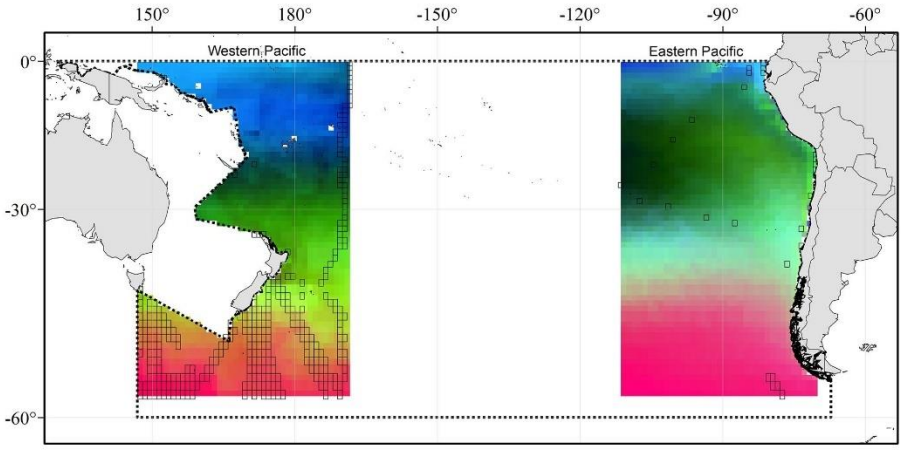

Fig 7. Predicted spatial variation in species composition of Copepoda at the western and eastern sides of the SPO based on a principal component analysis (PCA) of the Generalized Dissimilarity Modelling (GDM)-transformed environmental predictors. Colors represent gradients in species composition. Locations with similar colors indicate more similar expected composition. Dashed line at both sides of the antemeridian (180˚ longitude) delimits the South Pacific Ocean. Map projection is WGS 84/PDC Mercator (EPSG 3832).

https://doi.org/10.1371/journal.pone.0306440.g007

Ecuador (~4˚S), where cool upwelled waters collide with warm tropical waters forming the Equatorial Front [81]. The South Pacific Subtropical Anticyclone or the South Pacific High, which spins counter-clockwise, is the most influential off the west coast of South America [74, 84] and acts as the dominant forcing of the subtropical gyre [85]. However, it presents seasonal variation, abiding at its northern position (26˚S, 86˚W) during the late austral fall and winter, when it is also closer to the South American continent and its intensity is weaker; whereas, during austral spring and summer the South Pacific High moves southwest (37˚S, 108˚W) and depicts its maximum intensity [85]. The latter (former) conditions generate stronger (weaker) Equatorward winds that favor (disfavor) coastal upwelling offshore central-south Chile [81]. In terms of sampling coverage for epipelagic copepods, only 4.02% of the total area of the epipelagic SPO has been sampled between 1993 and 2019. In fact, all the main current systems have been sampled over less than 2.5% of their area, each covering less than 1% of the total area of the SPO. An exception is the East Australian Current System with 17.28% of its area sampled and covering 2.76% of the total area of the SPO (Table 1).

Environmental data selection and predictive models. The routine VSURF selected five oceanographic factors to be tested for influence on species richness (arranged in decreasing order of importance): mean temperature (T_{mean}), salinity (S), dissolved oxygen concentration (O_2), chlorophyll-a concentration (Chla), and the mixed layer depth (MLD). For species composition, all seven oceanographic variables were selected (arranged in decreasing order of importance): mean temperature (T_{mean}), chlorophyll-a concentration (Chla), dissolved oxygen concentration (O_2), standard deviation of temperature (T_{sd}), salinity (S), temperature stability (T_{stab}), and mixed layer depth (MLD). The Spearman correlation matrices (S3A and S3B Fig) obtained for each subset of variables depicted that all were weakly correlated according to a Spearman's rank correlation coefficient $|\rho < 0{,}7|$, with exception of T_{mean} and O_2, which showed $\rho = -0.99$.

However, in addition to environmental variables, data on Copepoda richness within the upper 200 m of the SPO depicted that the species and assemblies were significantly associated

Table 1. Summary of spatial characteristics and cells sampled per each main surface current system of the SPO. CHC = Cape Horn Current; EAC = East Australian Current; HCS = Humboldt Current System; SEC = South Equatorial Current; SPSG = South Pacific Subtropical Gyre; WWD = West Wind Drift; n.a. = not applicable.

Current	Area (Km^2)	Total number of cells	Number of sampled cells	Total number of observations	Number of species observed per current	Sampled area per current (Km^2)	% of the current's area sampled	% of the area of the SPO sampled
CHC	$2.65 *10^6$	152	5	55	3	$6.16 *10^4$	2.32	0.05
EAC	$1.93 *10^7$	1468	270	18207	148	$3.33 *10^6$	17.28	2.76
HCS	$1.59 *10^7$	1230	16	2527	91	$1.97 *10^5$	1.24	0.16
SEC	$6.74 *10^6$	685	12	510	94	$1.48 *10^5$	2.19	0.12
SPSG	$6.14 *10^7$	4436	67	899	24	$8.26 *10^5$	1.34	0.68
WWD	$1.46 *10^7$	804	23	147	10	$2.83 *10^5$	1.94	0.24
Total	$1.21 *10^8$	8775	393	22345	n.a.	$4.84 *10^6$	n.a.	4.02

https://doi.org/10.1371/journal.pone.0306440.t001

over the space according to Moran's I statistics. This is shown by regression residuals which exhibited significant spatial autocorrelation, i.e., there are spatial-dependent elements in the regression residuals (I = 0.012, p-value = 0.015). Therefore, the residuals autocovariate (RAC) was added as a new variable for the model selection, after which the spatial autocorrelation according to Moran's I statistics was not significant (I = 0.003, p = 0.091).

When looking for environmental predictors to explain the distribution of species richness, the best GAM explaining species richness included Chla, S, T_{mean} and RAC (Table 2). The adjusted R^2 value revealed that 60% of the variability is explained by this model. The predicted values of alfa diversity were concordant with the observed data (r = 0.77; S4 Fig).

Regarding species composition within the 0–200 m range, a significant spatial correlation according to Moran's I statistics was observed, as regression residuals exhibited significant spatial autocorrelation, (I = 0.018, p-value = 0.005). After we added RAC as a new variable for the model selection, spatial autocorrelation did not occur based on Moran's I statistics (I = -0.006, p-value = 0.726).

The best GAM model explaining the species composition of copepods in the SPO included Chla, O_2, S, T_{mean} and RAC (Table 3). The adjusted R^2 value revealed that 70% of the variability is explained by this model. The predicted values of beta diversity were concordant with the observed data (r = 0.84; S5 Fig).

Discussion

Spatial patterns of biodiversity and their predictors

Hot and cold spots patterns of copepod distribution in the SPO do not seem to follow the previously reported latitudinal trends of global patterns of marine species with peaks of diversity

Table 2. GAM+RAC models for species richness. Statistics acronyms are BIC = Bayesian information criterion, ΔBIC = delta BIC (i.e., the difference in BIC score between the best model and the model being compared). Predictors' acronyms are: T_{mean} = mean temperature, S = salinity, Chla = chlorophyll-a concentration, MLD = mixed layer depth, autocovariate = residuals autocovariate. The best model is highlighted in bold.

	Model	BIC	ΔBIC
1	**Species richness ~ Chla, S, T_{mean} + autocovariate**	**2364.54**	**0**
2	Species richness ~ Chla, MLD, S, T_{mean} + autocovariate	2365.47	0.93

https://doi.org/10.1371/journal.pone.0306440.t002

Table 3. GAM+RAC models for species composition. Statistics acronyms are BIC = Bayesian information criterion, ΔBIC = delta BIC (i.e., the difference in BIC score between the best model and the model being compared). Predictors' acronyms are: T_{mean} = mean temperature, T_{stab} = temperature stability, S = salinity, Chla = chlorophyll-a concentration, DO_2 = dissolved oxygen concentration, MLD = mixed layer depth, autocovariate = residuals autocovariate. The best model is highlighted in bold.

	Model	BIC	ΔBIC
1	**Species composition ~ Chla, DO_2, S, T_{mean} + autocovariate**	**553.32**	**0**
2	Species composition ~ Chla, MLD, DO_2, S, T_{mean} + autocovariate	551.84	1.48
3	Species composition ~ Chla, MLD, DO_2, S, T_{mean}, T_{stab} + autocovariate	551.68	1.64

https://doi.org/10.1371/journal.pone.0306440.t003

at subtropical latitudes and a gradual decrease towards temperate and polar regions [23, 34, 86–90]. However, the presence of hot spots equatorial area off Peru and Ecuador (Fig 4) coincides with the Eastern margin biogeographic region where coastal (0–250 Km offshore) and eastern (250–1000 Km offshore) boundary currents that originate from the Humboldt Current and has high levels of production [91]; whereas the hotspots observed in western temperate-subpolar areas off Australia (Fig 4), corresponds, according to their zoning, to the South Subtropical Convergence and to the Chatham Rise zones, both frontal zones that marks the intersection of colder sub Antarctic waters with warmer tropical waters thus supporting substantial production [92]. The latitudinal trend, suggesting a plateau distribution of diversity from tropical to temperate regions, can be observed at the spatial distribution of the Shannon index shown in Fig 3, which shows greater diversity over a coastal band from the Equator towards the temperate area in the eastern zone, and higher diversity from subtropical areas towards temperate and subpolar zones at the western zone. Shannon Wiener, however exhibited some discrepancies with species richness. For instance, when comparing the northern vs. the southern portion of the eastern SPO (i.e. the Humboldt Current). In this regard, it is important to consider that we estimated the Shannon Wiener based on the species occurrences over the study period, not on species abundance, whereas species richness represents the total number of species throughout the study period, independently of their frequency of occurrence. Therefore, Shannon Wiener and species richness may show different patterns of diversity, when comparing regions where copepod populations are highly frequent, since their populations are more continuously present during their annual cycles, such as in tropical or subtropical regions, or they have very seasonal life cycles, with low frequency of occurrence, such as in temperate regions [93].

Regarding latitudinal trends, Woodd-Walker et al. (2002) [36] suggested that the decreasing trend with latitude may arise from a more stable seasonal cycle of productivity in the tropical/subtropical area supporting a stable high-diversity community in comparison with a strongly seasonal productivity in temperate/polar regions which may limit the number of copepods species and so resulting in a low diversity pattern. This latitudinal pattern is reflected in our spatial distribution of Shannon-Wiener index in both sides of the SPO, but it is not clear for the spatial distribution of alpha diversity, that at its western side showed lower values of diversity and had a similar tendency with a peak in the tropical and temperate zone, decreasing towards higher latitudes, although the eastern side showed higher values peaking at the temperate area that decreased towards the Equator and from the coastal towards the oceanic zone.

The zonal pattern on the other hand, remains with much uncertainty due to a poor sampling coverage in the oceanic region of the SPO. Our study shows that maximum values of copepod richness occur around tropical-subtropical areas in both eastern and western sides, but with a strongly reduced diversity in the oceanic region in areas with too few sampled cells. In this regard, Rombouts et al. (2009) [23] suggested that temperature-predicted diversity of copepods should be higher in a subtropical band in both hemispheres, although with no

contrasting differences between coastal and oceanic regions. Such patterns have also been found in other planktonic groups, such as euphausiids [34], tintinnid ciliates [94], foraminifera [34, 95]; as well as benthic marine invertebrates, such as prosobranch gastropods [32]; and higher trophic level organisms, fishes [34, 96], sharks [34], squids [34] and cetaceans [34]. For instance, in a recent work [19] a total number of 121 species of copepods was reported from a single cruise carried out in the South Pacific Subtropical Gyre, indicating this area can be comparable to the North Pacific Subtropical Gyre in which 125 species were reported by McGowan and Walker (1979) [97], although more recently Vereshchaka et al. (2017) [98] indicated that more than 240 species can be found in the central-south Pacific region. Therefore, the species records available at OBIS may not represent the potentially rich copepod community in the central gyre of the SPO; and that is why we opted for dividing the basin into a eastern and western side and exclude the longitudinal band between -110˚–-170˚ for performing our analyses, as this area had too few sampling.

Temperature and its stability were the main factors, initially proposed in our hypothesis, as predictors of copepod biodiversity patterns in this basin. However, hot spots were also found off Chile, Peru and Ecuador along the main coastal upwelling system, which might be associated to 1) the habitat features hypothesis [34] related to ecosystem size and mesoscale processes, that are known to influence positively copepod diversity [34, 86, 90]; and 2) the productivity-richness hypothesis that predicts a positive effect of primary productivity on richness [34], supported by other studies finding a positive relationship between copepod diversity and chlorophyll-a concentration [86, 87, 89, 99]. Biogeographic patterns can also be explained on the basis of evolutionary [100, 101] and spatial processes [102] which are considered as the historical context for observed spatial distribution. Nevertheless, as stressed above, limited data coverage precludes a clear conclusion on underlying mechanisms explaining observed patterns of diversity.

Considered the above-mentioned potential mechanisms, we selected environmental variables to evaluate factors explaining copepod species richness and species composition. All variables were correlated to each other with a Spearman's rank correlation coefficient of $|\rho < 0{,}7|$, except for T_{mean} and O_2, that showed $\rho = -0.99$. In general, variables with correlation values of $|\rho|$ less than 0.7 are not recommended for selection [103]; nevertheless, despite this high value of $|\rho|$, we chose to include both variables instead of conducting further testing. This is because dissolved gases in the ocean tend to decrease their concentration with higher temperature [104], and so this relationship would not reflect a systematic bias. The oceanographic factors explaining copepod species richness (Chla, S, T_{mean}) and species composition (Chla, O_2, S, T_{mean}) in the SPO are of significance in a lesser or greater degree at different zones of the study area; and, they have also been documented to be of importance on a macroscale basis for copepod abundance and body size [25]. Moreover, the GDM-based spatial analysis conducted for evaluating species composition showed that the stronger predictors of the observed dissimilarities were the same variables (S, O_2, T_{mean}, Chla; S3 Fig).

It has been found that chlorophyll strongly correlates with copepod abundance in the ocean [34, 86, 99, 105]. Oxygen is also a significant factor influencing copepod distribution in the ocean, because its availability is a major driver for temperature-size responses in aquatic organisms [106], and the variation in its concentration, for example, due to deoxygenation, can affect copepod physiology, with drastic impacts in both coastal [11, 107] and oceanic [108] species. Warmer water increases copepod growth, development and molting rates [107], with an associated increase in the oxygen demand. This can lead to a reduction in population growth by limiting the hatching success and naupliar growth in early life stages [11], as well as reducing egg production and somatic growth in adults [107], together with shifts in their depth distribution [108]. This involves physiological adaptations that may vary according to

the species, their body weight and extent of motion [109]. Altogether, these combined drivers have a potential effect on copepod ecology and, consequently, on their biogeographic patterns.

Salinity and its variation also affects copepod distribution [110], biomass [111], reproduction [112, 113], growth [114, 115], body size [25] or fatty acid synthesis [115], with various ranges of tolerance that may or may not be favorable, according to their biology and location. This may be relevant since global warming in some areas of the ocean can lead to an increase in salinity (evaporation or greater circulation) or a reduction of the same (greater run-off of fresh water into the ocean, rainfall, or ice melt), producing osmotic stress that may be costly for their physiology.

Temperature itself plays a fundamental role in the marine ecosystem, since it controls physiological rates [116], metabolism [116], body size [25], reproduction [10], mortality [117] and community structure [24, 118], even at large spatial scales [25, 35, 41, 119]. Thus, it may be thought that temperature also influences the distribution of organisms in the ocean, as it can substantially vary in its three dimensions. Over the meridional axis, temperature exhibits a strong gradient from the equator to the poles, with a similar gradient commonly present from coastal areas to central gyres, whereas in the vertical axis, it has a strong temperature gradient from the upper mixed layer down to the deep, cold waters. These gradients in the water column structure may contribute to the generation of large-scale spatial trends in the distribution of organisms such as copepods [120]. Although this study did not separate copepods into functional groups according certain traits more specifically linked to environmental variations, the fact that composition changed mainly due to oceanographic factors that influence the nesting of functional groups, highlights and support those findings [121], as beta diversity is a proxy of difference in number of species among ecosystems, thus reflecting changes or gradients in the environment as well.

Species distribution and the structure of species assemblages may additionally obey some physical processes (e.g., large-scale circulation, currents, eddies, fronts, interaction with the atmosphere) and the effect of local conditions. In this sense, it is possible that in addition to more direct effects on copepod populations, temperature is reflecting variability in water masses distribution controlled by large-scale circulation. The distribution of drifting plankton, including copepods, is largely affected by near-surface currents, allowing species radiation and colonization processes [122], and so influencing diversity patterns.

Regarding the structure of the copepod community, we found that some dominant species were representing different current systems, and thus distinct plankton communities. However, we could only assess most occurrences of species (not abundance) for each main surface current system of the SPO (S1 Table). The occurrences distribution of dominant species seemed to be concordant with patterns documented for copepod diversity on a large scale, with cyclopoids showing greater diversity in the subtropics and calanoids in the temperate zone [25, 123]. Dominant species in the each of the major currents are mostly represented by small Calanoid copepods and the widely distributed Cyclopoid *Oithona similis*. Some of the recurrent species are *Paracalanus parvus* and *P. indicus*. Both species are possibly a single species traditionally known as *P. parvus*, but morphologically close to *P. indicus*, although most likely being a new, non-described species [124]. Lately, it has been referred as *P. cf. indicus* in the Eastern SPO [125]. The other recurrent species are *Calocalanus* spp. They are also known as small-sized copepods and mostly found in oceanic waters [126]. The high occurrence of small-sized oceanic copepods, and low presence of large-sized Calanoids, such as *Calanus* spp., *Calanoides* spp., and *Pleurommama* spp., which are abundant in coastal areas of the SPO [38, 93] may indicate that small copepods prevail, or are numerically more abundant than large-sized ones. Also, most data sets do not include harpacticoids or other cyclopoid copepods, such as *Oncaea* spp. which may be highly abundant in oligotrophic waters of the SPO [127].

The OBIS data base does not include the observed number of species in each of the surface current systems (see S1 Table) when compared to total species inventories. For example, the maximum species richness available in OBIS for the East Australian Current (EAC) and the Humboldt Current System (HCS) is 148 and 91, respectively (see Table 1); that account for ca. a quarter of the species inventory compiled by the Banyuls Observatory data base on copepods for those areas [128]. In the other current systems, similar levels of differences between OBIS data and species inventories can be applied.

Current data limitations over space and time

Sampling biases must be considered when validating the robustness of the derived spatial patterns and the role of environmental drivers. For example, it is crucial to consider that due to spatial gaps of data (Fig 1, Table 1), our results may be strongly constrained be sampling coverage [129, 130].

The spatial sampling effort was evaluated over the SPO through rarefaction/extrapolation curves by grouping the cells into the main surface current systems of the SPO (Fig 5A). It was found that species richness counts did not reach a clear asymptote at any of the defined current systems. Thus, the SPO is under-sampled for copepods. This aspect may have had an influence on Shannon-Wiener index values (Fig 3), as moderate to high values (from 1.7 on) were estimated only for a small area of the SPO. Subsequently, large areas exhibiting much lower values of richness and biodiversity may result from lack of sampling, description, and digitization of copepod data rather than having a relatively low diversity of species on a significant part of its extension. Moreover, the GDM-based spatial analysis done for evaluating species composition was performed with ecological data based on occurrence instead of abundance, which requires the assumption that any location where the species has not been observed can be treated as absence; therefore, making under-sampled locations more problematic [72]. Although invertebrates are the most common group documented after plants [131], and that an increasing number of data papers over time reflects progress in digitization and online platforms development for reporting observations that serve for biodiversity research [131, 132], it has been estimated that less than 10% of specimens' registers are digitized [133], with even less data available online [134]. The lack of description and cataloguing of species and the incomplete knowledge regarding their geographic distribution (i.e., Linnean and Wallacean shortfalls, respectively) are among the most common setbacks for biodiversity research using databases [130], representing a practical limit for biodiversity knowledge that may lead to misidentification of ecological processes [130]. We further addressed this issue by estimating redundancy index, that indicated a middling sampling over the SPO (S6 Fig) with a lower coverage on its eastern side, that highlights the gaps on great extensions and depicts higher values for areas where a greater sampling effort was seen. Moreover, through Moran's I index, it is possible to infer that the distribution of richness is more spatially clustered than expected if underlying spatial processes were random, as biodiversity aspects of species and communities are linked to complex interactions between physical, chemical, and biological factors. Considering this, and the developments in statistical modeling making possible to account for biases within heterogeneous data [135], we chose to use the RAC approximation [67] for the GAM analyses. This allows the incorporation of another variable into the models to take spatial autocorrelation into account and maintain strong predictive and inferential performance [67]. However, despite the usefulness of these methodologies, more effort is needed for improving the number and quality of distribution records used as primary data in macroecological studies [136], with databasing focused on georeferencing the information obtained from data collections [129].

Copepod resilience to climate forcing

Copepod diversity may have remained stable over a long time and large space due to a strong resilience to environmental variability. In this aspect and when dissecting species composition into turnover and nestedness, we observed that the former was higher in areas where hot spots were also identified (Figs 6 and 4, respectively), coinciding with the flow of cold currents (Humboldt current, Zeehan Current in southern Australia, and southern part of the East Australian current off New Zealand into the West Wind Drift). Therefore, basin-scale ocean currents seem to be an important oceanographic driver explaining the distribution of copepods in the SPO. The potential of large-scale ocean currents generating distributional patterns at various levels in the ocean has recently been studied more across different taxa [137–141], showing results that support the hypothesis and suggest that it may be a general process transcending taxa and spatial scales [141]. All these large-scale circulation patterns may allow the recolonization and mixing of copepod assemblies, thereby acting as a buffer to cope with the local impact of warming, deoxygenation, or other altered environmental conditions driven by natural perturbations or anthropogenic origin. This buffering effect may allow planktonic organisms such as copepods to exhibit a high resilience to large-scale changes in hydrographic conditions due to global warming.

Conclusion

The diversity distribution of copepods in the SPO follows general patterns observed in other organisms in the ocean, although patterns over a basin scale with presence of hot and cold spots do not replicate observed patterns reported for the North Pacific or Atlantic Ocean. The key environmental correlates for such biodiversity patterns were found to be mean temperature, chlorophyll-a concentration, salinity, oxygen concentration, and residuals autocovariate. A significant role for causing and maintaining copepod diversity patterns was also attributed to large-scale circulation processes, which may act as a buffer for changes in local conditions and allow species recolonization. Therefore, we suggest that planktonic copepods may exhibit a strong resilience to climate change impact.

However, caution should be taken in interpreting our findings since our modeling approaches and spatial analyses were strongly constrained by spatial and temporal gaps in sampling efforts and data availability. Future analyses are expected to improve observed patterns with the completion of global biodiversity data bases.

Supporting information

S1 Fig. Kriging interpolation analysis done for the western and eastern side of the SPO with 394 cells accounting for number of genera. Transparent squares are the 1˚ sampled cells used for Kriging interpolation, whereas the grey dotted line delimits the South Pacific Ocean. Map projection is WGS 84/PDC Mercator (EPSG 3832).
(JPG)

S2 Fig. Maximum height of the spline function (hence the maximum value of the transformed predictors), indicating the stronger predictors of the observed dissimilarities for the Generalized Dissimilarity Modelling (GDM)-based spatial analysis. Their acronyms are: s = salinity, o2 = dissolved oxygen concentration, tmean = mean temperature, chla = chlorophyll-a concentration, mld = mixed layer depth, tstab = temperature stability, tsd = standard deviation of temperature. The spatial layers were generated and plotted with the predictors with heights over zero (i.e., s, o2, tmean and chla).
(JPG)

S3 Fig. Spearman correlation matrices of environmental variables used in GAM models for (a) alfa diversity and (b) beta diversity. Positive correlations are displayed in red and negative correlations in blue color. Color intensity is proportional to the correlation coefficients. In the right side of the correlogram, the legend color shows the correlation coefficients and the corresponding colors. Their acronyms are: Tmean = mean temperature, Tstab = temperature stability, Tsd = standard deviation of temperature, S = salinity, Chla = chlorophyll-a concentration, O2 = dissolved oxygen concentration, MLD = mixed layer depth.
(JPG)

S4 Fig. Correlation between observed and predicted species richness. Pearson's r coefficient: 0.77 (p-value<0.01). Negative residuals (below the reference line) indicate knowledge shortfalls, whereas positive residuals (above the reference line) indicate underestimated species richness.
(JPG)

S5 Fig. Correlation between observed and predicted species composition. Pearson's r coefficient: 0.84 (p-value<0.01). Negative residuals (below the reference line) indicate knowledge shortfalls, whereas positive residuals (above the reference line) indicate underestimated species composition.
(JPG)

S6 Fig. Redundancy index obtained for the western and eastern side of the SPO. Values close to 1 indicate good sampling, whereas values close to 0 indicate poor sampling. Transparent squares are the 1˚ sampled cells used for Kriging interpolation, whereas the grey dotted line delimits the South Pacific Ocean. Map projection is WGS 84/PDC Mercator (EPSG 3832).
(JPG)

S1 Table. Dominant copepod species in terms of occurrence for the main surface current systems of the South Pacific Ocean. CHC = Cape Horn Current; EAC = East Australian Current; HCS = Humboldt Current System; SEC = South Equatorial Current; SPSG = South Pacific Subtropical Gyre; WWD = West Wind Drift.
(DOCX)

S2 Table. Dominant copepod species of the South Pacific Ocean in terms of occurrence for all ranges values of beta diversity and its components turnover and nestedness.
(DOCX)

Acknowledgments

We are grateful to all the scientific community providing data on marine biodiversity to OBIS portal, and special thanks to ESPOBIS, the Eastern South Pacific Node of OBIS. Two anonymous reviewers greatly helped to improve our work.

Author Contributions

Conceptualization: Manuela Pérez-Aragón, Ruben Escribano, Reinaldo Rivera.

Data curation: Reinaldo Rivera, Pamela Hidalgo.

Formal analysis: Manuela Pérez-Aragón.

Funding acquisition: Ruben Escribano.

Investigation: Manuela Pérez-Aragón, Ruben Escribano, Reinaldo Rivera, Pamela Hidalgo.

Methodology: Manuela Pérez-Aragón, Ruben Escribano, Reinaldo Rivera.

Resources: Ruben Escribano, Pamela Hidalgo.

Software: Manuela Pérez-Aragón, Reinaldo Rivera.

Supervision: Ruben Escribano.

Validation: Manuela Pérez-Aragón, Ruben Escribano, Reinaldo Rivera.

Visualization: Ruben Escribano, Reinaldo Rivera.

Writing – original draft: Manuela Pérez-Aragón, Ruben Escribano, Reinaldo Rivera.

Writing – review & editing: Ruben Escribano, Reinaldo Rivera, Pamela Hidalgo.

References

1. Angel MV. Biodiversity of the Pelagic Ocean. Conserv Biol. 1993; 7: 760–772.
2. Ormond RFG, Gage JD, Angel M V. Marine Biodiversity: Patterns and Processes. Cambridge University Press. 1997.
3. Currie DJ, Francis AP, Kerr JT. Some general propositions about the study of spatial patterns of species richness. Ecoscience. 1999; 6: 392–399. https://doi.org/10.1080/11956860.1999.11682541
4. Dornelas M, Gotelli NJ, McGill B, Shimadzu H, Moyes F, Sievers C, et al. Assemblage Time Series Reveal Biodiversity Change but Not Systematic Loss. Science (80-). 2014; 344: 296–300. https://doi.org/10.1126/science.1248484 PMID: 24744374
5. Renema W, Bellwood DR, Braga JC, Bromfield K, Hall R, Johnson KG, et al. Hopping Hotspots: Global Shifts in Marine Biodiversity. Science (80-). 2008; 321: 654–657. https://doi.org/10.1126/science.1155674 PMID: 18669854
6. Dornelas M, Antão LH, Moyes F, Et al. BioTIME: A database of biodiversity time series for the Anthropocene. Glob Ecol Biogeogr. 2018; 27: 760–786. https://doi.org/10.1111/geb.12729 PMID: 30147447
7. Verity PG, Smetacek V. Organism life cycles, predation, and the structure of marine pelagic ecosystems. Mar Ecol Prog Ser. 1996; 130: 277–293. https://doi.org/10.3354/meps130277
8. Lombard F, Boss E, Waite AM, Vogt M, Uitz J, Stemmann L, et al. Globally Consistent Quantitative Observations of Planktonic Ecosystems. Front Mar Sci. 2019; 6. https://doi.org/10.3389/fmars.2019.00196
9. Valdés V, Carlotti F, Escribano R, Donoso K, Pagano M, Molina V, et al. Nitrogen and phosphorus recycling mediated by copepods and response of bacterioplankton community from three contrasting areas in the western tropical South Pacific (20˚S). 2018; 6019–6032.
10. Escribano R, Hidalgo P, Valdés V, Frederick L. Temperature effects on development and reproduction of copepods in the Humboldt Current: the advantage of rapid growth. J Plankton Res. 2014; 36: 104–116. https://doi.org/10.1093/plankt/fbt095
11. Ruz PM, Hidalgo P, Escribano R, Keister JE, Yebra L, Franco-Cisterna B. Hypoxia effects on females and early stages of Calanus chilensis in the Humboldt Current ecosystem (23˚S). J Exp Mar Bio Ecol. 2018; 498: 61–71. https://doi.org/10.1016/j.jembe.2017.09.018
12. Thor P, Dupont S. Transgenerational effects alleviate severe fecundity loss during ocean acidification in a ubiquitous planktonic copepod. Glob Chang Biol. 2015; 21: 2261–2271. https://doi.org/10.1111/gcb.12815 PMID: 25430823
13. Lewis CN, Brown KA, Edwards LA, Cooper G, Findlay HS. Sensitivity to ocean acidification parallels natural pCO2 gradients experienced by Arctic copepods under winter sea ice. Proc Natl Acad Sci. 2013; 110: E4960–E4967. https://doi.org/10.1073/pnas.1315162110 PMID: 24297880
14. Peterson WT, Bellantoni DC. Relationships between water-column stratification, phytoplankton cell size and copepod fecundity in long island sound and off central Chile. South African J Mar Sci. 1987; 5: 411–421. https://doi.org/10.2989/025776187784522748
15. Williams R, Conway DVP, Hunt HG. The role of copepods in the planktonic ecosystems of mixed and stratified waters of the European shelf seas. Hydrobiologia. 1994; 292–293: 521–530. https://doi.org/10.1007/BF00229980
16. Kiørbe T, Nielsen TG. Regulation of zooplankton biomass and production in a temperate, coastal ecosystem. 1. Copepods. 1994; 39: 493–507. Available: https://play.google.com/store/apps/details?id=com.evozi.deviceid&hl=pl

17. Berline L, Siokou-Frangou I, Marasovic I, Vidjak O, Fernández de Puelles ML, Mazzocchi MG, et al. Intercomparison of six Mediterranean zooplankton time series. Prog Oceanogr. 2012; 97–100: 76–91. https://doi.org/10.1016/j.pocean.2011.11.011

18. Pino-Pinuer P, Escribano R, Hidalgo P, Riquelme-Bugueño R, Schneider W. Copepod community response to variable upwelling conditions off central-southern Chile during 2002–2004 and 2010–2012. Mar Ecol Prog Ser. 2014; 515: 83–95. https://doi.org/10.3354/meps11001

19. Medellín-Mora J, Escribano R, Schneider W. Community response of zooplankton to oceanographic changes (2002–2012) in the central/southern upwelling system of Chile. Prog Oceanogr. 2016; 142: 17–29. https://doi.org/10.1016/j.pocean.2016.01.005

20. Frederick L, Escribano R, Morales CE, Hormazabal S, Medellín-Mora J. Mesozooplankton respiration and community structure in a seamount region of the eastern South Pacific. Deep Res Part I. 2018; 135: 74–87. https://doi.org/10.1016/j.dsr.2018.03.008

21. Costello MJ, Chaudhary C. Marine Biodiversity, Biogeography, Deep-Sea Gradients, and Conservation. Curr Biol. 2017; 27: R511–R527. https://doi.org/10.1016/j.cub.2017.04.060 PMID: 28586689

22. Ocean Biogeografic Information System (OBIS). Available: http://iobis.org/

23. Rombouts I, Beaugrand G, Ibañez F, Gasparini S, Chiba S, Legendre L. Global latitudinal variations in marine copepod diversity and environmental factors. Proc R Soc B Biol Sci. 2009; 276: 3053–3062. https://doi.org/10.1098/rspb.2009.0742 PMID: 19515670

24. Hooff RC, Peterson WT. Copepod Biodiversity as an Indicator of Changes in Ocean and Climate Conditions of the Northern California Current Ecosystem. Limnol Oceanogr. 2006; 51: 2607–2620.

25. Brandão MC, Benedetti F, Martini S, Soviadan YD, Irisson JO, Romagnan JB, et al. Macroscale patterns of oceanic zooplankton composition and size structure. Sci Rep. 2021; 11: 1–19. https://doi.org/10.1038/s41598-021-94615-5 PMID: 34344925

26. Muller-Karger FE, Canonico G, Aguilar CB, Bax NJ, Appeltans W, Yarincik K, et al. Marine Life 2030: building global knowledge of marine life for local action in the Ocean Decade. ICES J Mar Sci. 2023; 80: 355–357. https://doi.org/10.1093/icesjms/fsac084

27. Reid JL, Brinton E, Fleminger A, Venrick EL, McGowan JA. Ocean Circulation and Marine Life. Adv Oceanogr. 1978; 65–130. https://doi.org/10.1007/978-1-4615-8273-1_3

28. Wright DH. Species-energy theory: an extension of species-area theory. Oikos. 1983; 41: 496–506.

29. Currie DJ. Energy and large-scale patterns of animal and plant species richness. Am Nat. 1991; 137: 27–49. https://doi.org/10.1086/285144

30. Allen AP, Brown JH, Gillooly JF. Global biodiversity, biochemical kinetics, and the energetic-equivalence rule. Science (80-). 2002; 297: 1545–1548. https://doi.org/10.1126/science.1072380 PMID: 12202828

31. Rohde K. Latitudinal Gradients in Species Diversity: The Search for the Primary Cause. Oikos. 1992; 65: 514–527.

32. Roy K, Jablonski D, Valentine JW, Rosenberg G. Marine latitudinal diversity gradients: Tests of causal hypotheses. Proc Natl Acad Sci. 2002; 95: 3699–3702. https://doi.org/10.1073/pnas.95.7.3699 PMID: 9520429

33. Brown JH, Gillooly JF, Allen AP, Savage VM, West GB. Toward a metabolic theory of ecology. Ecology. 2004; 85: 1771–1789.

34. Tittensor DP, Mora C, Jetz W, Lotze HK, Ricard D, Berghe E Vanden, et al. Global patterns and predictors of marine biodiversity across taxa. Nature. 2010; 466: 1098–1101. https://doi.org/10.1038/nature09329 PMID: 20668450

35. Beaugrand G, Edwards M, Legendre L. Marine biodiversity, ecosystem functioning, and carbon cycles. Proc Natl Acad Sci. 2010; 107: 10120–10124. https://doi.org/10.1073/pnas.0913855107 PMID: 20479247

36. Woodd-Walker RS, Ward P, Clarke A. Large-scale patterns in diversity and community structure of surface water copepods from the Atlantic Ocean. Mar Ecol Prog Ser. 2002; 236: 189–203. https://doi.org/10.3354/meps236189

37. Richardson AJ, Schoeman DS. Climate impact on plankton ecosystems in the Northeast Atlantic. Science (80-). 2004; 305: 1609–1612. https://doi.org/10.1126/science.1100958 PMID: 15361622

38. González CE, Medellín-Mora J, Escribano R. Environmental Gradients and Spatial Patterns of Calanoid Copepods in the Southeast Pacific. Front Ecol Evol. 2020; 8: 1–16. https://doi.org/10.3389/fevo.2020.554409

39. Suckow MA, Weisbroth SH, Franklin CL. Temperature in the oceans. Seawater: Its Composition, Properties and Behaviour. 1995. pp. 14–28. https://doi.org/10.1016/B978-075063715-2/50003-4

40. Ibarbalz FM, Henry N, Brandão MC, Martini S, Busseni G, Byrne H, et al. Global Trends in Marine Plankton Diversity across Kingdoms of Life. Cell. 2019; 179: 1084–1097.e21. https://doi.org/10.1016/j.cell.2019.10.008 PMID: 31730851

41. Rombouts I, Beaugrand G, Ibañez F, Gasparini S, Chiba S, Legendre L. A multivariate approach to large-scale variation in marine planktonic copepod diversity and its environmental correlates. Limnol Oceanogr. 2010; 55: 2219–2229. https://doi.org/10.4319/lo.2010.55.5.2219

42. Costello MJ, Cheung A, De Hauwere N. Surface Area and the Seabed Area, Volume, Depth, Slope, and Topographic Variation for the World's Seas, Oceans, and Countries. Environ Sci Technol. 2010; 44: 8821–8828. https://doi.org/10.1021/es1012752 PMID: 21033734

43. International Hydrographic Organization. Limits of Oceans and Seas, 3rd Edition. Mónaco; 1953. pp. 1–42.

44. International Hydrographic Organization. South Pacific Ocean and its sub-divisions. 4th Editio. Limits of Oceans and Seas, 4th Edition. 4th Editio. Mónaco; 2002. pp. 1–16. Available: https://www.iho.int/mtg_docs/com_wg/S-23WG/S-23WG_Misc/Draft_2002/Draft_2002.htm

45. Provoost P, Bosch S. robis: Ocean Biodiversity Information System (OBIS) Client. R package version 2.8.2. 2021. Available: https://cran.r-project.org/package=robis

46. Wickham H, Hester J, Chang W. devtools: Tools to Make Developing R Packages Easier. R package version 2.4.3. 2021. Available: https://cran.r-project.org/package=devtools

47. Desportes C, Drévillon M, Clavier M, Gounou A. Global Ocean Ensemble Physics Reanalysis—Low resolution. Available: https://data.marine.copernicus.eu/product/GLOBAL_REANALYSIS_PHY_001_026/description

48. Le Galloudec O, Perruche C, Derval C, Tressol M, Dussurget R. Global ocean biogeochemistry hindcast. Available: https://data.marine.copernicus.eu/product/GLOBAL_MULTIYEAR_BGC_001_029/description

49. Guinehut S. Multi Observation Global Ocean 3D Temperature Salinity Height Geostrophic Current and MLD. Available: https://data.marine.copernicus.eu/product/MULTIOBS_GLO_PHY_TSUV_3D_MYNRT_015_012/description

50. Owens HL, Guralnick R. climateStability: An R package to estimate climate stability from time-slice climatologies. Biodivers Informatics. 2019; 14: 8–13. https://doi.org/10.17161/bi.v14i0.9786

51. Genuer R, Poggi J-M, Tuleau-Malot C. Variable Selection Using Random Forests. 2019. Available: https://cran.r-project.org/web/packages/VSURF/VSURF.pdf

52. Genuer R, Poggi J-M, Tuleau-Malot C. VSURF: An R Package for Variable Selection Using Random Forests. R J. 2015; 7: 19–33. Available: https://journal.r-project.org/archive/2015-2/genuer-poggi-tuleaumalot.pdf

53. Barbosa AM. fuzzySim: Applying fuzzy logic to binary similarity indices in ecology. Methods Ecol Evol. 2015; 6: 853–858. https://doi.org/10.1111/2041-210X.12372

54. Hammer Ø, Harper DAT, Ryan PD. Past: Paleontological Statistics Software Package for Education and Data Analysis. Palaeontol Electron. 2001; 4: 9pp. Available: http://palaeo-electronica.orghttp://palaeo-electronica.org/2001_1/past/issue1_01.htm.

55. Getis A, Ord JK. The Analysis of Spatial Association by Use of Distance Statistics. Geogr Anal. 1992; 24: 189–206. https://doi.org/10.1111/j.1538-4632.1992.tb00261.x

56. Swingland IR. Biodiversity, Definition of. Encycl Biodivers. 2013; 1: 377–391. https://doi.org/10.1016/B978-0-12-384719-5.00009–5

57. Koleff P, Gaston KJ, Lennon JJ. Measuring beta diversity for presence–absence data. J Anim Ecol. 2003; 72: 367–382. https://doi.org/10.1007/s00228-017-2223-5

58. Baselga A, Gómez-Rodríguez C. Alpha, beta and gamma diversity: measuring differences in biological communities. Nov Acta Científica Compostel. 2019; 26: 39–45.

59. Qian H, Ricklefs RE, White PS. Beta diversity of angiosperms in temperate floras of eastern Asia and eastern North America. Ecol Lett. 2005; 8: 15–22. https://doi.org/10.1111/j.1461-0248.2004.00682.x

60. Laffan SW, Lubarsky E, Rosauer DF. Biodiverse, a tool for the spatial analysis of biological and related diversity. Ecography (Cop). 2010; 33: 643–647. https://doi.org/10.1111/j.1600-0587.2010.06237.x

61. Baselga A, Orme CDL. Betapart: An R package for the study of beta diversity. Methods Ecol Evol. 2012; 3: 808–812. https://doi.org/10.1111/j.2041-210X.2012.00224.x

62. Sanches Melo A. Package "CommEcol", Community Ecology Analyses. 2021. pp. 1–34.

63. Vilela B, Villalobos F. LetsR: A new R package for data handling and analysis in macroecology. Methods Ecol Evol. 2015; 6: 1229–1234. https://doi.org/10.1111/2041-210X.12401

64. Laffan SW. Indices available in Biodiverse. 2022. Available: https://github.com/shawnlaffan/biodiverse/wiki/Indices#simpson-and-shannon

65. Hsieh TC, Ma KH, Chao A. iNEXT: an R package for rarefaction and extrapolation of species diversity (Hill numbers). Methods Ecol Evol. 2016; 7: 1451–1456. https://doi.org/10.1111/2041-210X.12613

66. Hamilton S. Ocean Currents Data and Map. Harvard Dataverse, V1; 2018. https://doi.org/10.7910/DVN/TKGO2Z

67. Crase B, Liedloff AC, Wintle BA. A new method for dealing with residual spatial autocorrelation in species distribution models. Ecography (Cop). 2012; 35: 879–888. https://doi.org/10.1111/j.1600-0587.2011.07138.x

68. Bivand RS, Wong DWS. Comparing implementations of global and local indicators of spatial association. Test. 2018; 27: 716–748. https://doi.org/10.1007/s11749-018-0599-x

69. Bivand R. spdep: Spatial Dependence: Weighting Schemes, Statistics. 2023. p. 168. https://doi.org/10.1111/gean.12319

70. Fabozzi FJ, Focardi SM, Rachev ST, Arshanapalli BG. Model Selection Criterion: AIC and BIC. The Basics of Financial Econometrics. John Wiley & Sons, Inc.; 2014. pp. 399–403. https://doi.org/10.1002/9781118856406.app5

71. Bartoń K. Package MuMIn: Multi-Model Inference. 2022. Available: https://cran.r-project.org/web/packages/MuMIn/

72. Mokany K, Ware C, Woolley SNC, Ferrier S, Fitzpatrick MC. A working guide to harnessing generalized dissimilarity modelling for biodiversity analysis and conservation assessment. Glob Ecol Biogeogr. 2022; 31: 802–821. https://doi.org/10.1111/geb.13459

73. Fitzpatrick M, Mokany K, Manion G, Nieto-Lugilde D, FFerrier S, Lisk M, et al. Package "gdm." 2022. https://doi.org/10.1111/geb.13459

74. Schneider W, Fukasawa M, Garcés-Vargas J, Bravo L, Uchida H, Kawano T, et al. Spin-up of South Pacific subtropical gyre freshens and cools the upper layer of the eastern South Pacific Ocean. Geophys Res Lett. 2007; 34: 1–5. https://doi.org/10.1029/2007GL031933

75. Reid J. On the total geostrophic circulation of the South Pacific Ocean: Flow patterns. Tracers. 1986; and transp: Vol. 16.

76. Qu T, Lindstrom EJ. A Climatological Interpretation of the Circulation in the Western South Pacific*. J Phys Oceanogr. 2011; 32: 2492–2508. https://doi.org/10.1175/1520-0485-32.9.2492

77. Ganachaud A, Cravatte S, Melet A, Schiller A, Holbrook NJ, Sloyan BM, et al. The Southwest Pacific circulation and climate experiment (SPICE). J Geophys Res Ocean. 2014; 119: 7660–7686. https://doi.org/10.1002/2013JC009678.Received

78. Ridgway KR, Dunn JR. Mesoscale structure of the mean East Australian Current System and its relationship with topography. Prog Oceanogr. 2003; 56: 189–222. https://doi.org/10.1016/S0079-6611(03)00004-1

79. Rintoul SR, Hughes CW, Olbers D. The Antarctic Circumpolar Current System. In: Siedler G, Church J, Gould J, editors. Ocean Circulation and Climate: Observing and Modelling the Global Ocean. 2001. pp. 271–302.

80. Stramma L, Peterson RG, Tomczak M. The South Pacific Current. J Phys Oceanogr. 1995; 25: 77–91. https://doi.org/10.1175/1520-0485(1995)025<0077:tspc>2.0.co;2

81. Montecino V, Lange CB. The Humboldt Current System: Ecosystem components and processes, fisheries, and sediment studies. Prog Oceanogr. 2009; 83: 65–79. https://doi.org/10.1016/j.pocean.2009.07.041

82. Merino-Campos V, De Pol-Holz R, Southon J, Latorre C, Collado-Fabbri S. Marine radiocarbon reservoir age along the chilean continental margin. Radiocarbon. 2019; 61: 195–210. https://doi.org/10.1017/RDC.2018.81

83. García-Reyes M, Sydeman WJ, Schoeman DS, Rykaczewski RR, Black BA, Smit AJ, et al. Under Pressure: Climate Change, Upwelling, and Eastern Boundary Upwelling Ecosystems. Front Mar Sci. 2015; 2: 1–10. https://doi.org/10.3389/fmars.2015.00109

84. Strub PT, Mesías JM, Montecino V, Rutllant J, Salinas S. Coastal Ocean Circulation off Western South America. Volume 11. The Sea. Volume 11. John Wiley & Sons, Inc.; 1998. pp. 273–313.

85. Ancapichun, Santiago; Garcés-Vargas J. Variability of the Southeast Pacific Subtropical Anticyclone and its impact on sea surface temperature off north-central Chile. Ciencias Mar. 2015; 41: 1–20. https://doi.org/10.7773/cm.v41i1.2338

86. Carlotti F, Pagano M, Guilloux L, Donoso K, Valdés V, Grosso O, et al. Meso-zooplankton structure and functioning in the western tropical South Pacific along the 20th parallel south during the OUTPACE survey (February-April 2015). Biogeosciences. 2018; 15: 7273–7297. https://doi.org/10.5194/bg-15-7273-2018

87. Le Borgne R, Rodier M. Net zooplankton and the biological pump: A comparison between the oligotrophic and mesotrophic equatorial Pacific. Deep Res Part II Top Stud Oceanogr. 1997; 44: 2003–2023. https://doi.org/10.1016/S0967-0645(97)00034-9

88. Le Borgne R, Champalbert G, Gaudy R. Mesozooplankton biomass and composition in the equatorial Pacific along 180. J Geophys Res Ocean. 2003; 108: 1–10. https://doi.org/10.1029/2000jc000745

89. Dai L, Li C, Yang G, Sun X. Zooplankton abundance, biovolume and size spectra at western boundary currents in the subtropical North Pacific during winter 2012. J Mar Syst. 2016; 155: 73–83. https://doi.org/10.1016/j.jmarsys.2015.11.004

90. Fernández-Álamo MA, Färber-Lorda J. Zooplankton and the oceanography of the eastern tropical Pacific: A review. Prog Oceanogr. 2006; 69: 318–359. https://doi.org/10.1016/j.pocean.2006.03.003

91. Pennington JT, Mahoney KL, Kuwahara VS, Kolber DD, Calienes R, Chavez FP. Primary production in the eastern tropical Pacific: A review. Prog Oceanogr. 2006; 69: 285–317. https://doi.org/10.1016/j.pocean.2006.03.012

92. Dunstan PK, Hayes D, Woolley S, Allain V, Leduc D, Flynn A, et al. Bioregions of the South West Pacific Ocean. 2018. Available: https://rmi-data.sprep.org/system/files/Preliminary-worskop-report-Pacific_v2_1.pdf

93. Hidalgo P, Escribano R, Vergara O, Jorquera E, Donoso K, Mendoza P. Patterns of copepod diversity in the Chilean coastal upwelling system. Deep Res Part II. 2010; 57: 2089–2097. https://doi.org/10.1016/j.dsr2.2010.09.012

94. Dolan JR, Lemée R, Gasparini S, Mousseau L, Heyndrickx C. Probing diversity in the plankton: using patterns in Tintinnids (planktonic marine ciliates) to identify mechanisms. Hydrobiologia. 2006; 555: 143–157. https://doi.org/10.1007/s10750-005-1112-6

95. Rutherford S, Hondt SD, Prell W. Environmental controls on the geographic distribution of zooplankton diversity. Nature. 1999; 400: 749–753.

96. Worm B, Sandow M, Oschlies A, Lotze HK, Myers RA. Global patterns of predator diversity in the open oceans. Science (80-). 2005; 309: 1365–1369. https://doi.org/10.1126/science.1113399 PMID: 16051749

97. McGowan JA, Walker PW. Structure in the Copepod Community of the North Pacific Central Gyre. Ecol Monogr. 1979; 49: 195–226. Available: http://www.jstor.org/stable/1942513

98. Vereshchaka A, Abyzova G, Lunina A, Musaeva E. The deep-sea zooplankton of the North, Central, and South Atlantic: Biomass, abundance, diversity. Deep Res Part II Top Stud Oceanogr. 2017; 137: 89–101. https://doi.org/10.1016/j.dsr2.2016.06.017

99. Rivera R, Escribano R, González CE, Pérez-Aragón M. Modeling present and future distribution of plankton populations in a coastal upwelling zone: the copepod Calanus chilensis as a study case. Sci Rep. 2023; 13. https://doi.org/10.1038/s41598-023-29541-9 PMID: 36823290

100. Rigby S, Milsom C. Benthic origins of zooplankton: An environmentally determined macroevolutionary effect. Geology. 1996; 24: 52–54. https://doi.org/10.1130/0091-7613(1996)024<0052:BOOZAE>2.3.CO;2

101. Bradford-Grieve JM. Colonization of the pelagic realm by calanoid copepods. Hydrobiologia. 2002; 485: 223–244. https://doi.org/10.1023/A:1021373412738

102. Braga E, Zardoya R, Meyer A, Yen J. Mitochondrial and nuclear rRNA based copepod phylogeny with emphasis on the Euchaetidae (Calanoida). Mar Biol. 1999; 133: 79–90. https://doi.org/10.1007/s002270050445

103. Dormann CF, Elith J, Bacher S, Buchmann C, Carl G, Carré G, et al. Collinearity: A review of methods to deal with it and a simulation study evaluating their performance. Ecography (Cop). 2013; 36: 27–46. https://doi.org/10.1111/j.1600-0587.2012.07348.x

104. Sverdrup HU, Johnson MW, Fleming RH. Dissolved Gases in Sea Water. Chapter VI: Chemistry of Sea Water. The Oceans: Their Physics, Chemistry, and General Biology. New York: Prentice-Hall, Inc.; 1942. pp. 186–191. Available: https://publishing.cdlib.org/ucpressebooks/view?docId=kt167nb66r;brand=eschol

105. White JR, Zhang X, Welling LA, Roman MR, Dam HG. Latitudinal gradients in zooplankton biomass in the tropical Pacific at 140˚W during the JGOFS EqPac study: Effects of El Niño. Deep Res Part II. 1995; 42: 715–733. https://doi.org/10.1016/0967-0645(95)00033-M

106. Forster J, Hirst AG, Atkinson D. Warming-induced reductions in body size are greater in aquatic than terrestrial species. Proc Natl Acad Sci U S A. 2012; 109: 19310–19314. https://doi.org/10.1073/pnas.1210460109 PMID: 23129645

107. Roman MR, Pierson JJ. Interactive Effects of Increasing Temperature and Decreasing Oxygen on Coastal Copepods. Biol Bull. 2022; 000–000. https://doi.org/10.1086/722111 PMID: 36548979

108. Wishner KF, Seibel B, Outram D. Ocean deoxygenation and copepods: Coping with oxygen minimum zone variability. Biogeosciences. 2020; 17: 2315–2339. https://doi.org/10.5194/bg-17-2315-2020

109. Paffenhöfer G-A. Oxygen consumption in relation to motion of marine planktonic copepods. Mar Ecol Prog Ser. 2006; 317: 187–192.

110. Cervetto G, Gaudy R, Pagano M. Influence of salinity on the distribution of Acartia tonsa (Copepoda, Calanoida). J Exp Mar Bio Ecol. 1999.

111. Vuorinen I, Hänninen J, Viitasalo M, Helminen U, Kuosa H. Proportion of copepod biomass declines with decreasing salinity in the Baltic Sea. ICES J Mar Sci. 1998.

112. Choi SY, Lee EH, Soh HY, Jang MC. Effects of Temperature and Salinity on Egg Production, Hatching, and Mortality Rates in Acartia ohtsukai (Copepoda, Calanoida). Front Mar Sci. 2021; 8. https://doi.org/10.3389/fmars.2021.704479

113. Dutz J, Christensen AM. Broad plasticity in the salinity tolerance of a marine copepod species, Acartia longiremis, in the Baltic Sea. J Plankton Res. 2018; 40: 342–355. https://doi.org/10.1093/plankt/fby013

114. Milione M, Zeng C. The effects of temperature and salinity on population growth and egg hatching success of the tropical calanoid copepod, Acartia sinjiensis. Aquaculture. 2008; 275: 116–123. https://doi.org/10.1016/j.aquaculture.2007.12.010

115. Lee SH, Lee MC, Puthumana J, Park JC, Kang S, Hwang DS, et al. Effects of salinity on growth, fatty acid synthesis, and expression of stress response genes in the cyclopoid copepod Paracyclopina nana. Aquaculture. 2017; 470: 182–189. https://doi.org/10.1016/j.aquaculture.2016.12.037

116. Pörtner HO. Climate variations and the physiological basis of temperature dependent biogeography: Systemic to molecular hierarchy of thermal tolerance in animals. Comp Biochem Physiol—A Mol Integr Physiol. 2002; 132: 739–761. https://doi.org/10.1016/s1095-6433(02)00045-4 PMID: 12095860

117. Elliott DT, Tang KW. Influence of carcass abundance on estimates of mortality and assessment of population dynamics in acartia tonsa. Mar Ecol Prog Ser. 2011; 427: 1–12. https://doi.org/10.3354/meps09063

118. Sorte CJB, Jones SJ, Miller LP. Geographic variation in temperature tolerance as an indicator of potential population responses to climate change. J Exp Mar Bio Ecol. 2011; 400: 209–217. https://doi.org/10.1016/j.jembe.2011.02.009

119. Mackas DL, Batten S, Trudel M. Effects on zooplankton of a warmer ocean: Recent evidence from the Northeast Pacific. Prog Oceanogr. 2007; 75: 223–252. https://doi.org/10.1016/j.pocean.2007.08.010

120. Barton AD, Pershing AJ, Litchman E, Record NR, Edwards KF, Finkel Z V., et al. The biogeography of marine plankton traits. Ecol Lett. 2013; 16: 522–534. https://doi.org/10.1111/ele.12063 PMID: 23360597

121. Benedetti F, Wydler J, Vogt M. Copepod functional traits and groups show contrasting biogeographies in the global ocean. BioRxiv. 2022. https://doi.org/10.1101/2022.02.24.481747

122. González CE, Goetze E, Escri R, Ulloa O, Victoriano P. Genetic diversity and novel lineages in the cosmopolitan copepod Pleuromamma abdominalis in the Southeast Pacific. Sci Rep. 2020; 1–15. https://doi.org/10.1038/s41598-019-56935-5 PMID: 31980660

123. Turner JT. Latitudinal Patterns of Calanoid and Cyclopoid Copepod Diversity in Estuarine Waters of Eastern North America. J Biogeogr. 1981; 8: 369–382. https://doi.org/10.2307/2844757

124. Cornils A, Blanco-Bercial L. Phylogeny of the Paracalanidae Giesbrecht, 1888 (Crustacea: Copepoda: Calanoida). Mol Phylogenet Evol. 2013; 69: 861–872. https://doi.org/10.1016/j.ympev.2013.06.018 PMID: 23831457

125. Escribano R, Bustos-ríos E, Hidalgo P, Morales CE. Non-limiting food conditions for growth and production of the copepod community in a highly productive upwelling zone. Cont Shelf Res. 2016; 126: 1–14. https://doi.org/10.1016/j.csr.2016.07.018

126. Brun P, Payne MR, Kiørboe T. A trait database for marine copepods. Earth Syst Sci Data. 2017; 9: 99–113. https://doi.org/10.5194/essd-9-99-2017

127. Medellín-Mora J, Escribano R, Corredor-Acosta A, Hidalgo P, Schneider W. Uncovering the Composition and Diversity of Pelagic Copepods in the Oligotrophic Blue Water of the South Pacific Subtropical Gyre. Front Mar Sci. 2021; 8: 1–18. https://doi.org/10.3389/fmars.2021.625842

128. Razouls C, Desreumaux N, Kouwenberg J, de Bovée F. Biodiversity of Marine Planktonic Copepods (morphology, geographical distribution and biological data), 2005–2023. In: Sorbonne University, CNRS. [Internet]. 2023 [cited 25 Jan 2024]. Available: http://copepodes.obs-banyuls.fr/en

129. Boakes EH, McGowan PJK, Fuller RA, Chang-Qing D, Clark NE, O'Connor K, et al. Distorted views of biodiversity: Spatial and temporal bias in species occurrence data. PLoS Biol. 2010;8. https://doi.org/10.1371/journal.pbio.1000385 PMID: 20532234

130. Hortal J, De Bello F, Diniz-Filho JAF, Lewinsohn TM, Lobo JM, Ladle RJ. Seven Shortfalls that Beset Large-Scale Knowledge of Biodiversity. Annu Rev Ecol Evol Syst. 2015; 46: 523–549. https://doi.org/10.1146/annurev-ecolsys-112414-054400

131. Ball-Damerow JE, Brenskelle L, Barve N, Soltis PS, Sierwald P, Bieler R, et al. Research applications of primary biodiversity databases in the digital age. PLoS One. 2019; 14. https://doi.org/10.1371/journal.pone.0215794 PMID: 31509534

132. Nelson G, Ellis S. The history and impact of digitization and digital data mobilization on biodiversity research. Philosophical Transactions of the Royal Society B: Biological Sciences. Royal Society Publishing; 2019. https://doi.org/10.1098/rstb.2017.0391 PMID: 30455209

133. Page LM, Macfadden BJ, Fortes JA, Soltis PS, Riccardi G. Digitization of Biodiversity Collections Reveals Biggest Data on Biodiversity. BioScience. Oxford University Press; 2015. pp. 841–842. https://doi.org/10.1093/biosci/biv104

134. Ariño AH. Approaches to estimating the universe of natural history collections data. Biodivers Informatics. 2010; 7: 81–92. https://doi.org/10.17161/bi.v7i2.3991

135. Isaac NJB, van Strien AJ, August TA, de Zeeuw MP, Roy DB. Statistics for citizen science: Extracting signals of change from noisy ecological data. Methods Ecol Evol. 2014; 5: 1052–1060. https://doi.org/10.1111/2041-210X.12254

136. García-Roselló E, Guisande C, Manjarrés-Hernández A, González-Dacosta J, Heine J, Pelayo-Villamil P, et al. Can we derive macroecological patterns from primary Global Biodiversity Information Facility data? Glob Ecol Biogeogr. 2015; 24: 335–347. https://doi.org/10.1111/geb.12260

137. Gaylord B, Gaines SD. Temperature or transport? Range limits in marine species mediated solely by flow. Am Nat. 2000; 155: 769–789. https://doi.org/10.1086/303357

138. Navarrete SA, Broitman B, Wieters EA, Finke GR, Venegas RM, Sotomayor A. Recruitment of intertidal invertebrates in the southeast Pacific: Interannual variability and the 1997–1998 El Niño. Limnol Ocean. 2002; 47: 791–802. Available: http://www.pfeg.noaa.gov

139. Watson JR, Hays CG, Raimondi PT, Mitarai S, Dong C, McWilliams JC, et al. Currents connecting communities: nearshore community similarity and ocean circulation. Ecology. 2011. https://doi.org/10.1890/10-1436.1 PMID: 21797147

140. Coleman MA, Feng M, Roughan M, Cetina-Heredia P, Connell SD. Temperate shelf water dispersal by Australian boundary currents: Implications for population connectivity. Limnol Oceanogr Fluids Environ. 2013; 3: 295–309. https://doi.org/10.1215/21573689-2409306

141. Wernberg T, Thomsen MS, Connell SD, Russell BD, Waters JM, Zuccarello GC, et al. The footprint of continental-scale ocean currents on the biogeography of seaweeds. PLoS One. 2013; 8. https://doi.org/10.1371/journal.pone.0080168 PMID: 24260352

Supporting Information

Pérez-Aragón et al. (2024) Biodiversity patterns of epipelagic copepods in the South Pacific Ocean: Strengths and limitations of current data bases

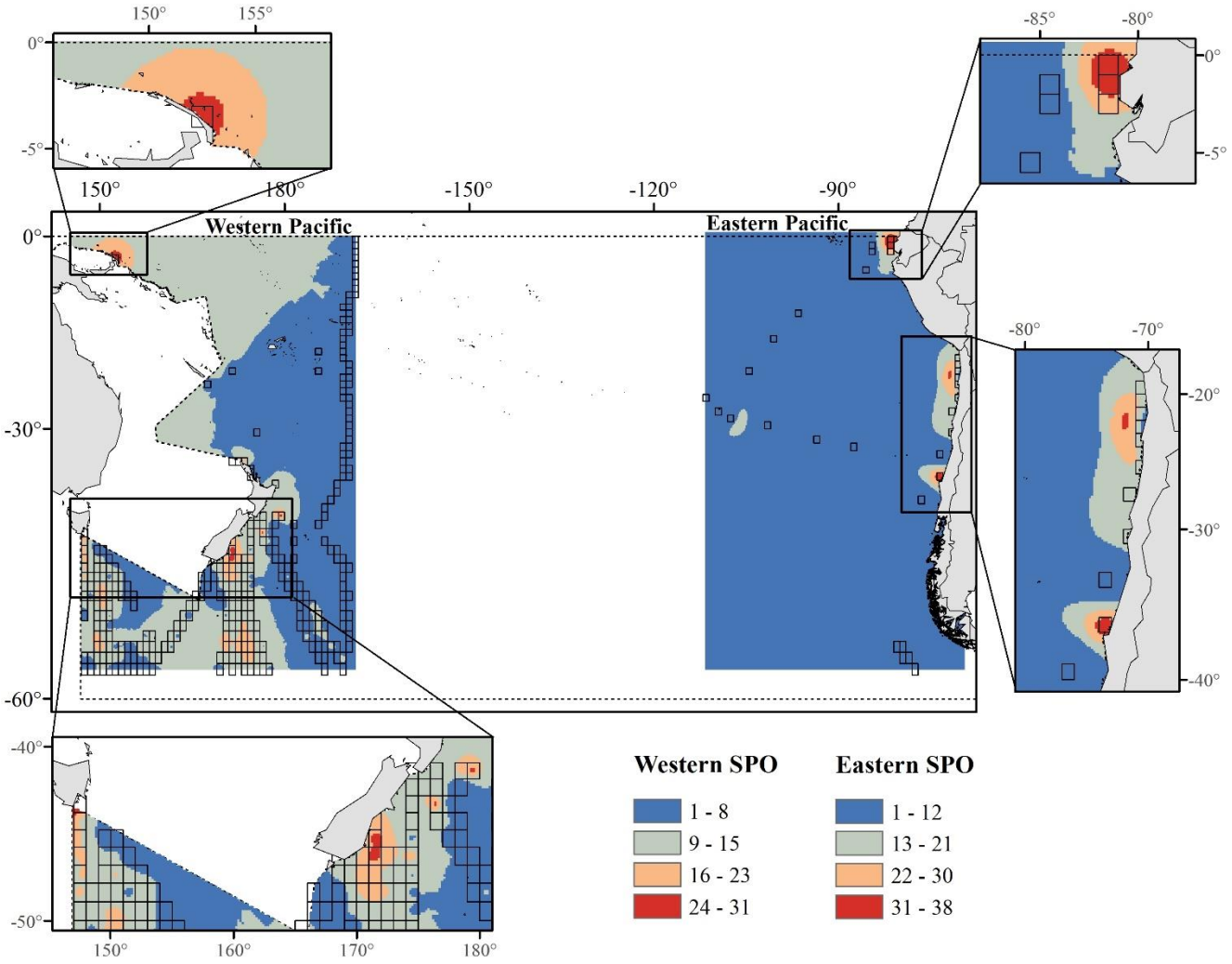

Figure S1: Kriging interpolation analysis done for the western and eastern side of the SPO with 394 cells accounting for number of genera. Transparent squares are the 1° sampled cells used for Kriging interpolation, whereas the grey dotted line delimits the South Pacific Ocean. Map projection is WGS 84/PDC Mercator (EPSG 3832).

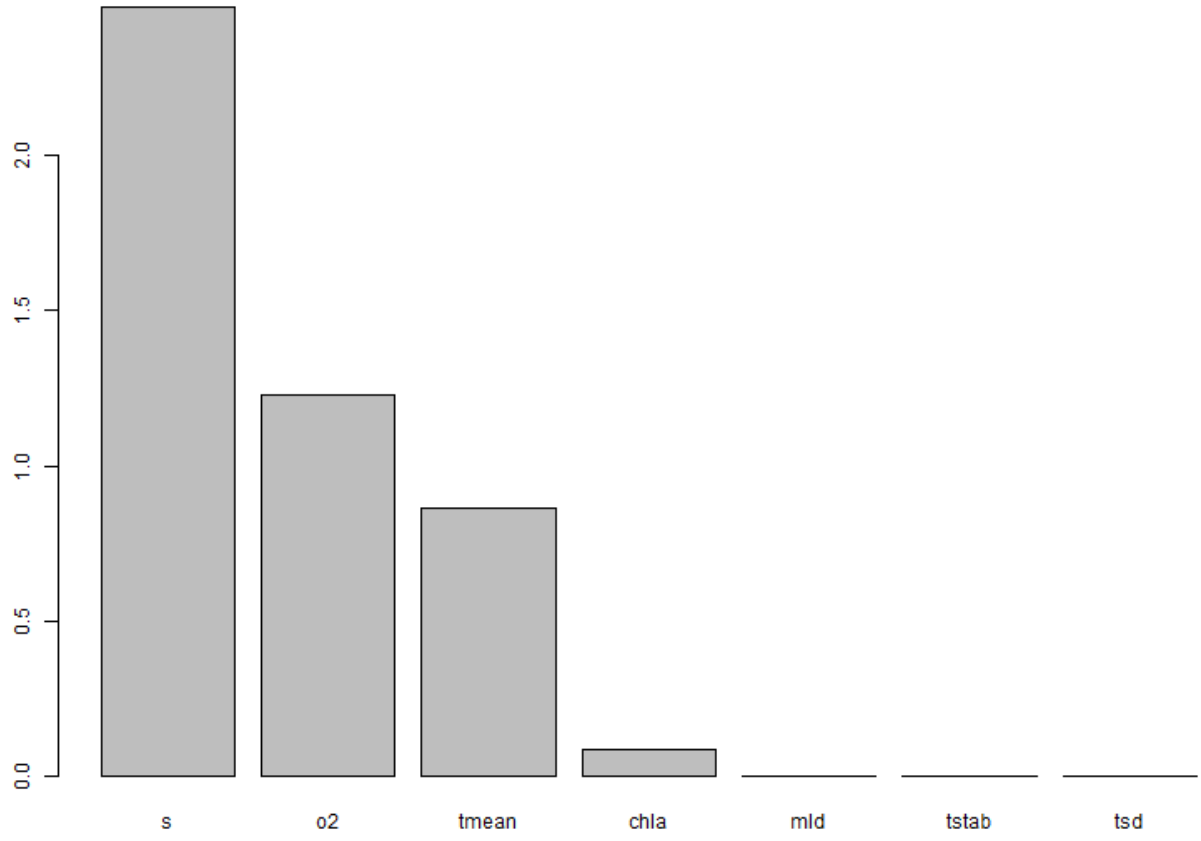

Figure S2: Maximum height of the spline function (hence the maximum value of the transformed predictors), indicating the stronger predictors of the observed dissimilarities for the Generalized Dissimilarity Modelling (GDM)-based spatial analysis. Their acronyms are: s = salinity, o2 = dissolved oxygen concentration, tmean = mean temperature, chla = chlorophyll-a concentration, mld = mixed layer depth, tstab= temperature stability, tsd = standard deviation of temperature. The spatial layers were generated and plotted with the predictors with heights over zero (i.e., s, o2, tmean and chla).

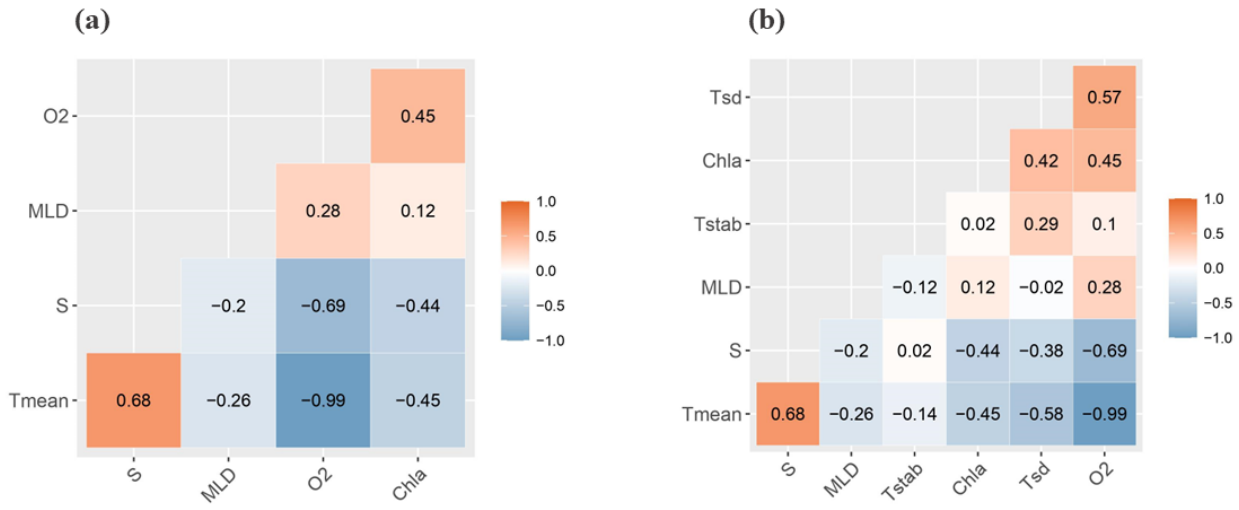

Figure S3: Spearman correlation matrices of environmental variables used in GAM models for (a) alfa diversity and (b) beta diversity. Positive correlations are displayed in red and negative correlations in blue color. Color intensity is proportional to the correlation coefficients. In the right side of the correlogram, the legend color shows the correlation coefficients and the corresponding colors. Their acronyms are: Tmean = mean temperature, Tstab= temperature stability, Tsd = standard deviation of temperature, S = salinity, Chla = chlorophyll-a concentration, O2 = dissolved oxygen concentration, MLD = mixed layer depth.

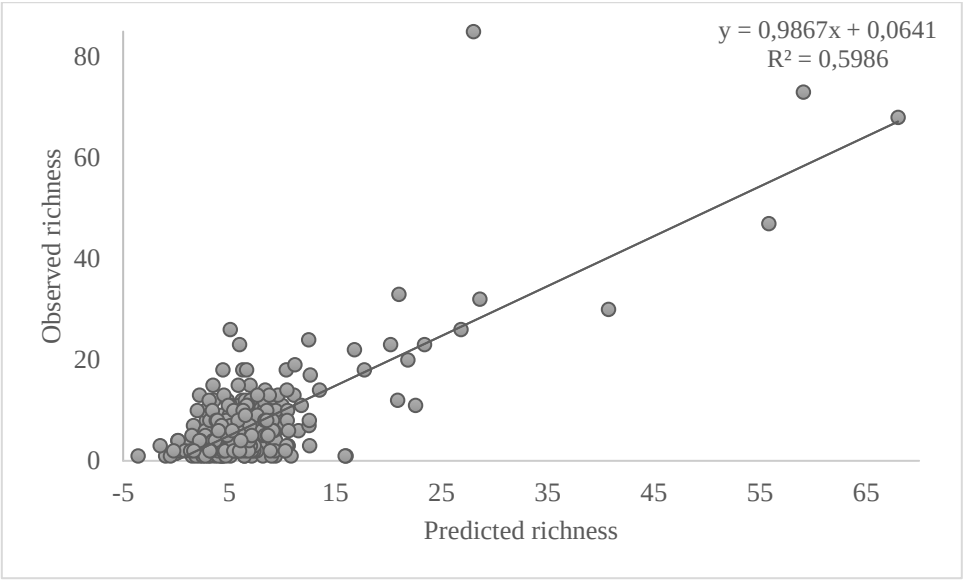

Figure S4: Correlation between observed and predicted species richness. Pearson's r coefficient: 0.77 (p-value<0.01). Negative residuals (below the reference line) indicate knowledge shortfalls, whereas positive residuals (above the reference line) indicate underestimated species richness.

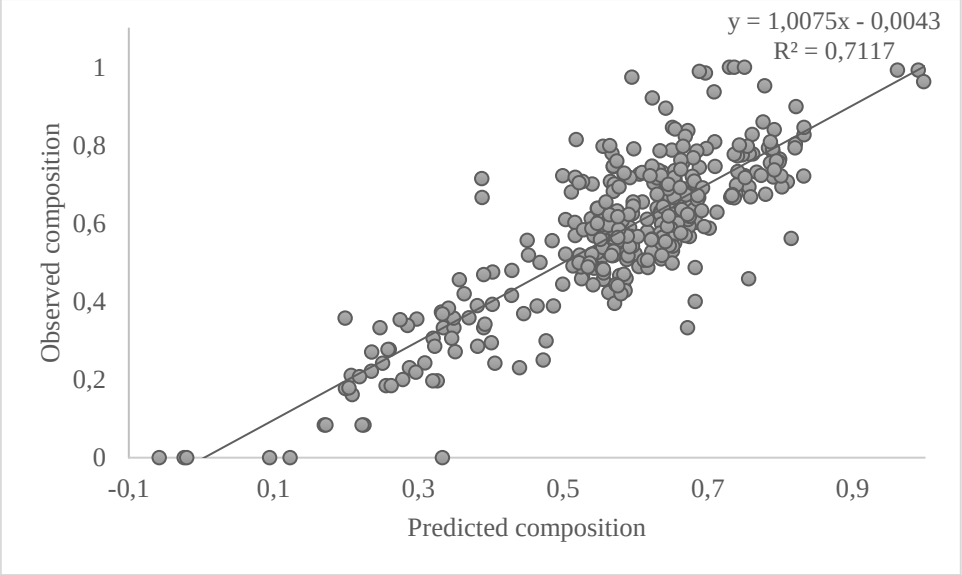

Figure S5: Correlation between observed and predicted species composition. Pearson's r coefficient: 0.84 (p-value<0.01). Negative residuals (below the reference line) indicate knowledge shortfalls, whereas positive residuals (above the reference line) indicate underestimated species composition.

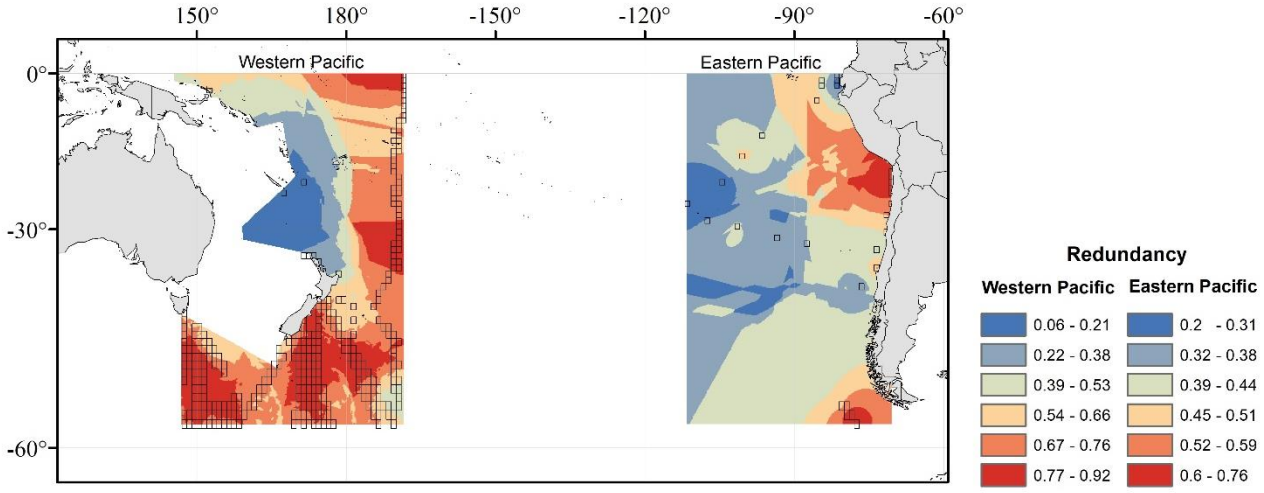

Figure S6: Redundancy index obtained for the western and eastern side of the SPO. Values close to 1 indicate good sampling, whereas values close to 0 indicate poor sampling. Transparent squares are the 1° sampled cells used for Kriging interpolation, whereas the grey dotted line delimits the South Pacific Ocean. Map projection is WGS 84/PDC Mercator (EPSG 3832).

Table S1: Dominant copepod species in terms of occurrence for the main surface current systems of the South Pacific Ocean. CHC=Cape Horn Current; EAC=East Australian Current; HCS=Humboldt Current System; SEC=South Equatorial Current; SPSG=South Pacific Subtropical Gyre; WWD=West Wind Drift.

	Species name	**Order**	**% of occurrence**
CHC	*Oithona similis*	Cyclopoida	61.8
	Calanus simillimus	Calanoida	36.4
	Pleuromamma robusta	Calanoida	1.8
EAC	*Oithona similis*	Cyclopoida	26.9
	Calanus simillimus	Calanoida	11.0
	Neocalanus tonsus	Calanoida	8.9
HCS	*Paracalanus indicus*	Calanoida	6.5
	Oithona similis	Cyclopoida	5.9
	Acartia tonsa	Calanoida	5.8
SEC	*Paracalanus parvus*	Calanoida	18.4
	Calocalanus kristalli	Calanoida	11.1
	Calocalanus plumulosus	Calanoida	11.1
SPSG	*Calocalanus kristalli*	Calanoida	42.2
	Paracalanus parvus	Calanoida	29.1
	Calocalanus plumulosus	Calanoida	14.6
WWD	*Calocalanus kristalli*	Calanoida	59.9
	Paracalanus parvus	Calanoida	27.9
	Calocalanus plumulosus	Calanoida	4.1

Table S2: Dominant copepod species of the South Pacific Ocean in terms of occurrence for all ranges values of beta diversity and its components turnover and nestedness.

	Species name	Order
Beta	*Acartia longiremis*	Calanoida
	Calocalanus kristalli	Calanoida
	Calocalanus pavo	Calanoida
	Paracalanus parvus	Calanoida
Turnover	*Acartia longiremis*	Calanoida
	Calocalanus kristalli	Calanoida
	Calocalanus plumulosus	Calanoida
	Paracalanus parvus	Calanoida
Nestedness	*Calocalanus pavo*	Calanoida
	Euterpina acutifrons	Harpacticoida
	Lucicutia flavicornis	Calanoida
	Mecynocera clausi	Calanoida

Table S3: Analysis of map overlay and Pearson correlation between the richness of species, genera and families.

Index	Overlap	Correlation
Species richness vs. family richness	0.799	0.549
Species richness vs. genus richness	0.883	0.850
Family richness vs. genus richness	0.881	0.787

4.2 Chapter 2: "The influence of environmental stability and upwelling variation on copepod diversity in the Humboldt Current System off Chile". Scientific manuscript submitted to "Frontiers in Ecology and Evolution" journal.

Abstract

The Humboldt Current System (HCS) is a highly dynamic upwelling system implying a strongly variable environment for zooplankton inhabiting the coastal zone. This variability has major consequences for population dynamics, community composition, and ultimately diversity patterns of planktonic copepods which dominate the bulk of zooplankton biomass. In this work, we tested the hypothesis that environmental stability is the key modulating mechanism of copepod diversity patterns in the HCS. We used a 17-years (1995-2011) database on species occurrence of copepods along with environmental data for the upper 500 m of the ocean (divided into five vertical strata) for the upwelling zone off Chile, distinguishing two regions (northern and southern) having different seasonal regimes of wind-driven upwelling. We estimated indices for copepod diversity and their distribution, segregated by regions and depth strata. The indices were then associated with oceanographic variables forced by upwelling intensity, along with an estimate of eddy kinetic energy (EKE), as a proxy of environmental stability. From the entire community, we found 18 dominant species widely distributed in the study area. Some were exclusive species for the upper depth stratum with differences in the number of exclusive species per region and depth. From Linear Mixed Models we found that the diversity indices significantly differed between regions and strata, and their variance was mainly explained by temperature, salinity, oxygen concentration, temperature stability, and eddy kinetic energy (EKE). Both temperature

stability and EKE were the best predictors of copepods diversity, suggesting that climate-oceanographic stability, forced by upwelling intensity, is the key driver for promoting and maintaining copepod diversity in the HCS.

Resumen

El Sistema de la Corriente de Humboldt (SCH) es un sistema de surgencia altamente dinámico que implica un ambiente muy variable para el zooplancton que habita la zona costera. Esta variabilidad tiene consecuencias importantes para la dinámica poblacional, la composición de la comunidad y, en última instancia, los patrones de diversidad de los copépodos planctónicos que dominan la mayor parte de la biomasa del zooplancton. En este trabajo, probamos la hipótesis de que la estabilidad ambiental es el mecanismo modulador clave de los patrones de diversidad de copépodos en el SCH. Utilizamos una base de datos de 17 años (1995-2011) sobre la ocurrencia de especies de copépodos junto con datos ambientales para los 500 m superiores del océano (divididos en cinco estratos verticales) para la zona de surgencia frente a Chile, distinguiendo dos regiones (norte y sur) con diferentes regímenes estacionales de surgencia impulsada por el viento. Estimamos índices para la diversidad de copépodos y su distribución, segregados por regiones y estratos de profundidad. Los índices fueron asociados con variables oceanográficas forzadas por la intensidad de surgencia, junto con una estimación de la energía cinética turbulenta (EKE), como un proxy de la estabilidad ambiental. De toda la comunidad, encontramos 18 especies dominantes ampliamente distribuidas en el área de estudio. Algunas son especies exclusivas para el estrato de profundidad superior con diferencias en el número de especies exclusivas por región y profundidad. A partir de modelos lineales mixtos, encontramos que los índices

de diversidad diferían significativamente entre regiones y estratos, y su varianza se explicaba principalmente por la temperatura, la salinidad, la concentración de oxígeno, la estabilidad de la temperatura y la energía cinética turbulenta (EKE). Tanto la estabilidad de la temperatura como la EKE fueron los mejores predictores de la diversidad de copépodos, lo que sugiere que la estabilidad climática-oceanográfica, forzada por la intensidad de surgencia, es el impulsor clave para promover y mantener la diversidad de copépodos en el SCH.

The influence of environmental stability and upwelling variation on copepod diversity in the Humboldt Current System off Chile

Manuela Pérez-Aragón[1], Reinaldo Rivera[2], Vera Oerder[2], Carolina E. González[2], Cristián E. Hernández[4,5] and Ruben Escribano[2,3]

[1] Doctoral Program in Oceanography, Facultad de Ciencias Naturales y Oceanográficas, Universidad de Concepción, P.O. Box 160 C, Concepción 4070386, Chile

[2] Instituto Milenio de Oceanografía, Universidad de Concepción, Concepción, Chile

[3] Department of Oceanography, Facultad de Ciencias Naturales y Oceanográficas, Universidad de Concepción, P.O. Box 160 C, Concepción 4070386, Chile

[4] Department of Zoology, Facultad de Ciencias Naturales y Oceanográficas, Universidad de Concepción, P.O. Box 160 C, Concepción 4070386, Chile

[5] Universidad Católica de Santa María, Urb. San José s/n, Umacollo, Arequipa, Perú

Correspondence to: Ruben Escribano (*rescribano@udec.cl*)

Abstract

The Humboldt Current System (HCS) is a highly dynamic upwelling system implying a strongly variable environment for zooplankton inhabiting the coastal zone. This variability has major consequences for population dynamics, community composition, and ultimately diversity patterns of planktonic copepods which dominate the bulk of zooplankton biomass. In this work, we tested the hypothesis that environmental stability is the key modulating mechanism of copepod diversity patterns in the HCS. We used a 17-years (1995-2011) database on species occurrence of copepods along with environmental data for the upper 500 m of the ocean (divided into five vertical strata) for the upwelling zone off Chile, distinguishing two regions (northern and southern) having different seasonal regimes of wind-driven upwelling. We estimated indices for copepod diversity and their distribution, segregated by regions and depth strata. The indices were then associated with oceanographic variables forced by upwelling intensity, along with an estimate of eddy kinetic energy (EKE), as a proxy of environmental stability. From the entire community, we found 18 dominant species widely distributed in the study area. Some were exclusive species for the upper depth stratum with differences in the number of exclusive species per region and depth. From Linear Mixed Models we found that the diversity indices significantly differed between regions and strata, and their variance was mainly explained by temperature, salinity, oxygen concentration, temperature stability, and eddy kinetic energy (EKE). Both temperature stability and EKE were the best predictors of copepods diversity, suggesting that climate-oceanographic stability, forced by upwelling intensity, is the key driver for promoting and maintaining copepod diversity in the HCS.

Introduction

The Humboldt Current System (HCS) extends from southern Chile (~42-45°S) to northern Peru and Ecuador (~4°S) (Montecino and Lange 2009; Thiel et al. 2007), being the largest of the four main Eastern Boundary Upwelling Systems, including the California, Canary, and Benguela Currents (García-Reyes et al. 2015). The HCS is also considered an important and unique biogeographic province that contains a large proportion of endemic fauna (Briggs and Bowen 2012; Costello et al. 2017; Spalding et al. 2007, 2012). It represents the equatorward-flowing, eastern portion of the basin-scale South Pacific Subtropical Gyre which, in terms of atmospheric forcing, is mainly influenced by the South Pacific Subtropical Anticyclone or the South Pacific High (Ancapichun and Garcés-Vargas 2015; Thiel et al. 2007), which spins counter-clockwise and is predominant off the west coast of South America (Schneider et al. 2007; Strub et al. 1998). The South Pacific Subtropical Anticyclone presents seasonal variation, abiding by its northern position (26°S, 86°W) during the late austral fall and winter, when it is also closer to the South American continent and its intensity is weaker. During austral spring and summer, it moves southwest (37°S, 108°W) and shows its maximum intensity (Ancapichun and Garcés-Vargas 2015). As a result, winds are upwelling-favorable during summer (all year round) southern (northern, respectively) than 30 °S (Montecino and Lange 2009). Four water masses have been found in the upper 500 m of the HCS: Subtropical Water (STW), Subantarctic Water (SAAW), Equatorial Subsurface Water (ESSW), and Antarctic Intermediate Water (AAIW) (Silva, Rojas, and Fedele 2009). Of these, STW and SAAW are surface waters containing the mixed layer. STW is found mostly in the north (<23°S) and the SAAW in the south (>28°S) (Silva et al. 2009). The HCS is also characterized by the presence of an Oxygen Minimum Zone (OMZ) caused by the shoaling of the oxygen-poor ESSW due to the upwelling events. This results in low concentrations of

dissolved oxygen near the surface (Morales, Hormazábal, and Blanco 1999). Therefore, the distribution of the OMZ along the water column in the HCS obeys latitudinal shifts in the upwelling regimes, with a shallower annual average depth of the upper OMZ in northern Chile (permanent upwelling) than in central south Chile (seasonal upwelling) (Yáñez, Hidalgo, and Escribano 2012).

Within the zooplankton community in the HCS, copepods are the most representative components (Escribano et al. 2007). These organisms respond rapidly to oceanographic and environmental variations (Escribano et al. 2014; Medellín-Mora, Escribano, and Schneider 2016; Peterson and Bellantoni 1987; Pino-Pinuer et al. 2014; Ruz et al. 2018; Yáñez et al. 2012). In the HCS, a large part of the oceanographic variation is controlled by changes in the wind-driven upwelling over a variety of time and spatial scales. Upwelling variation can have a major influence on the ecophysiology and distribution of copepods (Escribano and Hidalgo 2000; Peterson 1998), ultimately affecting their diversity patterns (Hidalgo et al. 2010; Rivera et al. 2023). However, the mechanisms underlying the influence of upwelling variation on copepod diversity remain unclear. From a broad ecological perspective, studies emphasize the importance of deterministic processes based on species niche differences (niche theory), suggesting that environmental factors maintain species richness and originate from environmental heterogeneity (e.g. Chesson, 2000; Tilman, 2004). From Pianka's major hypotheses (Pianka 1966), the climate stability hypothesis (Fischer 1960; Klopfer 1959) to explain observed patterns of diversity is the only one that remains essentially unchanged and relatively unexplored (Fine 2015; Fjeldså et al. 1997; Guerrina et al. 2024; Schemske and Mittelbach 2017). Notably, in the HCS, such environmental stability appears to be mostly linked to upwelling intensity, which can affect coastal circulation (Marín et al. 2001), water

column stratification and temperature (Schneider et al. 2017), distribution of the OMZ and oxygenation (Sobarzo et al. 2007), and availability of food resources (quantity and quality) (Anabalón et al. 2007; Vargas, Escribano, and Poulet 2006). All of these factors can have a fundamental role in the population and community dynamics of copepods in the HCS (Escribano et al. 2012), ultimately influencing their diversity patterns and potentially uploading the relevance of the climate stability hypothesis to the ocean. This is very relevant, considering that initially, the hypothesis was proposed by analyzing diversity patterns on a terrestrial two-dimensions planar scale. Still, the ocean is a three-dimensional (3D) space, and the habitats of different species in seawater are unevenly distributed within it (e.g. Fang et al., 2024). Consequently, evaluating the climate stability hypothesis from a 3D spatial perspective is necessary, revealing when different depths in the same sea area exhibit multiple diversity patterns, attributes, and causes (e.g. Moreno et al., 2008).

However, marine biodiversity can depend on regional biogeographical limits (e.g. Hernández et al., 2005; Miloslavich et al., 2011; Moreno et al., 2006), thus the relevance of the climate stability hypothesis can potentially change depending on these limits which, in the case of HCS, are in a latitudinal environmental gradient. Particularly on the South East Pacific, Camus (2001) review suggests two primary limits delimiting three principal spatial units: one at the 30ºS limiting the Peruvian Province (18º-30ºS) and Intermediate area (30º-41ºS), and the second at the 41ºS delimiting the southern Magellanic Province (41º-56ºS).

This study tested the climate stability hypothesis as the central modulating mechanism of copepod diversity patterns in the HCS. We used a long-term (17 years) database on copepod species occurrence in the upwelling zone off Chile. Our approach included the estimates of indices for copepod diversity and distribution from available species records within the upper

500 m, comparing upwelling regions with distinct seasonal regimes: a north zone (NZ, 20°-30°S) characterized by a permanent upwelling regime, and a south zone (SZ, 30°-40°S) characterized by a seasonal upwelling regime; and the association with environmental stability estimated from databases on oceanographic variables, including an estimate of kinetic energy in the water column, as driven by changes in upwelling intensity under different climatic forcing conditions. We evaluated the hypothesis that a more stable system would allow to find greater diversity, as a more stable system in terms of upwelling index, temperature and salinity would support greater diversity than more unstable areas. The objectives were a) to evaluate copepod species diversity variability and compare its vertical structure between north and south zones, at different depth ranges, b) to understand the environmental drivers influencing patterns of distribution of Copepoda as representatives of zooplankton in the HCS, c) to determine whether there are differences between strata and between NZ and SZ in terms of diversity, and d) to assess whether observed patterns obeyed to changes in environmental stability forced by upwelling intensity.

Methodology

Study Area

The study area is located within the HCS off Chile, between 20°S and 40°S, and between 70°W and 78°W. To evaluate when different depths in this sea area exhibit multiple diversity patterns attributes, we consider five depth strata: 0-100 m, 100-200 m, 200-300 m, 300-400 m, and 400-500 m. On the other hand, to consider the effect of regional biogeographical limits we separated between north and south zones (NZ and SZ, respectively) at 30°S (Figure 1). Due to a relatively low data availability, this area and strata were divided into 2x2 degrees grid-cells of 100 m depth each, to ensure adequate sample size and visualization of emerging diversity patterns.

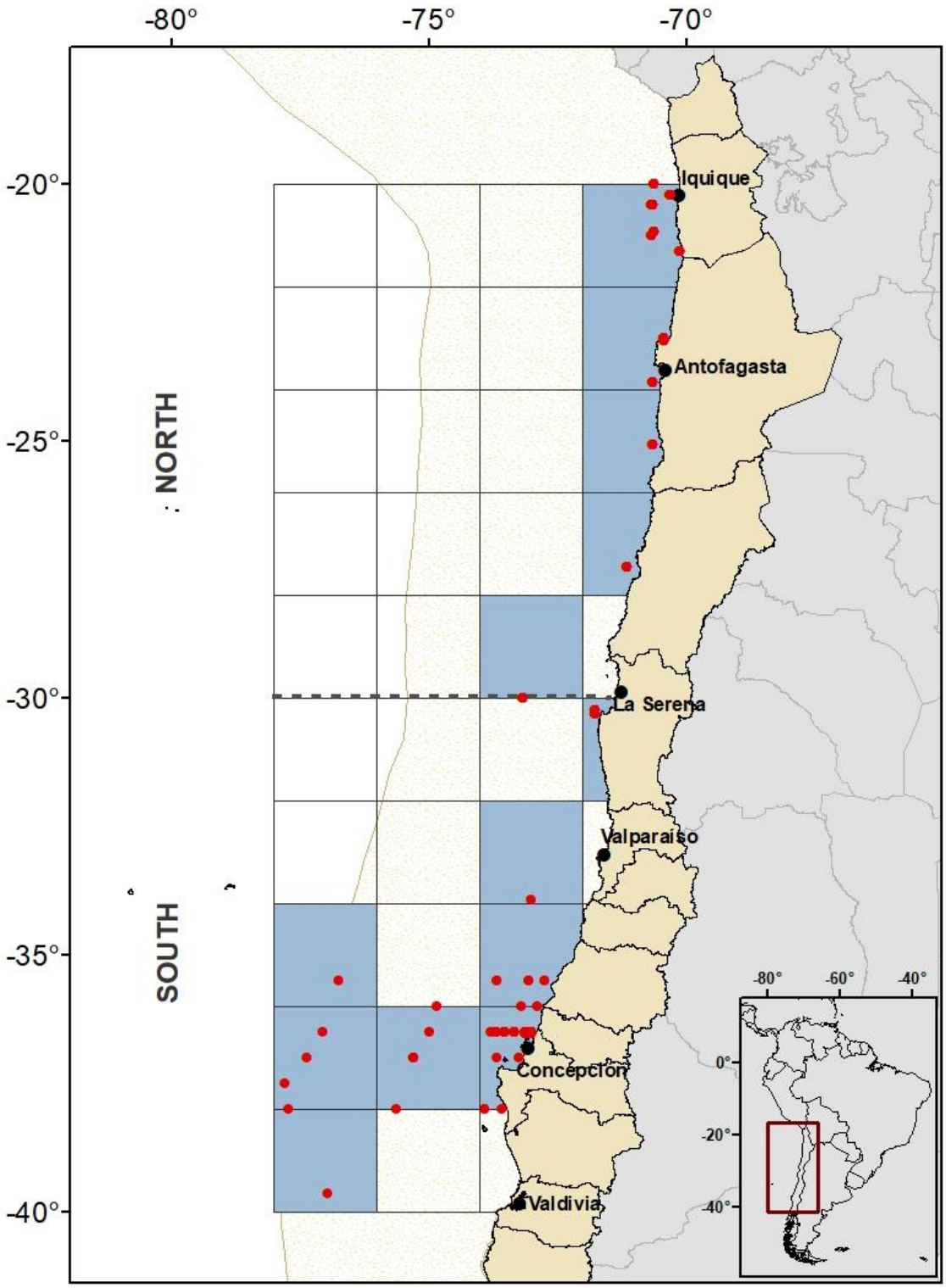

Figure 1: Study area at the Humboldt Current System (HCS, represented by the sand color dotted area) delimiting the 2x2 degrees grid cells forming the total grid. Blue grids represent the sampled ones, whereas the red dots represent the sampling stations from where data was obtained. The black dashed line at 30°S separates the north zone (NZ) and the south zone (SZ) of the HCS study area. Map projection is WGS 84 (EPSG 4326).

Data sources—Copepoda species and quality control procedures

Species occurrences were downloaded during August 2023 from the Ocean Biodiversity Information System (OBIS) database using its Mapper tool (https://mapper.obis.org/). The data were obtained for five strata of 100 m each between 500-0 m depth within the study area and within the time range from 1995 to 2011. Following the retrieval of the data, we eliminated occurrences without geographic coordinates, coordinates equal to zero, or those located inside the continent. We only selected occurrences at the species level and excluded duplicate records. This procedure allowed us to compile data to estimate species diversity indices, but also resulted in a reduction of information since many records are reported for genera or higher taxonomic levels (e.g. families), and in some cases without clear or wrong georeference. Taxonomy was revised and updated using the World Register of Marine Species (WoRMS) portal (http://www.marinespecies.org) through the *match_taxa* function of 'robis' package (Provoost and Bosch 2021) implemented in R software (R Core Team, 2021). After we had cleaned and curated the data, a total of 7013 occurrence records of Copepoda species were selected, and the number of species was counted by bathymetric strata and latitudinal zones (Table 1). The data on occurrences of Copepoda species are available in a Zenodo repository: https://doi.org/10.5281/zenodo.xxxxxx (version 1).

Table 1: Number of occurrence records at species level per strata and zone in the study area. N=north; S=south.

Stratum	Number of occurrences	Number of sampled points	Number of species per stratum
0-100 m N	2413	281	85
0-100 m S	1355	116	85
100-200 m N	889	116	74
100-200 m S	276	63	40
200-300 m N	649	98	69
200-300 m S	138	65	49
300-400 m N	543	108	69
300-400 m S	109	52	41
400-500 m N	559	116	72
400-500 m S	82	43	36
Total north zone	**5053**	**719**	**88**
Total south zone	**1960**	**339**	**90**
TOTAL	**7013**	**1058**	**126**

Data sources—Environmental data

Ten oceanographic and two atmospheric variables were selected for the analyses. The oceanographic variables were obtained from Copernicus Marine Environment Monitoring Service (CMEMS, https://marine.copernicus.eu) to a resolution of 1 x 1 degree and 0.25 x 0.25 degrees, namely: mean temperature and mean salinity, from global ocean reanalyses with data assimilation of satellite and in situ observations (Desportes et al. 2021); total chlorophyll-a concentration, dissolved oxygen concentration and pH from PISCES biogeochemical model forced by daily mean fields of ocean, sea ice and atmosphere coming from numerical simulation and reanalysis (Le Galloudec et al. 2021); geostrophic eastward sea water velocity (ugo) and geostrophic northward sea water velocity (vgo) from reprocessed in-situ and satellite data (Guinehut 2021); and particulate organic carbon (POC) from reprocessed in-situ and satellite data (Sauzède, Renosh, and Claustre 2023). The atmospheric variables of eastward and northward components of the wind at a height of 10 meters above the surface of the Earth (u10 y v10, respectively) were obtained from the Copernicus Climate Change Service (C3S) Climate Data Store (CDS) to a resolution of 0.25 x 0.25 degrees from reanalysis combining model data with in situ observations (Hersbach et al. 2023). Monthly surface (10 m height) wind velocity was used to compute the alongshore wind speed climatology. For each latitude, standard deviation is also computed from the monthly alongshore wind series to assess the wind variability.

All variables were retrieved within the time range from 1995 to 2011, except POC—which registers start from 1998, and averaged between those years, as well as for each depth range both in the north and south zones of the study area (i.e., 0-100 m, 100-200 m, 200-300 m, 300-400 m, 400-500 m).

To compute the Eddy Kinetic Energy (EKE), daily currents from the 1/12° horizontal resolution GLORYS12 reanalysis were downloaded from the CMEMS (https://marine.copernicus.eu/). Zonal and meridional current anomalies u' and v' were then computed from seasonal climatology. Finally, EKE is computed as (Jia, Wu, and Qiu 2011):

$$\mathrm{EKE} = \frac{1}{2}(\mathrm{u'}_{\mathrm{g}}^{2} + \mathrm{v'}_{\mathrm{g}}^{2})$$

Also, to evaluate the climate stability hypothesis, we calculated the stability of temperature and salinity. These variables were calculated by taking the inverse of the mean standard deviation between time slices over time. We then inverted variability to stability (as stability = 1/variability) and scaled it between 0 and 1. The calculations were performed with the package 'climateStability' (Owens and Guralnick 2019).

Data sources processing

All species occurring in each stratum from each zone were compared to the total to determine the number of shared and non-shared species and then to determine exclusive (restricted range) and more widely distributed species. These features were analyzed per stratum and zone in R software (R Core Team, 2021). The analysis was run by using the *%in%* operator and the *union*, *intersect* and *setdiff* functions that operate row-wise on data frames (in this case, lists of species as vectors for each stratum and zone). The script used for this analysis is available in a Zenodo repository: https://doi.org/10.5281/zenodo.xxxxxx (version 1).

All environmental variables were resampled to a resolution of 2 degrees (Figure 1) using QGIS 3.10 (QGIS.org, 2022). Initially, nine predictors were considered in our analyses (mean temperature, mean salinity, temperature stability, salinity stability, total chlorophyll-a concentration, dissolved oxygen concentration, pH, particulate organic carbon (POC), and EKE). Then, we obtained the Spearman rank-order correlation coefficient matrix with the 'corrplot' package (Wei T 2024), for visualizing their degree of association. Predictors showing correlation values over |0.7| were removed for further analyses (Dormann et al. 2013); then, particulate organic carbon (POC) and pH were no longer considered (Figure S1). The remaining predictors were later used to evaluate species richness, the Shannon-Wiener index, the Hurlbert index, and β-diversity and its additive components: turnover, and nestedness (eg., Baselga, 2010; Baselga and Gómez-Rodríguez, 2019).

To assess diversity patterns, species richness (measured as the number of species per grid-cell of 2°) was calculated using Biodiverse software (Laffan, Lubarsky, and Rosauer 2010). The Hulbert diversity index was also calculated. Although this index is designed to measure dominance in a community, where a lower value indicates greater diversity and a higher value indicates greater dominance, it can be used for presence-absence data, calculating the proportion of sample units where that species is present. To do this, count the number of sample units with the presence of the species and divide by the total number of sample units, as follows:

$$H = 1 - \frac{1}{N}\sum_{i=1}^{S} p_i^2$$

where:

- H is the Hulbert diversity index,
- N is the total number of sample units,
- p_i is the proportion of presence of species *i* in the sample units and
- S is the total number of species.

The calculations were performed with the 'vegan' package (Oksanen et al. 2024), and the script is available in the Zenodo repository: https://doi.org/10.5281/zenodo.xxxxxx (version 1).

Since we only have occurrence records, the Shannon-Wiener index was calculated considering that each species present has the same importance in the community. In this case, the proportions pi will be defined as the proportion of species present with respect to the total species in the set. Then, the Shannon-Wiener index for occurrence data was calculated in Biodiverse 3.1 software (Laffan et al. 2010), according to Laffan (2022):

$$H = -\sum_{i=1}^{n} p_i \cdot ln\, p_i$$

where p_i is the number of samples (in this case, occurrences) of the *i* species as a proportion of the total number of occurrences in the neighborhoods (2° x 2° sampling grid cells). This proportion is estimated as:

$$p_i = \frac{n_i}{N}$$

where n_i is the number of records of the i species and N is the total number of records at species level in the sampled cell.

We therefore calculated alpha diversity as species richness and beta diversity as species composition. In the latter, we differentiated between turnover and nestedness. Alpha diversity was calculated in Biodiverse 3.1 software (Laffan et al. 2010), whereas beta diversity was estimated using the packages 'betapart' (Baselga and Orme 2012), 'CommEcol' (Sanches Melo 2021) and 'letsR' (Vilela and Villalobos 2015) using the following equation:

$$\beta sor = \beta sim + \beta sne \equiv \frac{b+c}{2a+b+c} = \frac{b}{b+a} + \left(\frac{c-b}{2a+b+c}\right)\left(\frac{a}{b+a}\right)$$

where βsor is Sørensen dissimilarity, βsim is Simpson dissimilarity (i.e., turnover component of Sørensen dissimilarity), βsne is the nestedness component of Sørensen dissimilarity, *a* is the number of shared species between two cells, *b* the number of species unique to the poorest site, and *c* the number of species unique to the richest site.

For species richness, spatial hotspots were defined using spatial clustering analysis, Getis-Ord G* statistic (Getis and Ord 1992). This identifies spatial concentrations of an entity (in this case species richness per cell) or areas that contain higher/lower values than expected by chance for a given study area. Significant values of Z>0 provide evidence for significant hotspots whereas values of Z<0 provide evidence for groups of entities with lower values than expected by chance. The statistical determination of hotspots was performed in ArcMap 10.4.1 software (ESRI 2016) and were plotted by using the package 'ggridges' (Wilke 2024).

Statistical analysis

To evaluate differences in diversity and richness between strata, as well as between NZ and SZ, we used a two-way Permutational Multivariate Analysis of Variance (PERMANOVA) (Anderson 2001) since statistical inferences are made in a distribution-free setting using permutational algorithms (Anderson 2001, 2017). This analysis was performed in PAST v 4.17 software (Hammer, Harper, and Ryan 2001).

To assess the effect of the environmental variables on diversity, Linear Mixed Models (LMM) were used, which allow both fixed and random effects, thus serving for analyzing data that are non-independent (Arnqvist 2020; Bates 2005; Bolker 2015). First, we assessed normality using Shapiro-Wilk test. This analysis showed that species richness (W = 0.85695; p-value = 2.399e-05), Shannon index (W = 0.8206; p-value = 2.707e-06), Hurlbert index (W = 0.85695; p-value = 2.399e-05), β-diversity (W = 0.82175, p-value = 2.888e-06), and its additive components: turnover (W = 0.95377, p-value = 0.04883) and nestedness (W= 0.79035, p-value = 5.292e-07) had normal distribution. Then, a set of Linear Models (LM) and Linear Mixed Models (LMM) were developed for species richness, the Shannon-Wiener and Hurlbert indices, β-diversity and its two additive components: turnover, and nestedness. The residual diagnosis was carried out using the *simulateResiduals* function in 'DHARMa' package (Hartig 2024) to assess the distribution of data and their independence through observing the dispersion in variance. A lack of independence in the data can lead to overdispersion, which can be accounted for by fitting a random effect to the model. The residuals diagnosis showed that residuals for Linear Models (LM) and Linear Mixed Models (LMM) showed no deviation from the expected normal distribution (Figure S2, left panel), and that the difference between the observed and expected values was greater in the LM (i.e.,

they showed more unexplained variation of their residuals shown as an over-dispersion in their variance, Figure S2, right panel). Then, the analyses continued with the use of LMM, that included mean temperature, temperature stability, mean salinity, salinity stability, chlorophyll-a concentration, oxygen concentration, and EKE as fixed-effect predictors; whereas bathymetry (every 100 m strata) and zones (north and south) were included as random effects. These analyses were performed with the 'lme4' package (Bates et al. 2024). The environmental variables were normalized before the analysis. We generated a series of models to evaluate the drivers of diversity (Table S1); the models with the best fit were selected through the corrected Akaike Information Criterion (AICc), through the 'MuMIn' package (Bartoń 2022). Models with ΔAICc values (i.e., the difference in AICc score between the best model and the model being compared), within 2 units of the best model should be selected (Anderson, Gorley, and Clarke 2008). Finally, a marginal and conditional R^2 value was estimated for the best models with the *r.squaredGLMM* function of 'MuMIn' package (Bartoń 2022). The marginal R^2 (R^2m) estimates the fraction of the variance explained by the fixed effects in the model, whereas the conditional R^2 (R^2c) estimates the fraction explained by the fixed and random effects. The script of this analysis is available in the Zenodo repository: https://doi.org/10.5281/zenodo.xxxxxx (version 1).

Results

Spatial biodiversity

The integration of the northern and southern zones (NZ and SZ, respectively) for all associated cells and strata (i.e., five strata from both NZ and SZ), showed that there are 126 species in the whole study area. The NZ of the study area (i.e., five 100 m strata between 20 and 30°S) has 88 species. The SZ of the study area (i.e., five 100 m strata between 30 and 40°S) has 90 species. The stratum between 0 and 100 m depth has 85 species in the north and 85 species in the south. The stratum between 100 and 200 m depth has 74 species in the north and 40 species in the south. The stratum between 200 and 300 m depth has 69 species in the north and 49 species in the south. The stratum between 300 and 400 m depth has 69 species in the north and 41 species in the south. The stratum between 400 and 500 m depth has 72 species in the north and 36 species in the south. Only 18 species are common to all strata, thus distributed from 0 to 500 m at the NZ and SZ of the study area (Table S1 Supplemental Material): *Agetus typicus*, *Calanoides patagoniensis*, *Calanus chilensis*, *Euchaeta marina*, *Heterorhabdus papilliger*, *Metridia brevicauda*, *Metridia lucens*, *Oithona plumifera*, *Oithona setigera*, *Oithona similis*, *Oncaea curvata*, *Oncaea media*, *Oncaea mediterranea*, *Paracalanus indicus*, *Pleuromamma gracilis*, *Pleuromamma quadrungulata*, *Triconia conifera*, and *Triconia minuta*. There are 46 common species at the NS and SZ of the 0-100 m stratum (Table S1), whereas the 100-200 m, 200-300 m, 300-400 m, and the 400-500 m strata have 26, 29, 28, and 23 common species from the NS and SZ, respectively (Table S1).

We found that the NZ and SZ have 32 and 14 exclusive species, respectively (Table S1). This means that those species can only be found at the north or south zone, at different strata. Regarding exclusive species per zone and stratum, only three strata had species that were not

shared elsewhere within the study area: 0-100 m NZ, 0-100 m SZ and 400-500 m NZ. Four species were exclusively registered at the 0-100 m NZ stratum (Table S1), twenty-five species were exclusively registered at the 0-100 m SZ (Table S1), and two species were exclusively registered at the 400-500 m NZ stratum (Table S1).

From the common species for the north and south zone that occur along all strata (Table 2) the order Cyclopoida and Calanoida both present 50% relative occurrence, with nine species each (Table 2). From the order Cyclopoida, the family Oncaidae showed the greatest number of representatives (five species), followed by Oithonidae (three species) and Corycaeidae (one species) (Table 2). From the order Calanoida, four species belong to the Metridinidae family, two species to the Calanidae family, and one species to the Euchaetidae, Heterorhabdidae, and Paracalanidae families, respectively (Table 2). The observed distribution of these species occurrences at this study have been previously cited off Chile (Table 2).

Table 2: Dominant species of the HCS off Chile, occurring between 0 and 500 m depth and between 20°-40°S and 70°-78°S.

Scientific name (species level)	Order	Family	Reported previously at (location, depth range, author)
Agetus typicus	Cyclopoida	Corycaeidae	SPSG oligotrophic blue water, between 0-200 and 600-800 m (Medellín-Mora et al. 2021), supplementary material SZ of coastal HCS, between 0-200 m (Morales et al. 2010) SZ of oceanic HCS, between 0-100 m (Morales et al. 2010)
Calanoides patagoniensis	Calanoida	Calanidae	SZ of coastal HCS, between 0-100 m (Hidalgo et al. 2010)

			SPSG oligotrophic blue water, between 200-400 m (Medellín-Mora et al. 2021), supplementary material
Calanus chilensis	Calanoida	Calanidae	NZ and SZ of coastal HCS, between 0-100 m (Hidalgo et al. 2010)
Euchaeta marina	Calanoida	Euchaetidae	NZ and SZ of coastal HCS, between 0-600 m (Hidalgo et al. 2010) SPSG oligotrophic blue water, between 0-100 m (Medellín-Mora et al. 2021), supplementary material
Heterorhabdus papilliger	Calanoida	Heterorhabdidae	SZ of coastal HCS, between 0-100 m (Hidalgo et al. 2010) SZ of coastal HCS, between 0-200 m (Morales et al. 2010) SZ of oceanic HCS, between 0-100 m (Morales et al. 2010)
Metridia brevicauda	Calanoida	Metridinidae	SZ of coastal HCS, between 0-100 m (Hidalgo et al. 2010)
Metridia lucens	Calanoida	Metridinidae	NZ and SZ of oceanic HCS, between 0-100 m (Hidalgo et al. 2010) SZ of coastal HCS, between 0-200 m (Morales et al. 2010) SZ of oceanic HCS, between 0-100 m (Morales et al. 2010) Deep waters of the Southern Ocean (Park and Ferrari 2009)
Oithona plumifera	Cyclopoida	Oithonidae	NZ and SZ of oceanic HCS, between 0-100 m (Hidalgo et al. 2010) SPSG oligotrophic blue water, between 100-200 m (Medellín-Mora et al. 2021), supplementary material SZ of oceanic HCS, between 0-100 m (Morales et al. 2010)
Oithona setigera	Cyclopoida	Oithonidae	SZ of oceanic HCS, between 0-100 m (Hidalgo et al. 2010) SPSG oligotrophic blue water, between 0-600 m (Medellín-Mora et al. 2021) SZ of coastal HCS, between 0-200 m (Morales et al. 2010) SZ of oceanic HCS, between 0-100 m (Morales et al. 2010)
Oithona similis	Cyclopoida	Oithonidae	NZ and SZ of coastal HCS, between 0-100 m (Hidalgo et al. 2010) SPSG oligotrophic blue water, between 0-100 and 200-400 m (Medellín-Mora et al. 2021), supplementary material SZ of coastal HCS, between 0-200 m (Morales et al. 2010)

			SZ of oceanic HCS, between 0-100 m (Morales et al. 2010)
Oncaea curvata	Cyclopoida	Oncaeidae	SPSG oligotrophic blue water, between 200-400 m (Medellín-Mora et al. 2021), supplementary material
Oncaea media	Cyclopoida	Oncaeidae	NZ of coastal HCS, between 0-100 m (Hidalgo et al. 2010) SPSG oligotrophic blue water, between 0-800 m (Medellín-Mora et al. 2021) SZ of coastal HCS, between 0-200 m (Morales et al. 2010) SZ of oceanic HCS, between 0-100 m (Morales et al. 2010)
Oncaea mediterranea	Cyclopoida	Oncaeidae	NZ and SZ of coastal HCS, >100 m (Hidalgo et al. 2010) SPSG oligotrophic blue water, >800 m (Medellín-Mora et al. 2021)
Paracalanus indicus	Calanoida	Paracalanidae	NZ and SZ of coastal HCS, >100 m (Hidalgo et al. 2010) SPSG oligotrophic blue water, 100-800 m (Medellín-Mora et al. 2021), supplementary material
Pleuromamma gracilis	Calanoida	Metridinidae	SZ of oceanic HCS, between 0-100 m (Hidalgo et al. 2010) SPSG oligotrophic blue water, between 0-600 m (Medellín-Mora et al. 2021) SZ of coastal HCS, between 0-200 m (Morales et al. 2010) SZ of oceanic HCS, between 0-100 m (Morales et al. 2010)
Pleuromamma quadrungulata	Calanoida	Metridinidae	SZ of coastal HCS, between 0-100 m (Hidalgo et al. 2010) SZ of coastal HCS, between 0-200 m (Morales et al. 2010) SZ of oceanic HCS, between 0-100 m (Morales et al. 2010)
Triconia conifera	Cyclopoida	Oncaeidae	NZ and SZ of coastal HCS, between 0-100 m (Hidalgo et al. 2010) SPSG oligotrophic blue water, >400 m (Medellín-Mora et al. 2021) SZ of coastal HCS, between 0-200 m (Morales et al. 2010) SZ of oceanic HCS, between 0-100 m (Morales et al. 2010)
Triconia minuta	Cyclopoida	Oncaeidae	

Environmental stability

The Hovmöller diagram of the alongshore winds' climatology showed that there is seasonal upwelling south of 35°S, whereas north of this latitude upwelling is continuous (Figure 2a). Regarding wind's variability, its monthly standard deviation is greater towards the south (Figure 2b).

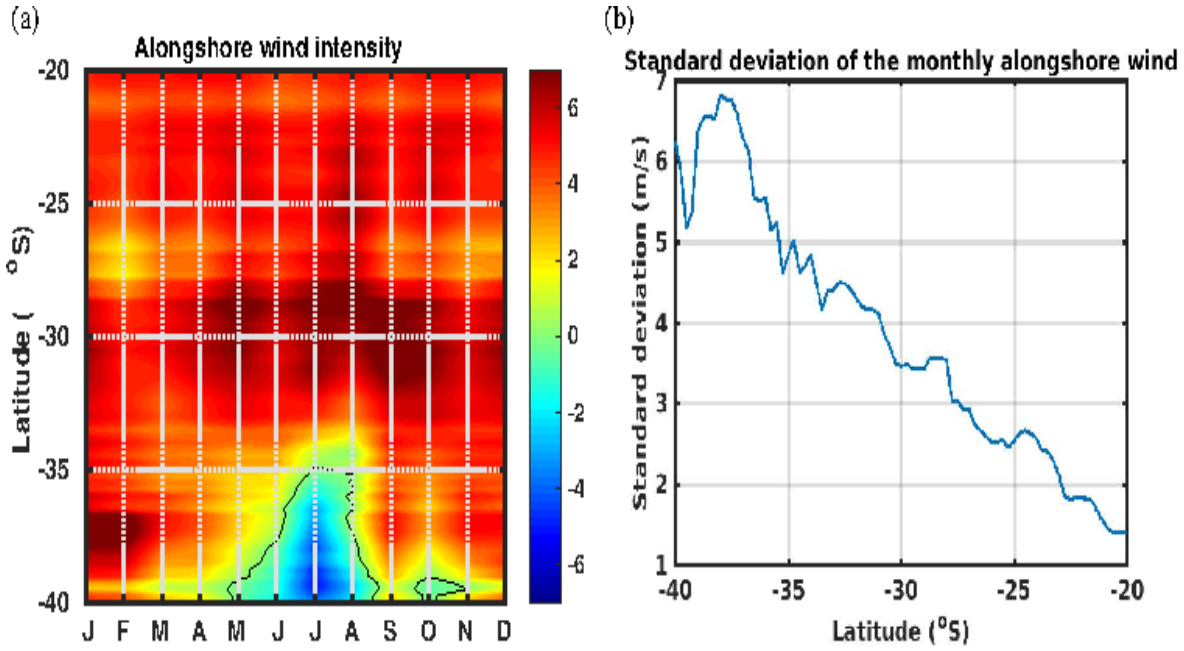

Figure 2: Alongshore surface wind speed (in m s^{-1}) from ERA5 reanalysis over the 1995-2011 period (a) Hovmöller diagram of the wind speed monthly climatology (b) latitudinal variation of the monthly wind standard deviation.

The turbulent kinetic energy at the surface analysis showed a zone with maximum EKE between 26 and 36°S (Figure 3a, detail in Figure S3), whereas the vertical EKE profiles averaged for each zone shows that the NZ has a more intense mesoscale activity compared

to the SZ (Figure 3b). For better assessing EKE latitudinal variations, it was averaged into 1° latitude bands and plotted along the strata, where it shows maximum intensity between 26 and 34°S over 100 m depth, decreasing with depth at all latitudes, and with a stronger decrease in the upper layers in the SZ than in the NZ (Figure 3c).

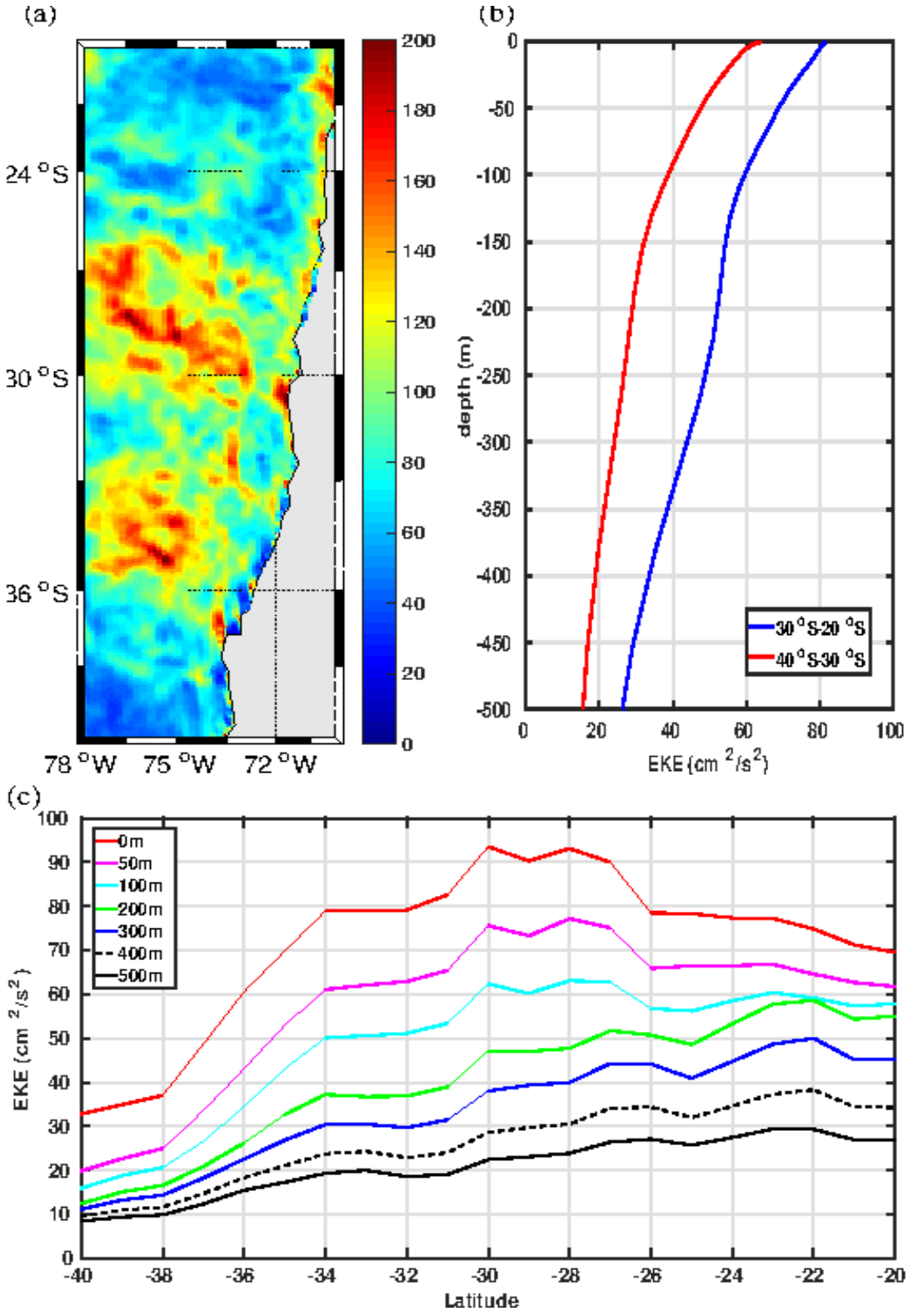

Figure 3: Mean Eddy Kinetic Energy (EKE in cm² s⁻²) computed from the daily outputs of the Glorys12 reanalysis over the 1995-2011 period. (a) surface EKE (b) vertical profile of the mean EKE averaged over the 20-30°S region (blue line) and the 30-40°S region (red line) (c) latitudinal variation of the mean EKE averaged from the coast to 78 °W and over 1° latitudinal bins, at different depths (0, 50, 100, 200, 300, 400 and 500 m).

Statistical outcomes

The two-way PERMANOVA analyses showed that species richness and Shannon-Wiener index were significantly different between zones, but not between strata (Table 3). These diversity measures showed that, on average, the NZ had higher species richness and a Shannon-Wiener index in all strata, excepting the 300-400 m depth range (Figures 4B and 4F, respectively). On the other hand, nestedness was significantly different between strata but not between zones (Table 3), indicating greater mean differences in the 100-200 m and the 200-300 m depth ranges, and lower mean differences in the 0-100m, 300-400 m, and 400-500 m depth ranges (Figure 4E). Hurlbert index, species composition and turnover were significantly different between zones, as well as between strata (Table 3). In particular, the Hurlbert index was on average greater in the NZ and upper strata (0-100 m, 100-200 m, and 200-300 m depth ranges; Figure 4D); whereas the species composition and turnover were on average greater in the NZ and lower strata (100-200 m, 200-300 m, 300-400 m and 400-500 m depth ranges; Figures 4A and 4C, respectively).

The clustering analysis (Getis-Ord Gi*) allowed us to identify high values of richness in all strata at the NZ, whereas cold spots (i.e., low species richness values) were greater at the SZ and at greater depths (Figure 5).

Table 3: Two-way PERMANOVA results for models of species richness, Shannon-Wiener index, Hulbert index, species composition and its components turnover and nestedness. Significant permutation p-values below the 0.05 level are highlighted in bold.

	Source	Sum of squares	df	Mean square	F	p-value
Species richness	Depth	15.606	4	0.390	18.277	0.058
	Zone	**16.854**	**1**	**16.854**	**78.955**	**0.002**
	Interaction	-1.599	4	-0.399	-18.727	0.999
	Residual	85.384	40	0.213		
	Total	10.185	49			
Shannon-Wiener index	Depth	10.208	4	0.255	0.992	0.318
	Zone	**0.986**	**1**	**0.986**	**38.331**	**0.017**
	Interaction	-26.926	4	-0.673	-2.618	1
	Residual	10.285	40	0.257		
	Total	95.988	49			
Hurlbert index	Depth	**156.057**	**4**	**0.390**	**23.068**	**0.045**
	Zone	**168.539**	**1**	**16.854**	**9.965**	**0.001**
	Interaction	0.174	4	0.044	0.258	0.966
	Residual	676.519	40	0.169		
	Total	10.185	49			
Species composition	Depth	**0.805**	**4**	**0.201**	**73.752**	**0.0003**
	Zone	**0.116**	**1**	**0.116**	**42.444**	**0.047**
	Interaction	144.088	4	0.360	13.199	0.0001
	Residual	109.167	40	0.027		
	Total	34.535	49			
Turnover	Depth	**0.872**	**4**	**0.218**	**34.584**	**0.005**
	Zone	**0.323**	**1**	**0.323**	**51.276**	**0.007**
	Interaction	271.197	4	0.678	10.761	0.0001
	Residual	252.026	40	0.063		
	Total	64.269	49			
Nestedness	Depth	**128.334**	**4**	**0.321**	**20.888**	**0.049**
	Zone	0.407	1	0.407	26.517	0.081
	Interaction	202.089	4	0.505	32.892	0.007
	Residual	614.399	40	0.1536		
	Total	98.555	49			

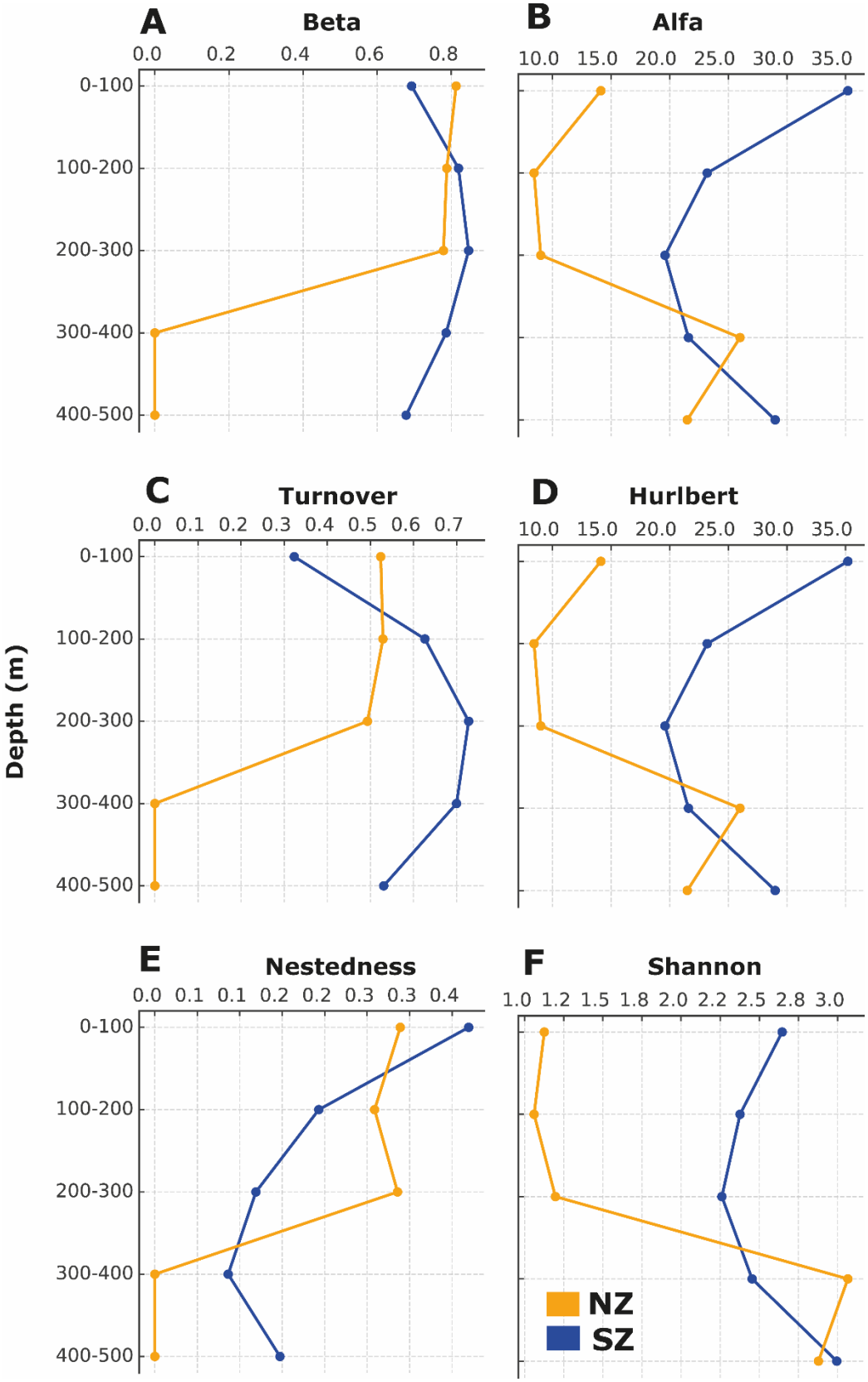

Figure 4: Diversity indices for the study area, separated by zone (NZ=north zone; SZ=south zone) and bathymetric range.

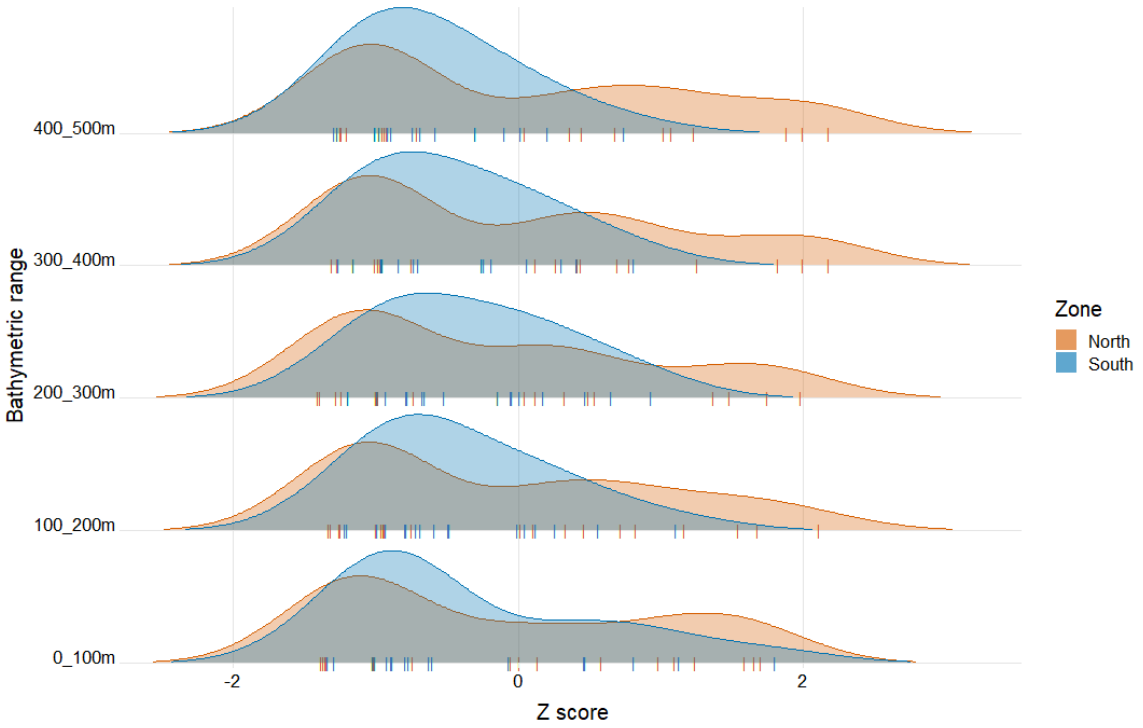

Figure 5: Getis-Ord Gi* statistic of species richness of Copepoda at each depth range and zone of the study area. A positive value for a standardized Z score suggests a hot spot, whereas a negative value indicates a cold spot.

The best-fitting LMM explaining species richness revealed that the variables mean temperature, mean salinity, and oxygen concentration were the most important predictors (Table 4). The R^2m and the R^2c explain a 44% and a 51% of the variability, respectively. The environmental predictors that explain the diversity evaluated through the Shannon-Wiener index included mean temperature, mean salinity, and oxygen concentration (Table 4). The R^2m and the R^2c explain a 43% and a 50% of the variability, respectively. The best-fitting model for diversity assessed through the Hurlbert index indicated that temperature, mean salinity, and oxygen concentration were significant predictors (Table 4). The R^2m and the R^2c explain a 44% and a 51% of the variability, respectively. The environmental predictors

explaining the distribution of beta diversity (species composition), included temperature stability and EKE (Table 4). The R^2m and the R^2c explain a 20% and a 53% of the variability, respectively. The environmental predictors that explain the distribution of turnover included temperature stability and EKE (Table 4). The R^2m and the R^2c explain a 4% and a 21% of the variability, respectively. The environmental drivers that explain the distribution of nestedness included temperature stability and EKE (Table 4). Both the R^2m and the R^2c explained 18% of the variability.

Table 4: LMM for species richness (SR), Shannon-Wiener index (SW), Hurlbert index (HI), species composition (SC) and its components turnover (TO) and nestedness (NE). Statistics acronyms are df=degrees of freedom, logLik=log-likelihood, AICc=corrected Akaike information criterion, ΔAICc=delta AICc, R^2m=marginal R^2, R^2c=conditional R^2. Predictors' acronyms are: T_{mean}=mean temperature, S_{mean}=mean salinity, Chla=chlorophyll-a concentration, O_2=dissolved oxygen concentration, EKE=Eddy Kinetic Energy, T_{stab}=temperature stability, S_{stab}=salinity stability. The best fitting models are highlighted in bold.

Model	df	log Lik	AICc	ΔAICc	Weight	R^2m	R^2c
SR ~ T_{mean}+S_{mean}+O_2	**7**	**-75.6**	**167.88**	**0.00**	**0.40**	**0.44**	**0.51**
SR ~ T_{stab}+S_{stab}+EKE	7	-76.8	170.32	2.44	0.12		
SR ~ T_{stab}+S_{stab}+O_2	7	-76.9	170.60	2.72	0.10		
SW ~ T_{mean}+S_{mean}+O_2	**7**	**-31.9**	**80.52**	**0.00**	**0.55**	**0.43**	**0.50**
SW~ T_{stab}+S_{stab}+EKE	7	-33.4	83.51	2.99	0.12		
SW ~ T_{stab}+S_{stab}+Chla	7	-33.5	83.60	3.08	0.12		
HI ~ T_{mean}+S_{mean}+O_2	**7**	**-75.6**	**167.88**	**0.00**	**0.40**	**0.44**	**0.51**
HI ~ T_{stab}+S_{stab}+EKE	7	-76.8	170.32	2.44	0.12		
HI ~ T_{stab}+S_{stab}+O_2	7	-76.9	170.60	2.72	0.10		
SC ~ T_{stab}+EKE	**6**	**15.1**	**16.2**	**0.00**	**0.90**	**0.20**	**0.53**
SC ~ T_{stab}+S_{stab}+EKE	7	13.29	-9.9	6.25	0.04		
SC ~ T_{stab}+S_{stab}+Chla	7	13.18	-9.7	6.46	0.04		
TO ~ T_{stab}+EKE	**6**	**4.55**	**4.86**	**0.00**	**0.79**	**0.04**	**0.21**
TO~ T_{stab}+S_{stab}+O_2	7	3.16	10.34	5.49	0.05		
TO ~ T_{stab}+S_{stab}+EKE	7	3.10	10.47	5.61	0.05		
NE ~ T_{stab}+EKE	**6**	**19.68**	**-25.41**	**0.00**	**0.78**	**0.18**	**0.18**
NE ~ T_{stab}+S_{stab}+Chla	7	19.27	-21.87	3.54	0.13		
NE ~ T_{mean}+S_{mean}+Chla	7	18.35	-20.04	5.37	0.05		

Discussion

The assessment of copepod diversity patterns in the HCS both, over the horizontal and vertical planes, clearly indicated a strong connection between the copepod community and upwelling variation. Changes in upwelling intensity over a seasonal time scale and according to the latitudinal regime can strongly influence the habitat conditions for copepods inhabiting the upper 500 m in the HCS. These changes can affect copepod populations and ultimately the community structure, including biodiversity. It is also important to highlight the strong link between the diversity indices and environmental stability as assessed by temperature stability and kinetic energy (EKE). More stable conditions throughout the year can allow populations to reproduce more continuously and so be present permanently, but also this stability may help maintaining the community composition more stable year-round. In this context, it can be inferred that fewer perturbations or a more predictable environment may also allow that species interactions along with their specific responses to environmental change can function more efficiently (Fischer et al. 2001) to promote a higher species richness.

It is important to stress that both temperature stability and EKE are driven by variation of upwelling intensity. Regarding latitudinal variation, it must be noted that permanent continuous upwelling regime north of 35°S derived from alongshore winds' climatology (Figure 2a) and greater surface EKE (Figure 3a) are masked by the delimitation of the zones for this study, as the southern region (SZ) starts at 30°S. However, when considering averages for each zone, a lower monthly standard deviation of wind's variability (Figure 2b) together with greater EKE along depth (Figures 3) can be observed in the northern region (NZ) than in the SZ, indicating more upwelling favorable conditions in the NZ throughout the year,

while the SZ shows more variability between seasons, giving lower average values. On the other hand, it has been documented that the SZ (data from 36,4°S) is characterized by a continuous alternation between strong southerly and weak northerlies (upwelling index < 0, downwelling favorable), even at a sub-seasonal scale (Aguirre et al. 2021), with implications on biogeochemical cycles and productivity. In addition, a more poleward location of the South Pacific High during winter has caused more summer-like hydrographic conditions on the continental shelf offshore central Chile (where the SZ was delimited), generating changes in the plankton community (Jacob et al. 2018; Schneider et al. 2017) that may explain increased coastal upwelling in the HCS, and the changes in species dominance associated with it in terms of abundance (Pino-Pinuer et al. 2014), as shifts in the upwelling regimes also affects phytoplankton composition that in turn are determinant for zooplankton reproductive pulses (Vargas et al. 2006). Besides that, NZ is characterized by an oxygen minimum zone that is relatively shallow (ca. 10-60 m depth of its upper limit) (Hidalgo et al. 2005, Morales et al. 1999) in the coastal upwelling area and adjacent oceanic waters, generating usually low oxygen concentrations to which organisms may respond in physiological or distributional terms (Morales et al. 1999). Despite zooplankton may tend to aggregate above the oxycline associated with more oxygenated surface waters (Tutasi and Escribano 2020), nauplii, small- and large-sized copepods are able to perform diel vertical migration the upwelling zone, withstanding severe hypoxia and being able to exhibit a large migration amplitude (∼500 m, large-sized copepods and copepods of the group Eucalanidae), remaining either temporarily or permanently during day or night conditions within the core of the OMZ (Tutasi and Escribano 2020). Therefore, considering that the OMZ occurs over the whole study area under different conditions and reaches depths of ca. 500 m, it appears as the dominant species of the HCS described here (Tables S1 and 2) may be adapted or have

evolved the capacity to cope with low oxygen conditions, temporally through vertical migration (Tutasi and Escribano 2020) or during more extended periods (Hidalgo et al. 2005). This also could explain the fewer exclusive species found in the 0-100 m depth range at NZ (Table S1), as different species may occur along the whole water column, whereas at the SZ more species may tend to aggregate in the upper layer for oxygen (Tutasi and Escribano 2020) or when the OMZ becomes shallower. The clustering analysis (Figure 5) indicated a similar tendency, with high values of richness in all strata at the north zone (NZ), whereas low species richness values (cold spots) were found at greater depths in the south zone (SZ).

Regarding copepod species diversity, the species common to all strata and zones can be considered, in terms of occurrence, dominant for the HCS off Chile as they occur between 0 and 500 m depth and between 20°-40°S. The observed distribution of these species occurrences at this study have been previously cited off Chile (Table 2), and complements the information previously documented.

From the dominant species of the HCS, *Calanus chilensis* has been considered as a coastal-neritic species endemic to the eastern South Pacific between 10° and 42°S (Marín, Espinoza, and Fleminger 1994), being later proposed as a biological indicator of the intrusion of the Humboldt Current in the Ecuadorian Pacific (Bucheli, Cajas, and Hidalgo 2019). More recently, a continuous distribution for the species has been modeled, that ranges from Ecuador to the southernmost area of South America between 0–200 m depth range, whereas the organisms occurring between 200–400 m have a modeled discontinuous distribution with greater suitability for the coast of Chile (Rivera et al. 2023). The neritic zone comprises the shallow coastal waters (down to 100-200 m) overlying the continental shelf (Boaden and Seed 1985); however, in this study the occurrence of *C. chilensis* has been registered down

to a depth of 500 m, supporting the modeled projection of this species. Together with *C. chilensis*, *Calanus patagoniensis* is another species considered endemic to the HCS, but with a more inshore distribution due to biological behavior involving vertical migration that may avoid them to be transported offshore by mesoscale processes (Morales et al. 2010). Our data can corroborate that for the south zone, that has more data available towards open ocean, where *C. chilensis* occurs along all its extension, while *C. patagoniensis* occurrences are restricted until the 73°W centroid. *Oithona similis*, *Paracalanus indicus*, *Pleuromamma gracilis* and *P. quadrungulata* are species that we found to be dominant in terms of occurrence and that have been described in other studies as dominant for the HCS (Escribano et al. 2012; Pino-Pinuer et al. 2014). Here, we found these species occurrence to be restricted until the 73°W centroid as well. *P. indicus* dominance in terms of abundance has been documented to vary strongly over the south zone, being outnumbered by *Drepanopus forcipatus* (Pino-Pinuer et al. 2014). In this study, *D. forcipatus* did not appear to be dominant in terms of occurrence as it only appeared between 0-200 m at NZ and SZ (Table S1), and restricted until the 73°W centroid, which is concordant with its known distribution restricted to coastal and shelf areas along southern South America (Park and Ferrari 2009). Additionally, it has been reported that the regional distribution of *C. chilensis* secondary production extends much further offshore in the HCS than what is typical for its ecological counterparts in other coastal upwelling systems, extending the area of high productivity which in turn maximizes trophic transfer efficiency towards economically important pelagic fish (Schukat et al. 2021). These aspects involve specific life-strategy traits and life-cycle adaptations (Schukat et al. 2021) that highlights *C. chilensis* importance as an endemic species adapted to the environmental variability of the HCS.

Acartia tonsa is a widely studied species in the HCS (e.g., Aguilera 2020; Aguilera and Bednaršek 2022; Ruz et al. 2015; Yáñez et al. 2018), considered cosmopolitan and characteristic of estuarine and upwelling systems, while also associated to the inshore area (Morales et al. 2010). In this study, this species did not appear to be dominant for the HCS, however it is present in both NZ and SZ between 0-300 m (Table S1) and restricted until the 73°W centroid, thus it may be considered an upper-mesopelagic species.

Paraeuchaeta barbata appeared as an exclusive species for the 400-500 m stratum of the NZ (Table S1). This calanoid species occurs in deep water throughout the world oceans (Park 1994), being a very common species between the Southern Ocean and the Arctic basin (Park and Ferrari 2009) associated with the Antarctic Intermediate Water (AAIW) during austral summer and winter when migrating from and arriving to the Chilean coast, respectively (Yamanaka 1976). This demonstrates that vertical zonation occurs in the HCS and is associated with seasonal physical-biological processes that in turn may be linked to temperature. Moreover, various species found in the HCS are characteristic of the Southern Ocean (SO) (Park and Ferrari 2009), such as *Metridia lucens* and *Pleuromamma quadrungulata*, deep water species in the SO considered dominant species in this study (found between 0-500 m depth and in both the NZ and SZ, Table 2); *Gaetanus brevispinus*, *G. kruppii*, *Lophothrix frontalis* (deep water species in the SO), *Metridia gerlachei* (very common herbivore calanoid in the SO), found between 0-500 m in the NZ in this study (Table S1); *Calanus propinquus, Neocalanus tonsus* (epipelagic calanoids of the SO, the latter can perform diapause), *Gaetanus tenuispinus* (very common deepwater species in the SO), found between 0-500 in the SZ in this study (Table S1); *Haloptilus oxycephalus*, *Scolecithricella minor* (very common deepwater calanoids of the SO that reach temperate and subarctic

regions, respectively), *Ctenocalanus citer* (epipelagic calanoid endemic to the SO) found between 0-100 m in the SZ in this study (Table S1). These examples indicate intrusion and colonization of epipelagic and deepwater copepods from the SO, that are adapted to that productive habitat (Park and Ferrari 2009), into the HCS. Thus, the HCS must be a suitable habitat for increasing regional diversity, especially that of calanoid copepods.

Generally, when several models produce quite similar AICc values (i.e., within 1 to 2 units of each other), it suggests that there is a reasonable amount of redundancy among predictor variables, as several different combinations of them could be used interchangeably to explain the observed relationship (Anderson et al. 2008). In this study, this was not the case (Table 4), so it can be inferred that the predictors are not inter-correlated. The fact that mean temperature, mean salinity, and oxygen concentration are the main predictors for richness indices such as alpha diversity, Shannon-Wiener index and Hurlbert index relates to the kinetic energy and the environmental stress hypotheses, as higher temperatures are beneficial for ectotherms development, which may lead to higher speciation rates (Fraser and Currie 1996; Tittensor et al. 2010); whereas environmental stress in terms of temperature and salinity extremes (Fraser and Currie 1996) and oxygen depletion (Tittensor et al. 2010) is negatively correlated with diversity. This also reflects the relevance that water masses and the OMZ may have on copepod populations, as the environmental conditions they generate have effects on different aspects of copepods ecology in the HCS (Escribano et al. 2014; Ruz et al. 2018). The importance of temperature stability and EKE as main predictors of species composition and its additive components turnover and nestedness, relates to the climate stability and historical factors hypotheses, that assumes higher diversity in more environmentally stable regions (Tittensor et al. 2010) and provide habitat features that favor

extant patterns of dispersal and richness (Fraser and Currie 1996), respectively. Therefore, mesoscale activity seems to be an important feature at a regional scale for zooplankton, as it has been documented how copepods are transported offshore by eddies, with some species potentially coupling their ontogeny to that process, such as *Calanus chilensis* (Schukat et al. 2021).

In summary, it appears that even at regional scale, different aspects related to basal hydrographic conditions, as well as the coupling of physical and biological processes are affecting diversity, with responses to their variations in terms of phenotypic plasticity that are species-specific. This, added to the individual variability (Bi and Liu 2017), may generate a variety of responses on copepod species. Moreover, within the context of climate change and global warming, it has been described that the effects of temperature variation on different marine communities at different scales are translated into a slowly replacement of cold-tolerant species with warm-tolerant counterparts, with the former being redistributed to greater depths (Burrows et al. 2019), without necessarily decreasing the system's functionality or shifting horizontal patterns, unless the species interact with the surface for the need of light, or as in the case of copepods, for feeding following DVM. Then, some increased depth range found in this study for some copepod species may be related to warming responses and vertical redistribution. However, this may represent an increase in the metabolic activity for some individuals not adapted for low oxygen conditions or that perform their life cycles associated with processes occurring at shallower depths. Considering the dynamism of the HCS and the increased capacity of plankton to rapidly respond to environmental shifts in temporal and special scales, greater assessments are required for better understanding copepods distribution and their shifts extent, with an

associated need for an enrichment of ecological data bases in terms of temporal and spatial coverage, for better implementing macroecological modeling techniques that yield more robust spatial patterns and their associated dominant drivers or processes.

Conflict of Interest

The authors declare that the research was conducted in the absence of any commercial or financial relationships that could be construed as a potential conflict of interest.

Author Contributions

M.P-A, RE and RR developed conceptual ideas and assessed diversity indices and statistical analyses, CG and VO performed analyses of environmental data and contributed with results descriptions, CH contributed with writing and conceptual ideas. All co-authors contributed with writing and editing the work.

Funding

This work was funded by the Instituto Milenio de Oceanografía (IMO) through the Agencia Nacional de Investigación Científica y Tecnológica de Chile (ANID) Grant AIM23-0003. The funders had no role in study design, data collection and analysis, decision to publish, or preparation of the manuscript.

Acknowledgments

We are grateful to all the scientific community providing data on marine biodiversity to OBIS portal, and especially thankful to Unesco/IODE/OBIS/ESPOBIS, the Eastern Southern Pacific-Oceanographic Biodiversity Information System and Programa de Biodiversidad Marina, 2024001000PG, Universidad de Concepción.

Data Availability Statement

All data used in this study on occurrences of Copepoda species and environmental variables are fully available in Zenodo repository https://doi.org/10.5281/zenodo.xxxxxx, together with the R scripts used to run the analyses (when applicable).

References

Aguilera, V.M. 2020. “PH and Other Upwelling Hydrographic Drivers in Regulating Copepod Reproduction during the 2015 El Niño Event: A Follow-up Study.” *Estuarine, Coastal and Shelf Science* 234(November 2019):106640. doi: 10.1016/j.ecss.2020.106640.

Aguilera, V.M., and N. Bednaršek. 2022. “Variations in Phenotypic Plasticity in a Cosmopolitan Copepod Species across Latitudinal Hydrographic Gradients.” *Frontiers in Ecology and Evolution* 10(October):1–19. doi: 10.3389/fevo.2022.925648.

Aguirre C., R. Garreaud, L. Belmar, L. Farías, L. Ramajo, and F. Barrera. 2021. “High-Frequency Variability of the Surface Ocean Properties Off Central Chile During the Upwelling Season.” *Frontiers in Marine Science* 8(3):1–19. doi: 10.3389/fmars.2021.702051.

Anabalón, V., C. E. Morales, R. Escribano, and M.A. Varas. 2007. “The Contribution of Nano- and Micro-Planktonic Assemblages in the Surface Layer (0-30 m) under Different Hydrographic Conditions in the Upwelling Area off Concepción, Central Chile.” *Progress in Oceanography* 75(3):396–414. doi: 10.1016/j.pocean.2007.08.023.

Ancapichun S. and J. Garcés-Vargas. 2015. “Variability of the Southeast Pacific Subtropical Anticyclone and Its Impact on Sea Surface Temperature off North-Central Chile.” *Ciencias Marinas* 41(1):1–20. doi: 10.7773/cm.v41i1.2338.

Anderson, M. J., R. N. Gorley, and K. R. Clarke. 2008. *PERMANOVA+ for PRIMER:*

Guide to Software and Statistical Methods. Plymouth, UK.

Anderson M.J. 2001. "A New Method for Non-Parametric Multivariate Analysis of Variance." *Austral Ecology* 26:32–46.

Anderson M.J. 2017. "Permutational Multivariate Analysis of Variance (PERMANOVA)." *Wiley StatsRef: Statistics Reference Online* 1–15. doi: 10.1002/9781118445112.stat07841.

Arnqvist G. 2020. "Mixed Models Offer No Freedom from Degrees of Freedom." *Trends in Ecology and Evolution* 35(4):329–35. doi: 10.1016/j.tree.2019.12.004.

Bartoń K. 2022. "Package MuMIn: Multi-Model Inference."

Baselga A. 2010. "Partitioning the Turnover and Nestedness Components of Beta Diversity." *Global Ecology and Biogeography* 19(1):134–43. doi: 10.1111/j.1466-8238.2009.00490.x.

Baselga A., and C. Gómez-Rodríguez. 2019. "Alpha, Beta and Gamma Diversity: Measuring Differences in Biological Communities." *Nova Acta Científica Compostelana (Bioloxía)* 26:39–45.

Baselga A. and C.D.L. Orme. 2012. "Betapart: An R Package for the Study of Beta Diversity." *Methods in Ecology and Evolution* 3(5):808–12. doi: 10.1111/j.2041-210X.2012.00224.x.

Bates D. 2005. "Fitting Linear Mixed Models in R: Using the Lme4 Package." *R News* 5(1):27–30. doi: 10.1108/13666282200300001.

Bates D., M. Maechler, B. Bolker, S. Walker, R.H.B. Christensen, H. Singmann, B. Dai, F.

Scheipl, G. Grothendieck, P. Green, J. Fox, P. N. Krivistsky, E. Tanaka, and M. Jagan. 2024. *Linear Mixed-Effects Models Using "Eigen" and S4: Package "Lme4."*

Bi R. and H. Liu. 2017. "Effects of Variability among Individuals on Zooplankton Population Dynamics under Environmental Conditions." *Marine Ecology Progress Series* 564:9–28. doi: 10.3354/meps11967.

Boaden P.J.S., and R. Seed. 1985. *An Introduction to Coastal Ecology*. London: Blackie Academic and Professional, an Imprint of Chapman and Hall.

Bolker B.M. 2015. "Linear and Generalized Linear Mixed Models." *Ecological Statistics* 309–33. doi: 10.1093/acprof:oso/9780199672547.003.0014.

Briggs J.C., and B.W. Bowen. 2012. "A Realignment of Marine Biogeographic Provinces with Particular Reference to Fish Distributions." *Journal of Biogeography* 39(1):12–30. doi: 10.1111/j.1365-2699.2011.02613.x.

Bucheli R., J. Cajas, and P. Hidalgo. 2019. "¿Es Calanus Chilensis Un Indicador de La Corriente de Humboldt En El Pacifico Ecuatoriano?" *Acta Oceanográfica Del Pacífico* 23.

Burrows M.T., A.E. Bates, M.J. Costello, M. Edwards, G.J. Edgar, C.J. Fox, B.S. Halpern, J.G. Hiddink, M.L. Pinsky, R.D. Batt, J. García Molinos, B.L. Payne, D.S. Schoeman, R.D. Stuart-Smith, and E.S. Poloczanska. 2019. "Ocean Community Warming Responses Explained by Thermal Affinities and Temperature Gradients." *Nature Climate Change* 9(December):1–5. doi: 10.1038/s41558-019-0631-5.

Camus, P.A. 2001. "Biogeografía Marina de Chile Continental." *Revista Chilena de Historia Natural* 74(3):587–617. doi: 10.4067/s0716-078x2001000300008.

Chesson, P. 2000. “Mechanisms of Maintainance of Species Diversity.” *Annual Review of Ecology and Systematics* 31:343–66. doi: 10.1146/annurev.ecolsys.31.1.343.

Costello, M.J., P. Tsai, P.S. Wong, A. Kwok, L. Cheung, Z. Basher, and C. Chaudhary. 2017. “Marine Biogeographic Realms and Species Endemicity.” *Nature Communications* 8(1057):1–9. doi: 10.1038/s41467-017-01121-2.

Desportes C., M. Drévillon, M. Clavier, and A. Gounou. 2021. “Global Ocean Ensemble Physics Reanalysis - Low Resolution.” Retrieved on September 11th, 2024 (https://data.marine.copernicus.eu/product/GLOBAL_REANALYSIS_PHY_001_026/description).

Dormann C.F., J. Elith, S. Bacher, C. Buchmann, G. Carl, G. Carré, J.R.G. Marquéz, B. Gruber, B. Lafourcade, P.J. Leitão, T. Münkemüller, C. Mcclean, P.E. Osborne, B. Reineking, B. Schröder, A.K. Skidmore, D. Zurell, and S. Lautenbach. 2013. “Collinearity: A Review of Methods to Deal with It and a Simulation Study Evaluating Their Performance.” *Ecography* 36(1):27–46. doi: 10.1111/j.1600-0587.2012.07348.x.

Escribano R. and P. Hidalgo. 2000. “Spatial Distribution of Copepods in the North of the Humboldt Current Region off Chile during Coastal Upwelling.” *Journal of the Marine Biological Association of the United Kingdom* 80(2):283–90. doi: 10.1017/S002531549900185X.

Escribano R., P. Hidalgo, M. Fuentes and K. Donoso. 2012. “Zooplankton Time Series in the Coastal Zone off Chile: Variation in Upwelling and Responses of the Copepod Community.” *Progress in Oceanography* 97–100:174–86. doi:

10.1016/j.pocean.2011.11.006.

Escribano R., P. Hidalgo, H. González, R. Giesecke, R. Riquelme-Bugueño, and K. Manríquez. 2007. “Seasonal and Inter-Annual Variation of Mesozooplankton in the Coastal Upwelling Zone off Central-Southern Chile.” *Progress in Oceanography* 75(3):470–85. doi: 10.1016/j.pocean.2007.08.027.

Escribano R., P. Hidalgo, V. Valdés, and L. Frederick. 2014. “Temperature Effects on Development and Reproduction of Copepods in the Humboldt Current: The Advantage of Rapid Growth.” *Journal of Plankton Research* 36(1):104–16. doi: 10.1093/plankt/fbt095.

Fang, J., Y. Cheng and B. Liu. 2024. “From Two-Dimensional to Three-Dimensional Marine Spatial Planning Methodology: A Case Study of Qidong.” *Ocean and Coastal Management* 253(April):107163. doi: 10.1016/j.ocecoaman.2024.107163.

Fine P.V.A. 2015. “Ecological and Evolutionary Drivers of Geographic Variation in Species Diversity.” *Annual Review of Ecology, Evolution, and Systematics* 46(October):369–92. doi: 10.1146/annurev-ecolsys-112414-054102.

Fischer A.G. 1960. “Latitudinal Variations in Organic Diversity.” *Evolution* 14(1):64. doi: 10.2307/2405923.

Fischer J.M., Frost T.M. and Ives A.R. 2001. Compensatory dynamics in zooplankton community responses to acidification: Measurement and mechanisms. Ecological Applications 11, 1060–1072. doi: 10.1890/1051-0761(2001)011[1060:CDIZCR]2.0.CO;2.

Fjeldså, J., D. Ehrlich, E. Lambin, and E. Prins. 1997. “Are Biodiversity ‘hotspots’

Correlated with Current Ecoclimatic Stability? A Pilot Study Using the NOAA-AVHRR Remote Sensing Data." *Biodiversity and Conservation* 6:401–22.

Fraser R.H., and D.J. Currie. 1996. "The Species Richness-Energy Hypothesis in a System Where Historical Factors Are Thought to Prevail: Coral Reefs." *The American Naturalist* 148(1):138–59.

Le Galloudec, O., C. Perruche, C. Derval, M. Tressol, and R. Dussurget. 2021. "Global Ocean Biogeochemistry Hindcast." Retrieved (https://data.marine.copernicus.eu/product/GLOBAL_MULTIYEAR_BGC_001_029/description).

García-Reyes M., W.J. Sydeman, D.S. Schoeman, R.R. Rykaczewski, B.A. Black, A.J. Smit, and S.J. Bograd. 2015. "Under Pressure: Climate Change, Upwelling, and Eastern Boundary Upwelling Ecosystems." *Frontiers in Marine Science* 2(December):1–10. doi: 10.3389/fmars.2015.00109.

Getis A. and J.K. Ord. 1992. "The Analysis of Spatial Association by Use of Distance Statistics." *Geographical Analysis* 24(3):189–206. doi: 10.1111/j.1538-4632.1992.tb00261.x.

Guerrina M., D. Dagnino, L. Minuto, F. Médail and G. Casazza. 2024. "Unveiling the Hypotheses of Endemic Richness: A Study Case in the Southwestern Alps." *Perspectives in Plant Ecology, Evolution and Systematics* 63(April). doi: 10.1016/j.ppees.2024.125792.

Guinehut, S. 2021. "Multi Observation Global Ocean 3D Temperature Salinity Height Geostrophic Current and MLD." Retrieved on September 11th, 2024

(https://data.marine.copernicus.eu/product/MULTIOBS_GLO_PHY_TSUV_3D_MYNRT_015_012/description).

Hammer Ø., D.A.T. Harper, and P.D. Ryan. 2001. “Past: Paleontological Statistics Software Package for Education and Data Analysis.” *Palaeontologia Electronica* 4(1):9pp.

Hartig F. 2024. “Residual Diagnostics for Hierarchical (Multi-Level/Mixed) Regression Models. Package ‘DHARMa.’” 73 pp.

Hernández C.E., R.A. Moreno, and N. Rozbaczylo. 2005. “Biogeographical Patterns and Rapoport’s Rule in Southeastern Pacific Benthic Polychaetes of the Chilean Coast.” *Ecography* 28(3):363–73.

Hersbach, H., B. Bell, P. Berrisford, G. Biavati, A. Horányi, J. Muñoz Sabater, J. Nicolas, C. Peubey, R. Radu, I. Rozum, D. Schepers, A. Simmons, C. Soci, D. Dee, and J. N. Thépaut. 2023. “ERA5 Hourly Data on Single Levels from 1940 to Present.” *Copernicus Climate Change Service (C3S) Climate Data Store (CDS)*. Retrieved July 30, 2024 (https://cds-beta.climate.copernicus.eu/datasets/reanalysis-era5-single-levels?tab=overview).

Hidalgo P., R. Escribano, and C.E. Morales. 2005. “Ontogenetic Vertical Distribution and Diel Migration of the Copepod Eucalanus Inermis in the Oxygen Minimum Zone off Northern Chile (20-21° S).” *Journal of Plankton Research* 27(6):519–29. doi: 10.1093/plankt/fbi025.

Hidalgo P., R. Escribano, O. Vergara, E. Jorquera, K. Donoso, and P. Mendoza. 2010. “Patterns of Copepod Diversity in the Chilean Coastal Upwelling System.” *Deep-Sea*

Research Part II 57(24–26):2089–97. doi: 10.1016/j.dsr2.2010.09.012.

Jacob, B.G., F.J. Tapia, R.A. Quiñones, R. Montes, M. Sobarzo, W. Schneider, G. Daneri, C.E. Morales, P. Montero, and H.E. González. 2018. "Major Changes in Diatom Abundance, Productivity, and Net Community Metabolism in a Windier and Dryer Coastal Climate in the Southern Humboldt Current." *Progress in Oceanography* 168(October):196–209. doi: 10.1016/j.pocean.2018.10.001.

Jia F., L. Wu, and B. Qiu. 2011. "Seasonal Modulation of Eddy Kinetic Energy and Its Formation Mechanism in the Southeast Indian Ocean." *Journal of Physical Oceanography* 41(4):657–65. doi: 10.1175/2010JPO4436.1.

Klopfer P.H. 1959. "Environmental Determinants of Faunal Diversity." *The American Naturalist* 93(873):337–42. doi: 10.1086/282092.

Laffan S.W. 2022. "Indices Available in Biodiverse." Retrieved (https://github.com/shawnlaffan/biodiverse/wiki/Indices#simpson-and-shannon).

Laffan S.W., E. Lubarsky, and D.F. Rosauer. 2010. "Biodiverse, a Tool for the Spatial Analysis of Biological and Related Diversity." *Ecography* 33(4):643–47. doi: 10.1111/j.1600-0587.2010.06237.x.

Marín V., S. Espinoza, and A. Fleminger. 1994. "Morphometric Study of Calanus Chilensis Males along the Chilean Coast." *Hydrobiologia* 292–293(1):75–80. doi: 10.1007/BF00229925.

Marín, V.H., R. Escribano, L.E. Delgado, G.Olivares, and P. Hidalgo. 2001. "Nearshore Circulation in a Coastal Upwelling Site off the Northern Humboldt Current System." *Continental Shelf Research* 21(13–14):1317–29. doi: 10.1016/S0278-4343(01)00022-

X.

Medellín-Mora J., R. Escribano, A. Corredor-Acosta, P. Hidalgo, and W. Schneider. 2021. "Uncovering the Composition and Diversity of Pelagic Copepods in the Oligotrophic Blue Water of the South Pacific Subtropical Gyre." *Frontiers in Marine Science* 8(July):1–18. doi: 10.3389/fmars.2021.625842.

Medellín-Mora J., R. Escribano and W. Schneider. 2016. "Community Response of Zooplankton to Oceanographic Changes (2002–2012) in the Central/Southern Upwelling System of Chile." *Progress in Oceanography* 142:17–29. doi: 10.1016/j.pocean.2016.01.005.

Miloslavich P., E. Klein, J. M. Díaz, C.E. Hernández, G. Bigatti, L. Campos, F. Artigas, J. Castillo, P.E. Penchaszadeh, P.E. Neill, A. Carranza, M.V. Retana, J.M. Díaz de Astarloa, M. Lewis, P. Yorio, M.L. Piriz, D. Rodríguez, Y.Y. Valentin, L. Gamboa, and A. Martín. 2011. "Marine Biodiversity in the Atlantic and Pacific Coasts of South America: Knowledge and Gaps." *PLoS ONE* 6(1):e14631. doi: 10.1371/journal.pone.0014631.

Montecino V. and C.B. Lange. 2009. "The Humboldt Current System: Ecosystem Components and Processes, Fisheries, and Sediment Studies." *Progress in Oceanography* 83(1–4):65–79. doi: 10.1016/j.pocean.2009.07.041.

Morales, C.E., S.E. Hormazábal, and J.L. Blanco. 1999. "Interannual Variability in the Mesoscale Distribution of the Depth of the Upper Boundary of the Oxygen Minimum Layer off Northern Chile (18–24S): Implications for the Pelagic System and Biogeochemical Cycling." *Journal of Marine Research* 57:909–32.

Morales, C. E., M. L. Torreblanca, S. Hormazabal, M. Correa-Ramírez, S. Nuñez, and P. Hidalgo. 2010. “Mesoscale Structure of Copepod Assemblages in the Coastal Transition Zone and Oceanic Waters off Central-Southern Chile.” Progress in Oceanography 84(3–4):158–73. doi: 10.1016/j.pocean.2009.12.001.

Moreno, R. A., C. E. Hernández, M. M. Rivadeneira, M. A. Vidal, and N. Rozbaczylo. 2006. “Patterns of Endemism in South-Eastern Pacific Benthic Polychaetes of the Chilean Coast.” Journal of Biogeography 33(4):750–59. doi: 10.1111/j.1365-2699.2005.01394.x.

Moreno, R. A., M. M. Rivadeneira, C. E. Hernández, S. Sampértegui, and N. Rozbaczylo. 2008. “Do Rapoport’s Rule, the Mid-Domain Effect or the Source-Sink Hypotheses Predict Bathymetric Patterns of Polychaete Richness on the Pacific Coast of South America?” Global Ecology and Biogeography 17(3):415–23. doi: 10.1111/j.1466-8238.2007.00372.x.

Oksanen, J., G. L. Simpson, R. Kindt, P. Legendre, P. R. Minchin, R. B. O’Hara, P. Solymos, M. H. H. Stevens, E. Szoecs, H. Wagner, M. Barbour, M. Bedward, B. Bolker, D. Borcard, H. B. Antoniazi Evangelista, R. FitzJohn, M. Friendly, B. Furneaux, G. Hannigan, M. O. Hill, L. Lahti, D. McGlinn, M. H. Ouellette, E. Ribeiro Cunha, T. Smith, A. Stier, C. J. F. Ter Braak, and J. Weedon. 2024. Community Ecology Package, “Vegan.”

Owens, H. L., and R. Guralnick. 2019. “ClimateStability: An R Package to Estimate Climate Stability from Time-Slice Climatologies.” Biodiversity Informatics 14:8–13. doi: 10.17161/bi.v14i0.9786.

Park, E. T., and F. D. Ferrari. 2009. Species Diversity and Distributions of Pelagic Calanoid Copepods (Crustacea) from the Southern Ocean.

Park, T. 1994. “Geographic Distribution of the Bathypelagic Genus Paraeuchaeta (Copepoda, Calanoida).” Hydrobiologia 292–293(1):317–32. doi: 10.1007/BF00229957.

Peterson, W. 1998. “Life Cycle Strategies of Copepods in Coastal Upwelling Zones.” Journal of Marine Systems 15(1–4):313–26. doi: 10.1016/S0924-7963(97)00082-1.

Peterson, W. T., and D. C. Bellantoni. 1987. “Relationships between Water-Column Stratification, Phytoplankton Cell Size and Copepod Fecundity in Long Island Sound and off Central Chile.” South African Journal of Marine Science 5(1):411–21. doi: 10.2989/025776187784522748.

Pianka, E. R. 1966. “Latitudinal Gradients in Species Diversity: A Review of Concepts.” The American Naturalist 100(910):33–46. doi: 10.1086/282398.

Pino-Pinuer, P., R. Escribano, P. Hidalgo, R. Riquelme-Bugueño, and W. Schneider. 2014. “Copepod Community Response to Variable Upwelling Conditions off Central-Southern Chile during 2002−2004 and 2010−2012.” Marine Ecology Progress Series 515:83–95. doi: 10.3354/meps11001.

Provoost, P., and S. Bosch. 2021. “Robis: Ocean Biodiversity Information System (OBIS) Client. R Package Version 2.8.2.”

Rivera, R., R. Escribano, C. E. González, and M. Pérez-Aragón. 2023. “Modeling Present and Future Distribution of Plankton Populations in a Coastal Upwelling Zone: The

Copepod Calanus Chilensis as a Study Case." Scientific Reports 13(1). doi: 10.1038/s41598-023-29541-9.

Ruz, P. M., P. Hidalgo, R. Escribano, J. E. Keister, L. Yebra, and B. Franco-Cisterna. 2018. "Hypoxia Effects on Females and Early Stages of Calanus Chilensis in the Humboldt Current Ecosystem (23°S)." Journal of Experimental Marine Biology and Ecology 498(September 2017):61–71. doi: 10.1016/j.jembe.2017.09.018.

Ruz, P. M., P. Hidalgo, S. Yáñez, R. Escribano, and J. E. Keister. 2015. "Egg Production and Hatching Success of Calanus Chilensis and Acartia Tonsa in the Northern Chile Upwelling Zone (23°S), Humboldt Current System." Journal of Marine Systems 148:200–212. doi: 10.1016/j.jmarsys.2015.03.007.

Sanches Melo, A. 2021. "Package 'CommEcol', Community Ecology Analyses." 1–34.

Sauzède, R., P. R. Renosh, and H. Claustre. 2023. "Global Ocean 3D Chlorophyll-a Concentration, Particulate Backscattering Coefficient and Particulate Organic Carbon." Retrieved (https://data.marine.copernicus.eu/product/MULTIOBS_GLO_BIO_BGC_3D_REP_015_010/description).

Schemske, D. W., and G. G. Mittelbach. 2017. "'Latitudinal Gradients in Species Diversity': Reflections on Pianka's 1966 Article and a Look Forward." American Naturalist 189(6):599–603. doi: 10.1086/691719.

Schneider, W., D. Donoso, J. Garcés-Vargas, and R. Escribano. 2017. "Water-Column Cooling and Sea Surface Salinity Increase in the Upwelling Region off Central-South

Chile Driven by a Poleward Displacement of the South Pacific High." Progress in Oceanography 151:38–48. doi: 10.1016/j.pocean.2016.11.004.

Schneider, W., M. Fukasawa, J. Garcés-Vargas, L. Bravo, H. Uchida, T. Kawano, and R. Fuenzalida. 2007. "Spin-up of South Pacific Subtropical Gyre Freshens and Cools the Upper Layer of the Eastern South Pacific Ocean." Geophysical Research Letters 34:1–5. doi: 10.1029/2007GL031933.

Schukat, A., W. Hagen, S. Dorschner, J. Correa Acosta, E. L. Pinedo Arteaga, P. Ayón, and H. Auel. 2021. "Zooplankton Ecological Traits Maximize the Trophic Transfer Efficiency of the Humboldt Current Upwelling System." Progress in Oceanography 193(September 2020). doi: 10.1016/j.pocean.2021.102551.

Silva, N., N. Rojas, and A. Fedele. 2009. "Water Masses in the Humboldt Current System: Properties, Distribution, and the Nitrate Deficit as a Chemical Water Mass Tracer for Equatorial Subsurface Water off Chile." Deep Sea Research Part II: Topical Studies in Oceanography 56:1004–20. doi: 10.1016/j.dsr2.2008.12.013.

Sobarzo, M., L. Bravo, D. Donoso, J. Garcés-Vargas, and W. Schneider. 2007. "Coastal Upwelling and Seasonal Cycles That Influence the Water Column over the Continental Shelf off Central Chile." Progress in Oceanography 75(3):363–82. doi: 10.1016/j.pocean.2007.08.022.

Spalding, M. D., V. N. Agostini, J. Rice, and S. M. Grant. 2012. "Pelagic Provinces of the World: A Biogeographic Classification of the World's Surface Pelagic Waters." Ocean and Coastal Management 60:19–30. doi: 10.1016/j.ocecoaman.2011.12.016.

Spalding, M. D., H. E. Fox, G. R. Allen, N. Davidson, Z. A. Ferdaña, M. Finlayson, B. S. Halpern, M. A. Jorge, A. Lombana, S. A. Lourie, K. D. Martin, E. McManus, J. Molnar, C. A. Recchia, and J. Robertson. 2007. "Marine Ecoregions of the World: A Bioregionalization of Coastal and Shelf Areas." BioScience 57(7):573–83. doi: 10.1641/B570707.

Strub, P. T., J. M. Mesías, V. Montecino, J. Rutllant, and S. Salinas. 1998. "Coastal Ocean Circulation off Western South America." Pp. 273–313 in The Sea. John Wiley and Sons, Inc.

Thiel, M., E. Macaya, E. Acuña, W. Arntz, H. Bastias, K. Brokordt, P. Camus, J. Castilla, L. Castro, M. Cortés, C. Dumont, R. Escribano, M. Fernandez, J. Gajardo, C. Gaymer, I. Gomez, A. González, H. González, P. Haye, J.-E. Illanes, J. Iriarte, D. Lancellotti, G. Luna-Jorquera, C. Luxoro, P. Manriquez, V. Marín, P. Muñoz, S. Navarrete, E. Perez, E. Poulin, J. Sellanes, H. Sepúlveda, W. Stotz, F. Tala, A. Thomas, C. Vargas, J. Vasquez, and J. M. A. Vega. 2007. "The Humboldt Current System of Northern and Central Chile." Oceanography and Marine Biology 45:195–344. doi: 10.1201/9781420050943.ch6.

Tilman, D. 2004. "Niche Tradeoffs, Neutrality, and Community Structure: A Stochastic Theory of Resource Competition, Invasion, and Community Assembly." Proceedings of the National Academy of Sciences of the United States of America 101(30):10854–61. doi: 10.1073/pnas.0403458101.

Tittensor, D. P., C. Mora, W. Jetz, H. K. Lotze, D. Ricard, E. Vanden Berghe, C. Mora, and B. Worm. 2010. “Global Patterns and Predictors of Marine Biodiversity across Taxa.” Nature 466(7310):1098–1101. doi: 10.1038/nature09329.

Tutasi, P., and R. Escribano. 2020. “Zooplankton Diel Vertical Migration and Downward C Flux into the Oxygen Minimum Zone in the Highly Productive Upwelling Region off Northern Chile.” Biogeosciences 17(2):455–73. doi: 10.5194/bg-17-455-2020.

Vargas, C. A., R. Escribano, and S. Poulet. 2006. “Phytoplankton Food Quality Determines Time Windows for Successful Zooplankton Reproductive Pulses.” Ecology 87(12):2992–99. doi: 10.1890/0012-9658(2006)87[2992:PFQDTW]2.0.CO;2.

Vilela, B., and F. Villalobos. 2015. “LetsR: A New R Package for Data Handling and Analysis in Macroecology.” Methods in Ecology and Evolution 6(10):1229–34. doi: 10.1111/2041-210X.12401.

Wei, T., and V. Simko. 2024. “R Package ‘Corrplot’: Visualization of a Correlation Matrix. (Version 0.94).” Retrieved (https://github.com/taiyun/corrplot).

Wilke, C. O. 2024. Ridgeline Plots in “Ggplot2”. Package “Ggridges.”

Yamanaka, N. 1976. “The Distribution of Some Copepods (Crustacea) in the Southern Ocean and Adjacent Regions from 40o to 81o W Long.” Boletim de Zoologia 1(1):161. doi: 10.11606/issn.2526-3358.bolzoo.1976.121576.

Yáñez, S., P. Hidalgo, and R. Escribano. 2012. “Mortalidad Natural de Paracalanus Indicus (Copepoda: Calanoida) En Áreas de Surgencia Asociada a La Zona de Mínimo de Oxígeno En El Sistema de Corrientes Humboldt: Implicancias En El Transporte

Pasivo Del Flujo de Carbono.” Revista de Biología Marina y Oceanografía 47(2):295–310.

Yáñez, S., P. Hidalgo, P. Ruz, and K. W. Tang. 2018. “Copepod Secondary Production in the Sea: Errors Due to Uneven Molting and Growth Patterns and Incidence of Carcasses.” Progress in Oceanography 165(July 2017):257–67. doi: 10.1016/j.pocean.2018.06.008.

Supporting Information

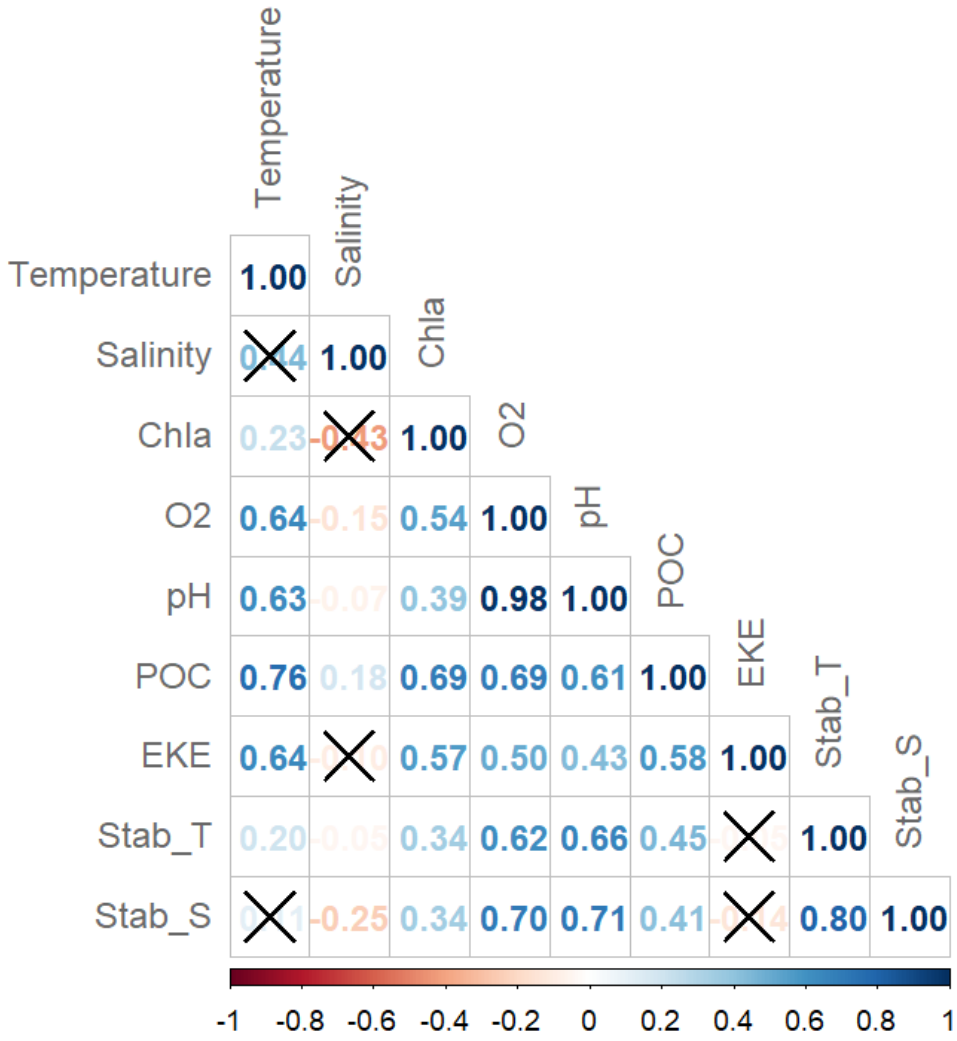

Figure S1: Spearman correlation matrix of environmental variables used in the Linear Mixed Models (LMM). Positive and negative correlations are displayed in blue and red color, respectively. Color intensity is proportional to the correlation coefficients, and the non-significant correlations are crossed out. The acronyms are: Temperature=mean temperature, Stab_T=temperature stability, Salinity=mean salinity, Stab_S=salinity stability Chla=chlorophyll-a concentration, O2=dissolved oxygen concentration, POC=particulate organic carbon, pH=potential of hydrogen, EKE=Eddy Kinetic Energy.

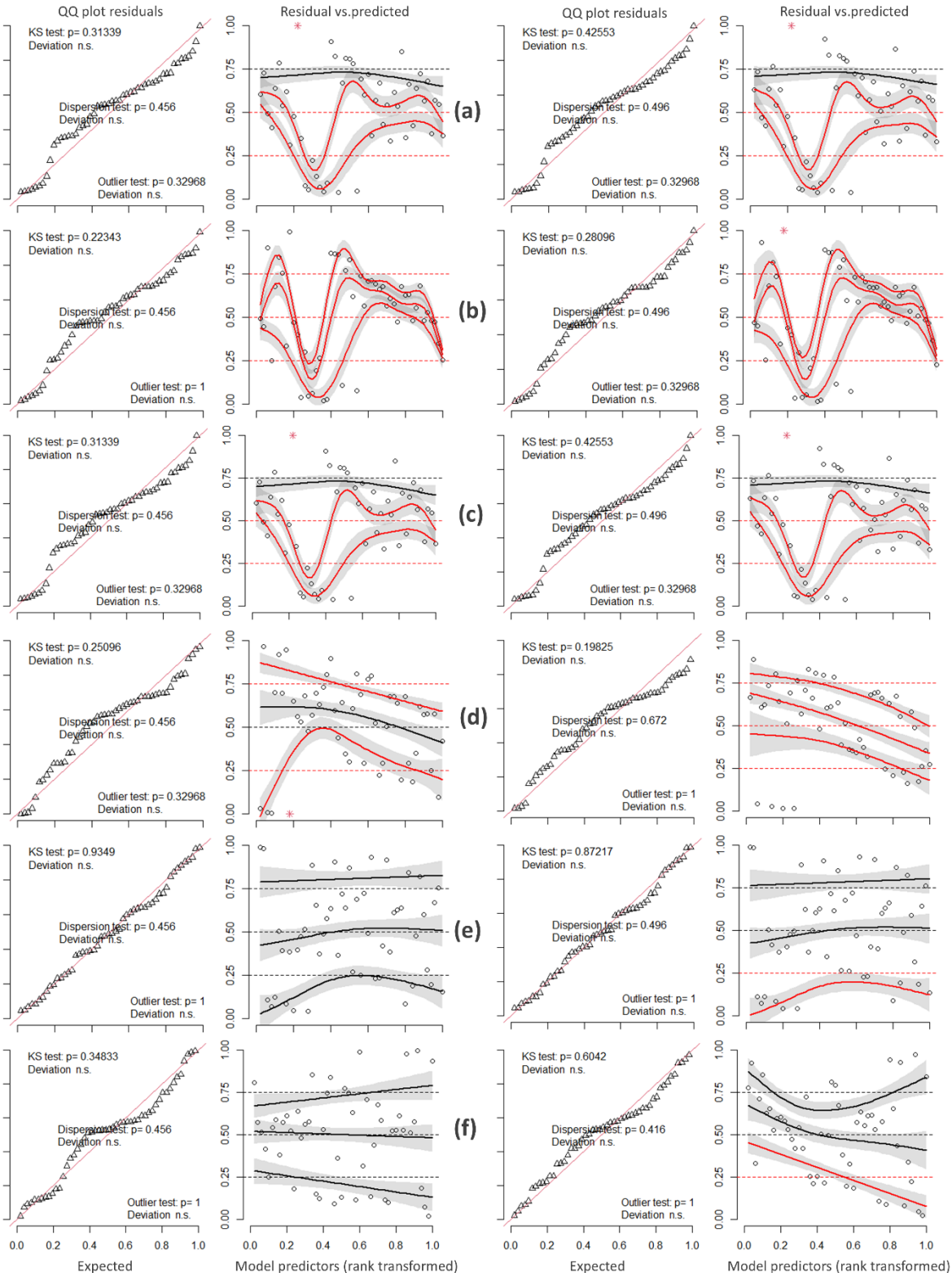

Figure S2: Residual diagnosis inferred from a linear model (LM, left panels) and a linear mixed model (LMM, right panels) for (a) species richness, (b) Shannon-Wiener index, (c) Hurlbert index, (d) β-diversity and its additive components (e) turnover and (f) nestedness. Each panel show a QQ plot (quantile-quantile plot) between observed and expected values, and the variation of their residuals. Kolmogorov-Smirnov (KS) test $p>0.05$.

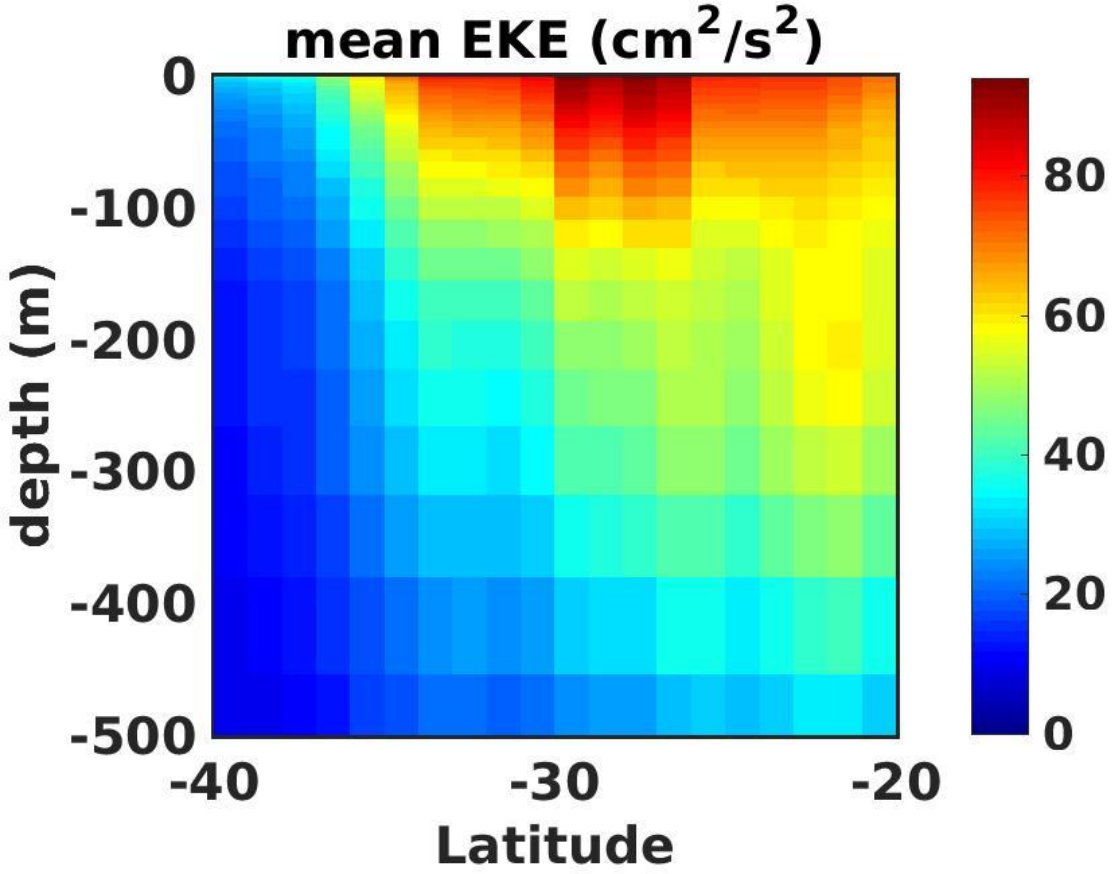

Figure S3: GLORYS12 EKE averaged between the coast and 78°W.

Table S1: Summary of common and exclusive species found in each zone and stratum of the study area.

	NORTH and SOUTH zones						NORTH zone			SOUTH zone	
	0-500 m	0-100 m	100-200 m	200-300 m	300-400 m	400-500 m	0-500 m	0-100 m	400-500 m	0-500 m	0-100 m
Acartia danae		x									
Acartia tonsa		x	x	x							
Aegisthus aculeatus							x				
Aetideus armatus		x									
Aetideus bradyi							x				
Agetus flaccus		x									
Agetus typicus	x	x	x	x	x	x					
Calanoides patagoniensis	x	x	x	x	x	x					
Calanus australis							x				
Calanus chilensis	x	x	x	x	x	x					
Calanus propinquus										X	
Calocalanus pavo											x
Calocalanus styliremis											x
Calocalanus tenuis											x
Candacia bipinnata							x				
Candacia catula											x
Candacia curta								x			
Candacia longimana										X	
Centropages brachiatus		x	x	x	x						
Centropages typicus							x				
Chiridius gracilis							x				
Chiridius poppei							x				
Clausocalanus arcuicornis		x									
Clausocalanus furcatus											x
Clausocalanus jobei											x
Clytemnestra scutellata										X	
Corycaeus speciosus										X	
Ctenocalanus citer											x
Ctenocalanus vanus		x									
Dioithona oculata							x				
Ditrichocorycaeus amazonicus		x									
Drepanopus forcipatus		x	x								
Euaugaptilus magnus							x				
Eucalanus elongatus		x									
Eucalanus hyalinus		x									
Eucalanus inermis		x									

Euchaeta marina	x	x	x	x	x	x					
Euchaeta media										X	
Euchirella amoena										X	
Euchirella maxima										X	
Euchirella messinensis							x		x		
Euchirella pulchra											x
Euchirella truncata							x				
Euterpina acutifrons											x
Gaetanus brevispinus							x				
Gaetanus kruppii							x				
Gaetanus miles							x				
Gaetanus tenuispinus										X	
Goniopsyllus rostratus		x									
Haloptilus acutifrons											x
Haloptilus longicornis											x
Haloptilus oxycephalus											x
Heterorhabdus clausi											x
Heterorhabdus lobatus											x
Heterorhabdus papilliger	x	x	x	x	x	x					
Heterorhabdus spinifrons										X	
Heterostylites longicornis							x				
Lophothrix frontalis							x				
Lubbockia squillimana											x
Lucicutia flavicornis		x		x	x	x					
Lucicutia grandis							x				
Lucicutia longiserrata							x				
Lucicutia magna							x				
Mecynocera clausi		x	x								
Mesocalanus tenuicornis											
Metridia brevicauda	x	x	x	x	x	x					
Metridia gerlachei							x				
Metridia lucens	x	x	x	x	x	x					
Microcalanus pygmaeus											x
Microsetella norvegica		x									
Microsetella rosea		x									
Mormonilla phasma		x		x	x	x					
Nannocalanus minor		x		x	x	x					
Neocalanus cristatus							x				
Neocalanus gracilis								x			
Neocalanus tonsus										X	
Neomormonilla minor							x				
Oculosetella gracilis											x
Oithona atlantica											

Oithona nana		x									
Oithona plumifera	x	x	x	x	x	x					
Oithona setigera	x	x	x	x	x	x					
Oithona similis	x	x	x	x	x	x					
Oncaea curvata	x	x	x	x	x	x					
Oncaea media	x	x	x	x	x	x					
Oncaea mediterranea	x	x	x	x	x	x					
Oncaea notopus					x	x					
Oncaea venusta		x	x	x							
Onchocalanus subcristatus							x				
Paracalanus indicus	x	x	x	x	x	x					
Paracalanus parvus							x				
Paraeuchaeta barbata							x		x		
Paraeuchaeta scotti							x				
Paraeuchaeta weberi										X	
Paraheterorhabdus vipera							x				
Pareucalanus attenuatus		x	x	x	x						
Phaenna spinifera							x				
Pleuromamma abdominalis										X	
Pleuromamma gracilis	x	x	x	x	x	x					
Pleuromamma piseki				x	x						
Pleuromamma quadrungulata	x	x	x	x	x	x					
Pleuromamma robusta				x	x						
Pleuromamma xiphias				x	x	x					
Pontellina plumata		x									
Pontoeciella abyssicola								x			
Pseudoamallothrix emarginata							x				
Pseudoamallothrix ovata											x
Pseudoamallothrix profunda		x									
Rhincalanus nasutus		x	x	x	x						
Scaphocalanus curtus											x
Scaphocalanus echinatus											x
Scaphocalanus elongatus							x				
Scolecithricella abyssalis											x
Scolecithricella minor											x
Scolecithrix bradyi		x	x								
Subeucalanus crassus		x									
Subeucalanus longiceps										X	x
Subeucalanus subtenuis							x				
Temora discaudata							x				
Temora stylifera		x									
Triconia antarctica										X	
Triconia conifera	x	x	x	x	x	x					

Triconia minuta	x	x	x	x	x	x					
Triconia similis											x
Urocorycaeus lautus								x			
Vettoria granulosa											x
TOTAL SPECIES	**18**	**46**	**26**	**29**	**28**	**23**	**32**	**4**	**2**	**14**	**25**

Table S2: Coefficients obtained by linear mixed models used to evaluate the best predictors for species richness, Shannon-Wiener index, Hurlbert index, beta diversity (species composition) and its additive components turnover and nestedness. Predictors' acronyms are: Chla=chlorophyll-a concentration, EKE=Eddy Kinetic Energy, O_2=dissolved oxygen concentration, S=mean salinity, S_{stab}=salinity stability, T_{stab} = temperature stability, T=mean temperature.

	Intercept	**Chla**	**EKE**	**O_2**	**S**	**S_{stab}**	**T_{stab}**	**T**
Species richness	2.23			-1.54	-0.51			1.44
	2.17		-0.26			-1.25	0.17	
	2.21			0.07		-1.09	0.09	
	2.20	-0.18				-1.13	0.21	
	2.22		-0.21	-1.50	-0.59			1.53
	2.19		-0.56	0.58		-1.67	0.18	
	2.23	0.07		-1.56	-0.49			1.44
	2.18	0.38	-1.01	-0.32	-0.52	-1.22	-0.06	1.34
	2.22	0.32	-0.53	-1.60	-0.63			1.75
	2.17	-0.13	-0.22			-1.27	0.23	
	2.21	-0.20		0.09		-1.19	0.23	
	2.19	-0.03	-0.54	0.56		-1.66	0.19	
	2.20		-0.23		0.14			0.18
	2.23	-0.13			0.18			0.08
	2.22	-0.05	-0.16		0.15			0.15
Shannon-Wiener index	0.97			-0.57	-0.15			0.49
	0.96		-0.08			-0.42	0.03	
	0.96	-0.08				-0.39	0.05	
	0.96			-0.01		-0.36	0.00	
	0.97		-0.05	-0.57	-0.17			0.52
	0.97	0.01		-0.57	-0.15			0.49
	0.96		-0.17	0.16		-0.54	0.03	
	0.96	-0.07	-0.06			-0.43	0.06	
	0.97	-0.09		0.01		-0.41	0.07	
	0.97	0.06	-0.11	-0.58	-0.18			0.56
	0.96	-0.04	-0.15	0.14		-0.53	0.05	
	0.95	0.11	-0.31	-0.16	-0.15	-0.38	-0.04	0.44
	0.96		-0.06		0.11			0.01
	0.98	-0.07			0.09			0.01
	0.99	-0.11	0.09		0.10			-0.03

	Intercept	**Chla**	**EKE**	**O_2**	**S**	**S_{stab}**	**T_{stab}**	**T**
Hurlbert index	2.23			-1.54	-0.51			1.44
	2.17		-0.26			-1.25	0.17	
	2.21			0.07		-1.09	0.09	
	2.20	-0.18				-1.13	0.21	
	2.22		-0.21	-1.50	-0.59			1.53
	2.19		-0.56	0.58		-1.67	0.18	
	2.23	0.07		-1.56	-0.49			1.44
	2.18	0.38	-1.01	-0.32	-0.52	-1.22	-0.06	1.34
	2.22	0.32	-0.53	-1.60	-0.63			1.75
	2.17	-0.13	-0.22			-1.27	0.23	
	2.21	-0.20		0.09		-1.19	0.23	
	2.19	-0.03	-0.54	0.56		-1.66	0.19	
	2.20		-0.23		0.14			0.18
	2.23	-0.13			0.18			0.08
	2.22	-0.05	-0.16		0.15			0.15
Species composition	0.52		0.06				0.08	
	0.52		0.06			-0.04	0.10	
	0.52	0.05				-0.05	0.10	
	0.52			0.01		-0.06	0.11	
	0.51	0.06			-0.01			0.02
	0.51		0.09		0.00			-0.02
	0.52		0.08	-0.06		0.01	0.11	
	0.52	0.03	0.03			-0.04	0.10	
	0.51	0.05		-0.02		-0.03	0.09	
	0.51			0.01	-0.02			0.01
	0.51	0.06	0.01		-0.004			0.01
	0.51	0.07		-0.01	-0.01			0.03
	0.52		0.09	0.01	0.01			-0.03
	0.52	0.02	0.06	-0.05		0.002	0.10	
	0.51	0.06	0.01	-0.01	-0.01			0.02
	0.52	0.02	0.05	-0.06	-0.03	-0.01	0.11	0.03

	Intercept	**Chla**	**EKE**	**O_2**	**S**	**S_{stab}**	**T_{stab}**	**T**
Turnover	0.39		0.04				0.005	
	0.39			0.02		-0.08	0.05	
	0.39		0.03			-0.06	0.04	
	0.39	-0.02				-0.06	0.07	
	0.39		0.07		0.02			-0.04
	0.39			-0.03	-0.04			0.04
	0.39	-0.03			-0.03			0.03
	0.39	-0.08	0.12		0.00			-0.05
	0.39	-0.06	0.07			-0.05	0.05	
	0.39		0.04	-0.02		-0.05	0.05	
	0.39	-0.03		0.04		-0.09	0.05	
	0.39		0.07	-0.03	0.01			-0.02
	0.39	-0.02		-0.02	-0.04			0.04
	0.39	-0.07	0.11	-0.05		-0.01	0.05	
	0.39	-0.08	0.13	0.02	0.01			-0.07
	0.39	-0.10	0.13	0.00	-0.01	-0.05	0.07	-0.06
Nestedness	0.18		0.04				0.06	
	0.18	0.06				-0.02	0.05	
	0.17	0.08			0.01			0.01
	0.18		0.04			0.00	0.05	
	0.18			0.04		-0.03	0.05	
	0.18			0.04	-0.01			0.01
	0.18	0.06		0.00		-0.02	0.05	
	0.18	0.06	0.00			-0.02	0.05	
	0.17	0.09	-0.04		0.00			0.04
	0.18		0.02		-0.03			0.03
	0.17	0.07		0.01	0.02			0.00
	0.18		0.05	-0.02		0.02	0.06	
	0.18	0.06	0.00	0.00		-0.02	0.05	
	0.18		0.02	0.05	0.00			-0.01
	0.17	0.10	-0.05	-0.02	-0.01			0.05
	0.17	0.11	-0.05	-0.09	-0.03	0.05	0.02	0.10

5. GENERAL DISCUSSION

For the South Pacific Ocean (SPO), the patterns of copepod distribution do not seem to follow the previously reported latitudinal trends of global patterns of marine species with peaks of diversity at subtropical latitudes and a gradual decrease towards temperate and polar regions (Le Borgne, Champalbert, and Gaudy 2003; Le Borgne and Rodier 1997; Carlotti et al. 2018; Dai et al. 2016; Fernández-Álamo and Färber-Lorda 2006; Rombouts et al. 2009; Tittensor et al. 2010). However, the presence of hot spots equatorial area off Peru and Ecuador (Figure 4, Chapter 1) coincides with the Eastern margin biogeographic region where coastal (0-250 Km offshore) and eastern (250-1000 Km offshore) boundary currents that originate from the Humboldt Current and has high levels of production (Pennington et al. 2006); whereas the hotspots observed in western temperate-subpolar areas off Australia (Figure 4, Chapter 1), corresponds, according to their zoning, to the South Subtropical Convergence and to the Chatham Rise zones, both frontal zones that marks the intersection of colder sub Antarctic waters with warmer tropical waters thus supporting substantial production (Dunstan et al. 2018). For the Humboldt Current System (HCS), copepods appear to inhabit the whole water column with shared species between zones, as well as distinct or exclusive species that were mainly occurring at the upper stratum (0-100 m) or intruding from deeper waters. The clustering analysis (Getis-Ord Gi*) allowed us to identify high values of richness in all strata at the NZ, whereas cold spots (i.e., low species richness values) were greater at the SZ and at greater depths (Figure 5, Chapter 2).

Regarding drivers of copepods diversity at regional and basin scales, various factors may serve to explain their patterns of horizontal and vertical zonation, based on different

hypotheses that appear not to be exclusive, and more likely revealing a combined effect. However, hydrographic conditions and processes determined as drivers of copepods diversity in the SPO and the HCS appear to be related to the kinetic energy hypothesis, highlighting the role of temperature on the biogeography of copepods and supporting our hypothesis where it is considered as a main driver of zooplankton distribution.

Our results described in both chapters of this thesis work highlight in one hand the dynamism of the ocean at basin (SPO) and regional (HCS) scales; and, on the other hand, the high ecological plasticity displayed by copepods to adapt to that natural environmental variability. However, more complete databases are required for better inferring macroecological patterns and determine to what extent they may cope with shifts in the timing, duration and extension of the hydrographic conditions and processes they rely on to survive, within the context of climate change and global warming.

6. CONCLUSIONS

- Our findings provide an overview of copepods diversity patterns and their potential drivers for the South Pacific Ocean (SPO, basin scale) and the Humboldt Current System (HCS, regional scale).
- Diversity patterns were detected zonally and meridionally for the SPO and the HCS. And, along the water column they were detected only at a regional scale (HCS), that counted with more data availability for performing analyses. For the basin scale study, we used integrated data from the upper 200 m of the water column of the eastern and western sides of the SPO as there was insufficient data both towards the South Pacific Central Gyre (open ocean) and greater depths. However, we were able to obtain emerging patterns despite these limitations and biases on databases, that undoubtedly may reveal in the future new evidence on the processes sustaining biodiversity.
- This thesis work stresses the need for strengthening the databases on planktonic organisms, as they can act as suitable indicators of ecosystem response to climate change at both basin (SPO) and regional (HCS) scales.
- The thesis supports the hypothesis that significant ecological zonation of copepods communities in the South Pacific region over the horizontal and vertical axes are strongly influenced by variation and stability of key environmental factors of which the variance of sea temperature and kinetic energy appeared as most important.

7. REFERENCES

van Aken, H. M. 2007. The Oceanic Thermohaline Circulation: An Introduction. Atmospheri. edited by L. A. Mysak and K. Hamilton. New York: Springer Science+Business Media.

Allen, A. P., J. H. Brown, and J. F. Gillooly. 2002. "Global Biodiversity, Biochemical Kinetics, and the Energetic-Equivalence Rule." Science 297(5586):1545–48. doi: 10.1126/science.1072380.

Allen, A. P., J. F. Gillooly, and J. H. Brown. 2007. "Recasting the Species–Energy Hypothesis: The Different Roles of Kinetic and Potential Energy in Regulating Biodiversity." Pp. 283–99 in Scaling Biodiversity, edited by D. Storch, P. A. Marquet, and J. H. Brown. New York: Cambridge University Press.

Anabalón, V., C. E. Morales, H. E. González, E. Menschel, W. Schneider, S. Hormazabal, L. Valencia, and R. Escribano. 2016. "Micro-Phytoplankton Community Structure in the Coastal Upwelling Zone off Concepción (Central Chile): Annual and Inter-Annual Fluctuations in a Highly Dynamic Environment." Progress in Oceanography 149:174–88. doi: 10.1016/j.pocean.2016.10.011.

Ancapichun, S., and J. Garcés-Vargas. 2015. "Variability of the Southeast Pacific Subtropical Anticyclone and Its Impact on Sea Surface Temperature off North-Central Chile." Ciencias Marinas 41(1):1–20. doi: 10.7773/cm.v41i1.2338.

Angel, M. V. 1982. "Ocean Trench Conservation. International Union for Conservation of Nature and Natural Resources." The Environmentalist 2(1):1–17. doi: 10.1016/S0251-1088(82)80001-6.

Appeltans, W., C. G. Messing, G. C. B. Poore, R. A. Bray, M. J. Costello, J. Lowry, M. N. Dawson, C. Nielsen, R. R. Hopcroft, B. W. Hoeksema, R. W. M. van Soest, C. B. Boyko, A. Warren, J. D. Reimer, W. Eschmeyer, R. M. Kristensen, W. Appeltans, S. Gofas, J. Norenburg, K. Fauchald, C. E. Mills, B. Neuhaus, W. Sterrer, I. Bartsch, G. Mapstone, E. Macpherson, H. Segers, D. Gibson, L. P. Madin, G. Lambert, L. Gómez-Daglio, N. Shenkar, M. Curini-Galletti, N. L. Bruce, P. Uetz, N. J. de Voogd, D. B. Lazarus, O. De Clerck, P. K. L. Ng, M. V. Angel, S. De Grave, E. V. Thuesen, B. Schierwater, J. Mees, G. Boxshall, F. Hernandez, S. P. Wilson, C. Self-Sullivan, P. Schuchert, E. Schwabe, B. Swalla, A. G. Collins, M. Longshaw, A. Gittenberger, T. Cribb, G. Walker-Smith, S. W. Feist, K. Meland, D. P. Gordon, V. Scarabino, P. Bock, R. Mooi, A. Berta, A. Kroh, S. Stöhr, W. Perrin, M. A. Todaro, S. N. Brandão, J. B. Kolb, M. L. Tasker, H. Furuya, A. Schmidt-Rhaesa, T. Artois, J. I. Saiz-Salinas, L. P. van Ofwegen, R. Bamber, R. Lemaitre, O. Garcia-Alvarez, G. C. Williams, G. B. Read, S. Koenemann, D. M. Opresko, T. C. Walter, C. Erséus, L. Cheng, G. Anderson, A. Barber, R. M. Rocha, P. Kirk, X. Turon, J. van der Land, K. E. Schnabel, N. Bailly, W. Decock, M. D. Guiry, C. C. Emig, N. Koedam, P. J. F. Davie, P. A. McLaughlin, D. P. Domning, T. N. Molodtsova, J. F. Pilger, S. Tyler, F. Dahdouh-Guebas, M. Schotte, T.-Y. Chan, T. Timm, D. G. Fautin, C. Mah, M. Osawa, G. Paulay, C. H. J. M. Fransen, J. Vanaverbeke, M. Rius, P. Pugh, B. Vanhoorne, S. Gerken, D. Jaume, M. Błażewicz-Paszkowycz, V. Siegel, S. D. Cairns, and S. T. Ahyong. 2012. “The Magnitude of Global Marine Species Diversity.” Current Biology 22(23):2189–2202. doi: 10.1016/j.cub.2012.09.036.

Barton, A. D., A. J. Pershing, E. Litchman, N. R. Record, K. F. Edwards, Z. V. Finkel, T.

Kiørboe, and B. A. Ward. 2013. “The Biogeography of Marine Plankton Traits.” Ecology Letters 16(4):522–34. doi: 10.1111/ele.12063.

Bartoń, K. 2022. “Package MuMIn: Multi-Model Inference.” R package version 1.47.5, <https://CRAN.R-project.org/package=MuMIn>.

Baselga, A., and C. Gómez-Rodríguez. 2019. “Alpha, Beta and Gamma Diversity: Measuring Differences in Biological Communities.” Nova Acta Científica Compostelana (Bioloxía) 26:39–45.

Baselga, A., and C. D. L. Orme. 2012. “Betapart: An R Package for the Study of Beta Diversity.” Methods in Ecology and Evolution 3(5):808–12. doi: 10.1111/j.2041-210X.2012.00224.x.

Bauer, J. E., and E. M. Druffel. 1998. “Ocean Margins as a Significant Source of Organic Matter to the Deep Open Ocean.” Nature 392(April):482–85.

Beaugrand, G., M. Edwards, and L. Legendre. 2010. “Marine Biodiversity, Ecosystem Functioning, and Carbon Cycles.” Proceedings of the National Academy of Sciences 107(22):10120–24. doi: 10.1073/pnas.0913855107.

Berline, L., I. Siokou-Frangou, I. Marasovic, O. Vidjak, M. L. F. de Puelles, M. G. Mazzocchi, G. Assimakopoulou, S. Zervoudaki, S. Fonda-umani, A. Conversi, C. Garcia-comas, F. Ibanez, S. Gasparini, L. Stemmann, and G. Gorsky. 2012. “Intercomparison of Six Mediterranean Zooplankton Time Series.” Progress in Oceanography 97–100:76–91. doi: 10.1016/j.pocean.2011.11.011.

Blanco-Bercial, L., J. Bradford-Grieve, and A. Bucklin. 2011. “Molecular Phylogeny of the Calanoida (Crustacea: Copepoda).” Molecular Phylogenetics and Evolution

59(1):103–13. doi: 10.1016/j.ympev.2011.01.008.

Boero, F., F. De Leo, S. Fraschetti, and G. Ingrosso. 2019. “The Cells of Ecosystem Functioning: Towards a Holistic Vision of Marine Space.” Pp. 1–25 in Advances in Marine Biology. Elsevier Ltd.

Boetius, A., S. Scheibe, A. Tselepides, and H. Thiel. 1996. “Microbial Biomass and Activities in Deep-Sea Sediments of the Eastern Mediterranean: Trenches Are Benthic Hotspots.” Deep-Sea Research Part I: Oceanographic Research Papers 43(9):1439–60. doi: 10.1016/S0967-0637(96)00053-2.

Le Borgne, R., G. Champalbert, and R. Gaudy. 2003. “Mesozooplankton Biomass and Composition in the Equatorial Pacific along 180.” Journal of Geophysical Research: Oceans 108(12):1–10. doi: 10.1029/2000jc000745.

Le Borgne, R., and M. Rodier. 1997. “Net Zooplankton and the Biological Pump: A Comparison between the Oligotrophic and Mesotrophic Equatorial Pacific.” Deep-Sea Research Part II: Topical Studies in Oceanography 44(9–10):2003–23. doi: 10.1016/S0967-0645(97)00034-9.

Bradford-Grieve, J. M. 2002. “Colonization of the Pelagic Realm by Calanoid Copepods.” Hydrobiologia 485:223–44. doi: 10.1023/A:1021373412738.

Braga, E., R. Zardoya, A. Meyer, and J. Yen. 1999. “Mitochondrial and Nuclear RRNA Based Copepod Phylogeny with Emphasis on the Euchaetidae (Calanoida).” Marine Biology 133(1):79–90. doi: 10.1007/s002270050445.

Brown, A., and S. Thatje. 2011. “Respiratory Response of the Deep-Sea Amphipod Stephonyx Biscayensis Indicates Bathymetric Range Limitation by Temperature and

Hydrostatic Pressure." PLoS ONE 6(12). doi: 10.1371/journal.pone.0028562.

Brown, A., S. Thatje, J. P. Morris, A. Oliphant, E. A. Morgan, C. Hauton, D. O. B. Jones, and D. W. Pond. 2017. "Metabolic Costs Imposed by Hydrostatic Pressure Constrain Bathymetric Range in the Lithodid Crab Lithodes Maja." Journal of Experimental Biology 220(November):3916–26. doi: 10.1242/jeb.158543.

Brown, J. H., J. F. Gillooly, A. P. Allen, V. M. Savage, and G. B. West. 2004. "Toward a Metabolic Theory of Ecology." Ecology 85(7):1771–89.

Carlotti, F., M. Pagano, L. Guilloux, K. Donoso, V. Valdés, O. Grosso, and B. P. V. Hunt. 2018. "Meso-Zooplankton Structure and Functioning in the Western Tropical South Pacific along the 20th Parallel South during the OUTPACE Survey (February-April 2015)." Biogeosciences 15(23):7273–97. doi: 10.5194/bg-15-7273-2018.

Chang, Y. L. K., Y. Miyazawa, M. Béguer-Pon, Y. S. Han, K. Ohashi, and J. Sheng. 2018. "Physical and Biological Roles of Mesoscale Eddies in Japanese Eel Larvae Dispersal in the Western North Pacific Ocean." Scientific Reports 8(1):1–11. doi: 10.1038/s41598-018-23392-5.

Cohen, J., K. Pfeiffer, and J. A. Francis. 2018. "Warm Arctic Episodes Linked with Increased Frequency of Extreme Winter Weather in the United States." Nature Communications 9(1):1–12. doi: 10.1038/s41467-018-02992-9.

Colwell, R. K., and D. C. Lees. 2000. "The Mid-Domain Effect: Geometric Constraints on the Geography of Species Richness." Trends Ecol. Evol. 15(2):70–76. doi: PII: S0169-5347(99)01767-X.

Colwell, R. K., C. Rahbek, and N. J. Gotelli. 2004. "The Mid-Domain Effect and Species

Richness Patterns: What Have We Learned so Far?" The American Naturalist 163(3):E1-23. doi: 10.1086/382056.

Costello, M. J., and C. Chaudhary. 2017. "Marine Biodiversity, Biogeography, Deep-Sea Gradients, and Conservation." Current Biology 27(11):R511–27. doi: 10.1016/j.cub.2017.04.060.

Costello, M. J., S. Wilson, and B. Houlding. 2012. "Predicting Total Global Species Richness Using Rates of Species Description and Estimates of Taxonomic Effort." Systematic Biology 61(5):871–83. doi: 10.1093/sysbio/syr080.

Costello, M. J., A. Cheung, and N. De Hauwere. 2010. "Surface Area and the Seabed Area, Volume, Depth, Slope, and Topographic Variation for the World's Seas, Oceans, and Countries." Environmental Science and Technology 44:8821–28.

Currie, D. J. 1991. "Energy and Large-Scale Patterns of Animal and Plant Species Richness." American Naturalist 137(1):27–49. doi: 10.1086/285144.

Currie, D. J., A. P. Francis, and J. T. Kerr. 1999. "Some General Propositions about the Study of Spatial Patterns of Species Richness." Ecoscience 6(3):392–99. doi: 10.1080/11956860.1999.11682541.

D'Hondt, S., A. J. Spivack, R. Pockalny, T. G. Ferdelman, J. P. Fischer, J. Kallmeyer, L. J. Abrams, D. C. Smith, D. Graham, F. Hasiuk, H. Schrum, and A. M. Stancin. 2009. "Subseafloor Sedimentary Life in the South Pacific Gyre." Proceedings of the National Academy of Sciences 106(28):11651–56. doi: 10.1073/pnas.0811793106.

Dai, L., C. Li, G. Yang, and X. Sun. 2016. "Zooplankton Abundance, Biovolume and Size Spectra at Western Boundary Currents in the Subtropical North Pacific during Winter

2012." Journal of Marine Systems 155:73–83. doi: 10.1016/j.jmarsys.2015.11.004.

Danovaro, R., N. Della Croce, A. Dell'Anno, and A. Pusceddu. 2003. "A Depocenter of Organic Matter at 7800 m Depth in the SE Pacific Ocean." Deep-Sea Research Part I: Oceanographic Research Papers 50(12):1411–20. doi: 10.1016/j.dsr.2003.07.001.

Danovaro, R., C. Gambi, and N. Della Croce. 2002. "Meiofauna Hotspot in the Atacama Trench, Eastern South Pacific Ocean." Deep-Sea Research Part I: Oceanographic Research Papers 49(5):843–57. doi: 10.1016/S0967-0637(01)00084-X.

Danovaro, R., A. Dell'anno, C. Corinaldesi, E. Rastelli, R. Cavicchioli, M. Krupovic, R. T. Noble, T. Nunoura, and D. Prangishvili. 2016. "Virus-Mediated Archaeal Hecatomb in the Deep Seafloor." Science Advances 2(10):1–9. doi: 10.1126/sciadv.1600492.

Danovaro, R., C. Gambi, A. Dell'Anno, C. Corinaldesi, S. Fraschetti, A. Vanreusel, M. Vincx, and A. J. Gooday. 2008. "Exponential Decline of Deep-Sea Ecosystem Functioning Linked to Benthic Biodiversity Loss." Current Biology 18(1):1–8. doi: 10.1016/j.cub.2007.11.056.

Danovaro, R., P. V. R. Snelgrove, and P. Tyler. 2014. "Challenging the Paradigms of Deep-Sea Ecology." Trends in Ecology and Evolution 29(8):465–75. doi: 10.1016/j.tree.2014.06.002.

von Dassow, P., and S. Collado Fabbri. 2014. "Biological Oceanography, Biogeochemical Cycles, and Pelagic Ecosystem Functioning of the East Central South Pacific Gyre: Focus on Easter Island and Salas y Gomez Island." Latin American Journal of Aquatic Research 42(4):703–42. doi: 10.3856/vol42-issue4-fulltext-4.

Desportes, C., M. Drévillon, M. Clavier, and A. Gounou. 2021. "Global Ocean Ensemble

Physics Reanalysis - Low Resolution." Retrieved on May 7th, 2021 and September 11th, 2024 (https://data.marine.copernicus.eu/product/GLOBAL_REANALYSIS_PHY_001_026/description).

Dolan, J. R., R. Lemée, S. Gasparini, L. Mousseau, and C. Heyndrickx. 2006. "Probing Diversity in the Plankton: Using Patterns in Tintinnids (Planktonic Marine Ciliates) to Identify Mechanisms." Hydrobiologia 555:143–57. doi: 10.1007/s10750-005-1112-6.

Dornelas, M., L. H. Antão, F. Moyes et al. 2018. "BioTIME : A Database of Biodiversity Time Series for the Anthropocene." Global Ecology and Biogeography 27(November 2017):760–86. doi: 10.1111/geb.12729.

Dornelas, M., N. J. Gotelli, B. McGill, H. Shimadzu, F. Moyes, C. Sievers, and A. E. Magurran. 2014. "Assemblage Time Series Reveal Biodiversity Change but Not Systematic Loss." Science 344(6181):296–300. doi: 10.1126/science.1248484.

Dunstan, P. K., D. Hayes, S. Woolley, V. Allain, D. Leduc, A. Flynn, K. Raumea, W. L. Long, P. Kumar, T. O. Hara, S. Singh, J.-a. Kerandel, A. L. Isechal, M. Keako, M. Satoa, H. Joseph, M. Fatia, A. L. Matoto, M. Falaile, J. C. Veron, B. Moore, V. Molisa, L. Fernandes, J. Sullivan, H. Wendt, J. Steffen, W. Lee, R. Przeslawski, and V. Zykov. 2018. Bioregions of the South West Pacific Ocean. CSIRO, Australia, 144 p. https://gobi.org/wp-content/uploads/2021/03/Final-workshop-report-Pacific_v5_1-1.pdf

Elliott, D. T., and K. W. Tang. 2011. "Influence of Carcass Abundance on Estimates of Mortality and Assessment of Population Dynamics in *Acartia tonsa*." Marine Ecology

Progress Series 427:1–12. doi: 10.3354/meps09063.

Escribano, R., P. Hidalgo, V. Valdés, and L. Frederick. 2014. “Temperature Effects on Development and Reproduction of Copepods in the Humboldt Current: The Advantage of Rapid Growth.” Journal of Plankton Research 36(1):104–16. doi: 10.1093/plankt/fbt095.

Falkowski, P. G., R. T. Barber, and V. Smetacek. 1998. “Biogeochemical Controls and Feedbacks on Ocean Primary Production.” Science 281(July):200–206. doi: 10.1126/science.281.5374.200.

Fernández-Álamo, M. A., and J. Färber-Lorda. 2006. “Zooplankton and the Oceanography of the Eastern Tropical Pacific: A Review.” Progress in Oceanography 69(2–4):318–59. doi: 10.1016/j.pocean.2006.03.003.

Francis, J. A., N. Skific, and S. J. Vavrus. 2018. “North American Weather Regimes Are Becoming More Persistent: Is Arctic Amplification a Factor?” Geophysical Research Letters 45(20):11,414-11,422. doi: 10.1029/2018GL080252.

Frederick, L., R. Escribano, C. E. Morales, S. Hormazabal, and J. Medellín-Mora. 2018. “Mesozooplankton Respiration and Community Structure in a Seamount Region of the Eastern South Pacific.” Deep-Sea Research Part I 135(March):74–87. doi: 10.1016/j.dsr.2018.03.008.

Le Galloudec, O., C. Perruche, C. Derval, M. Tressol, and R. Dussurget. 2021. “Global Ocean Biogeochemistry Hindcast.” Retrieved on May 7th, 2021 and September 11th, 2024 (https://data.marine.copernicus.eu/product/GLOBAL_MULTIYEAR_BGC_001_029/

description). DOI: https://doi.org/10.48670/moi-00019.

Gambi, C., A. Vanreusel, and R. Danovaro. 2003. “Biodiversity of Nematode Assemblages from Deep-Sea Sediments of the Atacama Slope and Trench (South Pacific Ocean).” Deep-Sea Research Part I: Oceanographic Research Papers 50(1):103–17. doi: 10.1016/S0967-0637(02)00143-7.

Ganachaud, A., S. Cravatte, A. Melet, A. Schiller, N. J. Holbrook, B. M. Sloyan, M. J. Widlansky, M. Bowen, J. Verron, P. Wiles, K. Ridgway, P. Sutton, J. Sprintall, C. Steinberg, G. Brassington, W. Cai, R. Davis, F. Gasparin, L. Gordeau, T. Hasegawa, W. Kessler, C. Maes, K. Takahashi, K. J. Richards, and U. Send. 2014. “The Southwest Pacific Circulation and Climate Experiment (SPICE).” Journal of Geophysical Research: Oceans 119:7660–86. doi: 10.1002/2013JC009678.Received.

García-Reyes, M., W. J. Sydeman, D. S. Schoeman, R. R. Rykaczewski, B. A. Black, A. J. Smit, and S. J. Bograd. 2015. “Under Pressure: Climate Change, Upwelling, and Eastern Boundary Upwelling Ecosystems.” Frontiers in Marine Science 2(December):1–10. doi: 10.3389/fmars.2015.00109.

Gaston, K. J., T. M. Blackburn, and J. I. Spicer. 1998. “Rapoport’s Rule: Time for an Epitaph?” Trends in Ecology and Evolution 13(2):70–74. doi: 10.1016/S0169-5347(97)01236-6.

Gentemann, C. L., M. R. Fewings, and M. García-Reyes. 2017. “Satellite Sea Surface Temperatures along the West Coast of the United States during the 2014–2016 Northeast Pacific Marine Heat Wave.” Geophysical Research Letters 44(1):312–19.

doi: 10.1002/2016GL071039.

Getis, A., and J. K. Ord. 1992. “The Analysis of Spatial Association by Use of Distance Statistics.” Geographical Analysis 24(3):189–206. doi: 10.1111/j.1538-4632.1992.tb00261.x.

Goldthwait, S. A., and D. K. Steinberg. 2008. “Elevated Biomass of Mesozooplankton and Enhanced Fecal Pellet Flux in Cyclonic and Mode-Water Eddies in the Sargasso Sea.” Deep-Sea Research Part II: Topical Studies in Oceanography 55(10–13):1360–77. doi: 10.1016/j.dsr2.2008.01.003.

Guinehut, S. 2021. “Multi Observation Global Ocean 3D Temperature Salinity Height Geostrophic Current and MLD.” Retrieved on May 7th, 2021 and September 11th, 2024 (https://data.marine.copernicus.eu/product/MULTIOBS_GLO_PHY_TSUV_3D_MYNRT_015_012/description). DOI: https://doi.org/10.48670/moi-00052.

Haury, L. R., J. J. Simpson, J. Peláez, C. J. Koblinsky, and D. Wiesenhahn. 1986. “Biological Consequences of a Recurrent Eddy off Point Conception, California.” Journal of Geophysical Research 91(Cll):12937–56.

Havermans, C., and V. Smetacek. 2018. “Bottom-up and Top-down Triggers of Diversification: A New Look at the Evolutionary Ecology of Scavenging Amphipods in the Deep Sea.” Progress in Oceanography 164:37–51. doi: 10.1016/j.pocean.2018.04.008.

Hernández-León, S., S. Putzeys, C. Almeida, P. Bécognée, A. Marrero-Díaz, J. Arístegui, and L. Yebra. 2019. “Carbon Export through Zooplankton Active Flux in the Canary Current.” Journal of Marine Systems 189(September 2018):12–21. doi:

10.1016/j.jmarsys.2018.09.002.

Hersbach, H., B. Bell, P. Berrisford, G. Biavati, A. Horányi, J. Muñoz Sabater, J. Nicolas, C. Peubey, R. Radu, I. Rozum, D. Schepers, A. Simmons, C. Soci, D. Dee, and J. N. Thépaut. 2023. "ERA5 Hourly Data on Single Levels from 1940 to Present." Copernicus Climate Change Service (C3S) Climate Data Store (CDS). Retrieved July 30, 2024 (https://cds-beta.climate.copernicus.eu/datasets/reanalysis-era5-single-levels?tab=overview). DOI: 10.24381/cds.adbb2d47.

Hobday, A. J., E. C. J. Oliver, A. Sen Gupta, J. A. Benthuysen, M. T. Burrows, M. G. Donat, N. J. Holbrook, P. J. Moore, M. S. Thomsen, T. Wernberg, and D. A. Smale. 2018. "Categorizing and Naming Marine Heatwaves." Oceanography 31(2):162–73. doi: https://doi.org/10.5670/oceanog.2018.205.

Hooff, R. C., and W. T. Peterson. 2006. "Copepod Biodiversity as an Indicator of Changes in Ocean and Climate Conditions of the Northern California Current Ecosystem." Limnology and Oceanography 51(6):2607–20.

International Hydrographic Organization. 1953. "Limits of Oceans and Seas, 3rd Edition." Pp. 1–42. International Hydrographic Organization (IHO), Bremerhaven, PANGAEA.

International Hydrographic Organization. 2002. "South Pacific Ocean and Its Sub-Divisions." Pp. 1–16 in Limits of Oceans and Seas, 4th Edition. Mónaco.

Ivanov, A. Y., and A. I. Ginzburg. 2002. "Oceanic Eddies in Synthetic Aperture Radar Images." Proceedings of the Indian Academy of Sciences, Earth and Planetary Sciences 111(3):281–95. doi: 10.1007/BF02701974.

Jacob, B. G., F. J. Tapia, R. A. Quiñones, R. Montes, M. Sobarzo, W. Schneider, G.

Daneri, C. E. Morales, P. Montero, and H. E. González. 2018. “Major Changes in Diatom Abundance, Productivity, and Net Community Metabolism in a Windier and Dryer Coastal Climate in the Southern Humboldt Current.” Progress in Oceanography 168(October):196–209. doi: 10.1016/j.pocean.2018.10.001.

Jahnke, R. A., C. E. Reimers, and D. B. Craven. 1990. “Intensification of Recycling of Organic Matter at the Seafloor near Ocean Margins.” Nature 348(November):50–54.

Jahnke, R. A., and D. B. Jahnke. 2000. “Rates of C, N, P and Si Recycling and Denitrification at the US Mid-Atlantic Continental Slope Depocenter.” Deep Sea Research Part I: Oceanographic Research Papers 47:1405–28.

Jamieson, A. J., T. Fujii, D. J. Mayor, M. Solan, and I. G. Priede. 2010. “Hadal Trenches: The Ecology of the Deepest Places on Earth.” Trends in Ecology and Evolution 25(3):190–97. doi: 10.1016/j.tree.2009.09.009.

Jordan, T. A., C. Martin, F. Ferraccioli, K. Matsuoka, H. Corr, R. Forsberg, A. Olesen, and M. Siegert. 2018. “Anomalously High Geothermal Flux near the South Pole.” Scientific Reports 8:16785. doi: 10.1038/s41598-018-35182-0.

Khodami, S., J. V. McArthur, L. Blanco-Bercial, and P. Martinez Arbizu. 2017. “Molecular Phylogeny and Revision of Copepod Orders (Crustacea: Copepoda).” Scientific Reports 7(1):1–11. doi: 10.1038/s41598-017-06656-4.

Kiørbe, T., and T. G. Nielsen. 1994. “Regulation of Zooplankton Biomass and Production in a Temperate, Coastal Ecosystem. 1. Copepods.” 39(3):493–507.

Kiørboe, T. 2011. “What Makes Pelagic Copepods so Successful?” Journal of Plankton Research 33(5):677–85. doi: 10.1093/plankt/fbq159.

Kitahashi, T., K. Kawamura, S. Kojima, and M. Shimanaga. 2014. “Bathymetric Patterns of α and β Diversity of Harpacticoid Copepods at the Genus Level around the Ryukyu Trench, and Turnover Diversity between Trenches around Japan.” Progress in Oceanography 123:54–63. doi: 10.1016/j.pocean.2014.02.007.

Koleff, P., K. J. Gaston, and J. J. Lennon. 2003. “Measuring Beta Diversity for Presence–Absence Data.” Journal of Animal Ecology 72(6):367–82. doi: 10.1007/s00228-017-2223-5.

Kostianoy, A. G., A. I. Ginzburg, O. V. Kopelevich, V. N. Kudryavtsev, O. Y. u. Lavrova, S. A. Lebedev, V. G. Smirnov, L. M. Mitnik, M. I. Mityagina, S. V. Stanichny, and Y. u. I. Troitskaya. 2018. “Ocean Remote Sensing in Russia.” Pp. 284–325 in Comprehensive Remote Sensing. Vol. 8, edited by S. Liang. Oxford: Elsiever.

Kretschmer, M., D. Coumou, L. Agel, M. Barlow, E. Tziperman, and J. Cohen. 2018. “More-Persistent Weak Stratospheric Polar Vortex States Linked to Cold Extremes.” Bulletin of the American Meteorological Society 99(1):49–60. doi: 10.1175/BAMS-D-16-0259.1.

Laffan, S. W. 2022. “Indices Available in Biodiverse.” Retrieved (https://github.com/shawnlaffan/biodiverse/wiki/Indices#simpson-and-shannon).

Laffan, S. W., E. Lubarsky, and D. F. Rosauer. 2010. “Biodiverse, a Tool for the Spatial Analysis of Biological and Related Diversity.” Ecography 33(4):643–47. doi: 10.1111/j.1600-0587.2010.06237.x.

Lange, S., and FR Schram. 1999. “Evolución y Filogenia de Los Crustáceos.” *Bol. S.E.A* (26):235–54.

Levin, L. A., R. J. Etter, M. A. Rex, A. J. Gooday, C. R. Smith, J. Pineda, C. T. Stuart, R. R. Hessler, and D. Pawson. 2001. “Environmental Influences on Regional Deep-Sea Species Diversity.” Annual Review of Ecology and Systematics 32:51–93.

Levitus, S., J. I. Antonov, T. P. Boyer, and C. Stephens. 2000. “Warming of the World Ocean.” Science 287(March):2225–29.

Lewis, C. N., K. A. Brown, L. A. Edwards, G. Cooper, and H. S. Findlay. 2013. “Sensitivity to Ocean Acidification Parallels Natural PCO2 Gradients Experienced by Arctic Copepods under Winter Sea Ice.” Proceedings of the National Academy of Sciences 110(51):E4960–67. doi: 10.1073/pnas.1315162110.

Lombard, F., E. Boss, A. M. Waite, M. Vogt, J. Uitz, L. Stemmann, H. M. Sosik, J. Schulz, J.-B. Romagnan, M. Picheral, J. Pearlman, M. D. Ohman, B. Niehoff, K. O. Möller, P. Miloslavich, A. Lara-López, R. Kudela, R. M. Lopes, R. Kiko, L. Karp-Boss, J. S. Jaffe, M. H. Iversen, J.-O. Irisson, K. Fennel, H. Hauss, L. Guidi, G. Gorsky, S. L. C. Giering, P. Gaube, S. Gallager, G. Dubelaar, R. K. Cowen, F. Carlotti, C. Briseño-Avena, L. Berline, K. Benoit-Bird, N. Bax, S. Batten, S. D. Ayata, L. F. Artigas, and W. Appeltans. 2019. “Globally Consistent Quantitative Observations of Planktonic Ecosystems.” Frontiers in Marine Science 6(April). doi: 10.3389/fmars.2019.00196.

Luo, M., J. Gieskes, L. Chen, X. Shi, and D. Chen. 2017. “Provenances, Distribution, and Accumulation of Organic Matter in the Southern Mariana Trench Rim and Slope: Implication for Carbon Cycle and Burial in Hadal Trenches.” Marine Geology 386:98–106. doi: 10.1016/j.margeo.2017.02.012.

Mackas, D. L., S. Batten, and M. Trudel. 2007. “Effects on Zooplankton of a Warmer

Ocean: Recent Evidence from the Northeast Pacific." Progress in Oceanography 75(2):223–52. doi: 10.1016/j.pocean.2007.08.010.

Mann, K. H., and J. R. N. Lazier. 2013a. "Vertical Structure in Coastal Waters: Freshwater Run-Off and Tidal Mixing." Pp. 118–61 in Dynamics of Marine Ecosystems.

Mann, K.H., Lazier, J.R.N., Mann, K.H. and Lazier, J.R.N. (2005). Vertical Structure of the Open Ocean: Biology of the Mixed Layer. In Dynamics of Marine Ecosystems (eds K.H. Mann and J.R.N. Lazier). https://doi.org/10.1002/9781118687901.ch3.

McCain, C. M. 2009. "Global Analysis of Bird Elevational Diversity." Global Ecology and Biogeography 18(3):346–60. doi: 10.1111/j.1466-8238.2008.00443.x.

McCain, C. M., and J.-A. Grytnes. 2010. "Elevational Gradients in Species Richness." Pp. 1–10 in Encyclopedia of Life Sciences (ELS). Chichester, UK.: John Wiley and Sons.

Medellín-Mora, J., R. Escribano, and W. Schneider. 2016. "Community Response of Zooplankton to Oceanographic Changes (2002–2012) in the Central/Southern Upwelling System of Chile." Progress in Oceanography 142:17–29. doi: 10.1016/j.pocean.2016.01.005.

Mestre, N. C., A. Brown, and S. Thatje. 2013. "Temperature and Pressure Tolerance of Larvae of *Crepidula fornicata* Suggest Thermal Limitation of Bathymetric Range." Marine Biology 160(4):743–50. doi: 10.1007/s00227-012-2128-x.

Monastersky, R. 2014. "Life — a Status Report." Nature 516:158–61. doi: 10.1038/516158a.

Montecino, V., and C. B. Lange. 2009. "The Humboldt Current System: Ecosystem

Components and Processes, Fisheries, and Sediment Studies." Progress in Oceanography 83(1–4):65–79. doi: 10.1016/j.pocean.2009.07.041.

Mora, C., D. P. Tittensor, S. Adl, A. G. B. Simpson, and B. Worm. 2011. "How Many Species Are There on Earth and in the Ocean?" PLoS Biology 9(8):1–8. doi: 10.1371/journal.pbio.1001127.

Morales, C. E., V. Anabalón, J. P. Bento, S. Hormazábal, M. Cornejo, M. A. Correa-Ramírez, and N. Silva. 2017. "Front-Eddy Influence on Water Column Properties, Phytoplankton Community Structure, and Cross-Shelf Exchange of Diatom Taxa in the Shelf-Slope Area off Concepción (~36–37°S)." Journal of Geophysical Research: Oceans 8944–65. doi: 10.1002/2017JC013111.

Morales, C. E., S. E. Hormazábal, and J. L. Blanco. 1999. "Interannual Variability in the Mesoscale Distribution of the Depth of the Upper Boundary of the Oxygen Minimum Layer off Northern Chile (18–24S): Implications for the Pelagic System and Biogeochemical Cycling." Journal of Marine Research 57:909–32.

OBIS. 2014. Ocean Biodiversity Information System (OBIS). Retrieved (http://iobis.org/).

Oliver, E. C. J., M. G. Donat, M. T. Burrows, P. J. Moore, D. A. Smale, L. V. Alexander, J. A. Benthuysen, M. Feng, A. Sen Gupta, A. J. Hobday, N. J. Holbrook, S. E. Perkins-Kirkpatrick, H. A. Scannell, S. C. Straub, and T. Wernberg. 2018. "Longer and More Frequent Marine Heatwaves over the Past Century." Nature Communications 9(1):1–12. doi: 10.1038/s41467-018-03732-9.

Owens, H. L., and R. Guralnick. 2019. "ClimateStability: An R Package to Estimate Climate Stability from Time-Slice Climatologies." Biodiversity Informatics 14:8–13.

doi: 10.17161/bi.v14i0.9786.

Pennington, J. T., K. L. Mahoney, V. S. Kuwahara, D. D. Kolber, R. Calienes, and F. P. Chavez. 2006. “Primary Production in the Eastern Tropical Pacific: A Review.” Progress in Oceanography 69(2–4):285–317. doi: 10.1016/j.pocean.2006.03.012.

Pereira, H. M., P. W. Leadley, V. Proença, R. Alkemade, J. P. W. Scharlemann, J. F. Fernández-Manjarrés, M. B. Araújo, P. Balvarena, R. Biggs, W. W. L. Cheung, L. Chini, H. D. Cooper, E. L. Gilman, S. Guénette, G. C. Hurtt, H. P. Huntington, G. M. Mace, T. Oberdorff, C. Revenga, P. Rodrigues, R. J. Scholes, U. R. Sumaila, and M. Walpole. 2010. “Scenarios for Global Biodiversity in the 21st Century.” Science 330:1496–1501. doi: 10.1126/science.1196624.

Pérez-Aragón, M., C. Fernandez, and R. Escribano. 2011. “Nitrogen Excretion by Mesozooplankton in a Coastal Upwelling Area: Seasonal Trends and Implications for Biological Production.” Journal of Experimental Marine Biology and Ecology 406:116–24. doi: 10.1016/j.jembe.2011.05.029.

Peterson, W. T., and D. C. Bellantoni. 1987. “Relationships between Water-Column Stratification, Phytoplankton Cell Size and Copepod Fecundity in Long Island Sound and off Central Chile.” South African Journal of Marine Science 5(1):411–21. doi: 10.2989/025776187784522748.

Pichevin, L. E., B. C. Reynolds, R. S. Ganeshram, L. Cacho, L. Pena, K. Keefe, and R. M. Ellam. 2009. “Enhanced Carbon Pump Inferred from Relaxation of Nutrient Limitation in the Glacial Ocean.” Nature 459(7250):1114–17. doi: 10.1038/nature08101.

Pineda, J., and H. Caswell. 1998. “Bathymetric Species-Diversity Patterns and Boundary Constraints on Vertical Range Distributions.” Deep Sea Research Part II: Topical Studies in Oceanography 45:83–101.

Pino-Pinuer, P., R. Escribano, P. Hidalgo, R. Riquelme-Bugueño, and W. Schneider. 2014. “Copepod Community Response to Variable Upwelling Conditions off Central-Southern Chile during 2002−2004 and 2010−2012.” Marine Ecology Progress Series 515:83–95. doi: 10.3354/meps11001.

Pörtner, H. O. 2002. “Climate Variations and the Physiological Basis of Temperature Dependent Biogeography: Systemic to Molecular Hierarchy of Thermal Tolerance in Animals.” Comparative Biochemistry and Physiology - A Molecular and Integrative Physiology 132(4):739–61. doi: 10.1016/S1095-6433(02)00045-4.

Provoost, P., and S. Bosch. 2021. “Robis: Ocean Biodiversity Information System (OBIS) Client. R Package Version 2.8.2.”

Qian, H., R. E. Ricklefs, and P. S. White. 2005. “Beta Diversity of Angiosperms in Temperate Floras of Eastern Asia and Eastern North America.” Ecology Letters 8(1):15–22. doi: 10.1111/j.1461-0248.2004.00682.x.

Qu, T., and E. J. Lindstrom. 2011. “A Climatological Interpretation of the Circulation in the Western South Pacific*.” Journal of Physical Oceanography 32(9):2492–2508. doi: 10.1175/1520-0485-32.9.2492.

Rapoport, E. H. 1975. Aerografía: Estrategias Geográficas de Las Especies. Primera Ed. México D.F.: Fondo de la Cultura Económica.

Reid, J. L. 1997. On the total geostrophic circulation of the pacific ocean: flow patterns,

tracers, and transports. Prog. Oceanogr. 39, 263–352.

Renema, W., D. R. Bellwood, J. C. Braga, K. Bromfield, R. Hall, K. G. Johnson, P. Lunt, C. P. Meyer, L. B. McMonagle, R. J. Morley, A. O'Dea, J. A. Todd, F. P. Wesselingh, M. E. J. Wilson, and J. M. Pandolfi. 2008. "Hopping Hotspots: Global Shifts in Marine Biodiversity." Science 321(August):654–57. doi: 10.1126/science.1155674.

Ridgway, K. R., and J. R. Dunn. 2003. "Mesoscale Structure of the Mean East Australian Current System and Its Relationship with Topography." Progress in Oceanography 56(2):189–222. doi: 10.1016/S0079-6611(03)00004-1.

Rigby, S., and C. Milsom. 1996. "Benthic Origins of Zooplankton: An Environmentally Determined Macroevolutionary Effect." Geology 24(1):52–54. doi: 10.1130/0091-7613(1996)024<0052:BOOZAE>2.3.CO;2.

Riquelme-Bugueño, R., M. Correa-Ramírez, R. Escribano, S. Núñez, and S. Hormazábal. 2015. "Mesoscale Variavility in the Habitat of the Humbboldt Current Krill, Spring 2007." Journal of Geophysical Research: Oceans 120:2769–83. doi: 10.1002/2014JC010460.Received.

Rohde, K. 1992. "Latitudinal Gradients in Species Diversity: The Search for the Primary Cause." Oikos 65(3):514–27.

Roman, J., and J. J. McCarthy. 2010. "The Whale Pump: Marine Mammals Enhance Primary Productivity in a Coastal Basin." PLoS ONE 5(10). doi: 10.1371/journal.pone.0013255.

Rombouts, I., G. Beaugrand, F. Ibañez, S. Gasparini, S. Chiba, and L. Legendre. 2009. "Global Latitudinal Variations in Marine Copepod Diversity and Environmental

Factors.” Proceedings of the Royal Society B: Biological Sciences 276(1670):3053–62. doi: 10.1098/rspb.2009.0742.

Rombouts, I., G. Beaugrand, F. Ibañez, S. Gasparini, S. Chiba, and L. Legendre. 2010. “A Multivariate Approach to Large-Scale Variation in Marine Planktonic Copepod Diversity and Its Environmental Correlates.” Limnology and Oceanography 55(5):2219–29. doi: 10.4319/lo.2010.55.5.2219.

Rowe, G., M. Sibuet, J. Deming, A. Khripounoff, J. Tietjen, S. Macko, and R. Theroux. 1991. “‘Total’ Sediment Biomass and Preliminary Estimates of Organic Carbon Residence Time in Deep-Sea Benthos.” Marine Ecology Progress Series 79(0):99–114.

Roy, K., D. Jablonski, J. W. Valentine, and G. Rosenberg. 2002. “Marine Latitudinal Diversity Gradients: Tests of Causal Hypotheses.” Proceedings of the National Academy of Sciences 95(7):3699–3702. doi: 10.1073/pnas.95.7.3699.

Rutherford, S., S. D. Hondt, and W. Prell. 1999. “Environmental Controls on the Geographic Distribution of Zooplankton Diversity.” Nature 400(August):749–53.

Ruz, P. M., P. Hidalgo, R. Escribano, J. E. Keister, L. Yebra, and B. Franco-Cisterna. 2018. “Hypoxia Effects on Females and Early Stages of Calanus Chilensis in the Humboldt Current Ecosystem (23°S).” Journal of Experimental Marine Biology and Ecology 498(September 2017):61–71. doi: 10.1016/j.jembe.2017.09.018.

Saito, R., A. Yamaguchi, I. Yasuda, H. Ueno, H. Ishiyama, H. Onishi, and I. Imai. 2014. “Influences of Mesoscale Anticyclonic Eddies on the Zooplankton Community South

of the Western Aleutian Islands during the Summer of 2010." Journal of Plankton Research 36(1):117–28. doi: 10.1093/plankt/fbt087.

Sanches Melo, A. 2021. "Package 'CommEcol', Community Ecology Analyses." 1–34.

Sauzède, R., P. R. Renosh, and H. Claustre. 2023. "Global Ocean 3D Chlorophyll-a Concentration, Particulate Backscattering Coefficient and Particulate Organic Carbon." Retrieved on September 11th, 2024 (https://data.marine.copernicus.eu/product/MULTIOBS_GLO_BIO_BGC_3D_REP_015_010/description). DOI: 10.48670/moi-00046.

Schneider, W., D. Donoso, J. Garcés-Vargas, and R. Escribano. 2017. "Water-Column Cooling and Sea Surface Salinity Increase in the Upwelling Region off Central-South Chile Driven by a Poleward Displacement of the South Pacific High." Progress in Oceanography 151:38–48. doi: 10.1016/j.pocean.2016.11.004.

Schneider, W., M. Fukasawa, J. Garcés-Vargas, L. Bravo, H. Uchida, T. Kawano, and R. Fuenzalida. 2007. "Spin-up of South Pacific Subtropical Gyre Freshens and Cools the Upper Layer of the Eastern South Pacific Ocean." Geophysical Research Letters 34:1–5. doi: 10.1029/2007GL031933.

Selden, P. A., R. Huys, M. H. Stephenson, A. P. Heward, and P. N. Taylor. 2010. "Crustaceans from Bitumen Clast in Carboniferous Glacial Diamictite Extend Fossil Record of Copepods." Nature Communications 1(5):1–6. doi: 10.1038/ncomms1049.

Smith, K. F., and J. H. Brown. 2002. "Patterns of Diversity, Depth Range and Body Size among Pelagic Fishes along a Gradient of Depth." Global Ecology and Biogeography 11(4):313–22.

Sorte, C. J. B., S. J. Jones, and L. P. Miller. 2011. “Geographic Variation in Temperature Tolerance as an Indicator of Potential Population Responses to Climate Change.” Journal of Experimental Marine Biology and Ecology 400(1–2):209–17. doi: 10.1016/j.jembe.2011.02.009.

Spears, T., and L. G. Abele. 2011. “Crustacean Phylogeny Inferred from 18S RDNA.” Arthropod Relationships 169–87. doi: 10.1007/978-94-011-4904-4_14.

Stramma, L., R. G. Peterson, and M. Tomczak. 1995. “The South Pacific Current.” Journal of Physical Oceanography 25(1):77–91. doi: 10.1175/1520-0485(1995)025<0077:tspc>2.0.co;2.

Strub, P. T., J. M. Mesías, V. Montecino, J. Rutllant, and S. Salinas. 1998. “Coastal Ocean Circulation off Western South America.” Pp. 273–313 in The Sea. John Wiley and Sons, Inc.

Stuiver, M., P. D. Quay, and H. G. Ostlund. 1983. “Abyssal Water Carbon-14 Distribution and the Age of the World Oceans.” Science 219(4586):849–51. doi: 10.1126/science.219.4586.849.

Suckow, M. A., S. H. Weisbroth, and C. L. Franklin. 1995. “Temperature in the Oceans.” Pp. 14–28 in Seawater: Its Composition, Properties and Behaviour.

Swingland, I. R. 2013. “Biodiversity, Definition Of.” Encyclopedia of Biodiversity 1(2001):377–91. doi: 10.1016/B978-0-12-384719-5.00009-5.

Thatje, S., L. Casburn, and J. A. Calcagno. 2010. “Behavioural and Respiratory Response of the Shallow-Water Hermit Crab *Pagurus cuanensis* to Hydrostatic Pressure and Temperature.” Journal of Experimental Marine Biology and Ecology 390(1):22–30.

doi: 10.1016/j.jembe.2010.04.028.

Thatje, S., and N. Robinson. 2011. “Specific Dynamic Action Affects the Hydrostatic Pressure Tolerance of the Shallow-Water Spider Crab *Maja brachydactyla*.” Naturwissenschaften 98(4):299–313. doi: 10.1007/s00114-011-0768-1.

Thiel, M., E. Macaya, E. Acuña, W. Arntz, H. Bastias, K. Brokordt, P. Camus, J. Castilla, L. Castro, M. Cortés, C. Dumont, R. Escribano, M. Fernandez, J. Gajardo, C. Gaymer, I. Gomez, A. González, H. González, P. Haye, J.-E. Illanes, J. Iriarte, D. Lancellotti, G. Luna-Jorquera, C. Luxoro, P. Manriquez, V. Marín, P. Muñoz, S. Navarrete, E. Perez, E. Poulin, J. Sellanes, H. Sepúlveda, W. Stotz, F. Tala, A. Thomas, C. Vargas, J. Vasquez, and J. M. A. Vega. 2007. “The Humboldt Current System of Northern and Central Chile.” Oceanography and Marine Biology 45:195–344. doi: 10.1201/9781420050943.ch6.

Thor, P., and S. Dupont. 2015. “Transgenerational Effects Alleviate Severe Fecundity Loss during Ocean Acidification in a Ubiquitous Planktonic Copepod.” Global Change Biology 21(6):2261–71. doi: 10.1111/gcb.12815.

Tian, J., L. Fan, H. Liu, J. Liu, Y. Li, Q. Qin, Z. Gong, H. Chen, Z. Sun, L. Zou, X. Wang, H. Xu, D. Bartlett, M. Wang, Y. Z. Zhang, X. H. Zhang, and C. L. Zhang. 2018. “A Nearly Uniform Distributional Pattern of Heterotrophic Bacteria in the Mariana Trench Interior.” Deep-Sea Research Part I: Oceanographic Research Papers 142(August):116–26. doi: 10.1016/j.dsr.2018.10.002.

Tittensor, D. P., C. Mora, W. Jetz, H. K. Lotze, D. Ricard, E. Vanden Berghe, C. Mora, and B. Worm. 2010. “Global Patterns and Predictors of Marine Biodiversity across Taxa.”

Nature 466(7310):1098–1101. doi: 10.1038/nature09329.

Toggweiler, J. R., and R. M. Key. 2001. “Theromohaline Circulation”. J. Steele, S. Thorpe, and K. Turekian (eds.). Encyclopedia of Ocean Sciences 2941–47. doi: 10.1006/rwos.2001.0111.

Valdés, V., F. Carlotti, R. Escribano, K. Donoso, M. Pagano, V. Molina, and C. Fernandez. 2018. “Nitrogen and Phosphorus Recycling Mediated by Copepods and Response of Bacterioplankton Community from Three Contrasting Areas in the Western Tropical South Pacific (20◦S).” 6019–32.

Valdés, V. P., C. Fernandez, V. Molina, R. Escribano, and F. Joux. 2017. “Dissolved Compounds Excreted by Copepods Reshape the Active Marine Bacterioplankton Community Composition.” Frontiers in Marine Science 4(November):343. doi: 10.3389/fmars.2017.00343.

Verity, P. G., and V. Smetacek. 1996. “Organism Life Cycles, Predation, and the Structure of Marine Pelagic Ecosystems.” Marine Ecology Progress Series 130(1–3):277–93. doi: 10.3354/meps130277.

Vilela, B., and F. Villalobos. 2015. “LetsR: A New R Package for Data Handling and Analysis in Macroecology.” Methods in Ecology and Evolution 6(10):1229–34. doi: 10.1111/2041-210X.12401.

Wickham, H., J. Hester, and W. Chang. 2021. “Devtools: Tools to Make Developing R Packages Easier. R Package Version 2.4.3.”

Williams, R., D. V. P. Conway, and H. G. Hunt. 1994. “The Role of Copepods in the Planktonic Ecosystems of Mixed and Stratified Waters of the European Shelf Seas.”

Hydrobiologia 292–293(1):521–30. doi: 10.1007/BF00229980.

Worm, B., M. Sandow, A. Oschlies, H. K. Lotze, and R. A. Myers. 2005. “Global Patterns of Predator Diversity in the Open Oceans.” Science 309(August):1365–69.

Yáñez, S., P. Hidalgo, and R. Escribano. 2012. “Mortalidad Natural de Paracalanus Indicus (Copepoda: Calanoida) En Áreas de Surgencia Asociada a La Zona de Mínimo de Oxígeno En El Sistema de Corrientes Humboldt: Implicancias En El Transporte Pasivo Del Flujo de Carbono.” Revista de Biología Marina y Oceanografía 47(2):295–310.

Zeppilli, D., A. Pusceddu, F. Trincardi, and R. Danovaro. 2016. “Seafloor Heterogeneity Influences the Biodiversity-Ecosystem Functioning Relationships in the Deep Sea.” Scientific Reports 6(March 2015):1–12. doi: 10.1038/srep26352.

Zhong, Y., A. Bracco, J. Tian, J. Dong, W. Zhao, and Z. Zhang. 2017. “Observed and Simulated Submesoscale Vertical Pump of an Anticyclonic Eddy in the South China Sea.” Scientific Reports 7(August 2016):44011. doi: 10.1038/srep44011.